Supercapacitor-Assisted Refrigerator for DC powered households

A thesis

submitted for fulfilment

of the requirements for the degree

of

Master of Engineering

at

The University of Waikato

by

Don Charles Themiya Sirimanne

THE UNIVERSITY OF
WAIKATO
Te Whare Wānanga o Waikato

2023

Table of Contents

Abstract ..... *i*

Acknowledgements ..... *ii*

List of Figures ..... *iii*

List of Tables ..... *vi*

Chapter 1: Introduction *1*

1.1 New approach to powering a DC refrigerator **2**

1.2 Project Development and objectives **2**

1.3 Thesis structure **3**

Chapter 2: CONCEPTS OF POWER DISTRIBUTION SYSTEMS, ENERGY STORAGE AND PHOTOVOLTAIC FUNDAMENTALS *4*

2.1 POWER SYSTEM ARCHITECTURE **4**

2.1.1 CENTRALIZED GENERATION AND DISTRIBUTED GENERATION 4

2.1.2 DC MICROGRID AND DC HOME CONCEPT 6

2.2 ENERGY STORAGE TECHNOLOGIES FOR RENEWABLE ENERGY **11**

2.2.1 KEY PARAMETERS FOR ESS [4] 11

2.2.2 ENERGY STORAGE SYSTEM CLASSIFICATIONS 15

2.2.3 ENERGY STORAGE SYSTEMS (ESS) 16

2.2.4 RAGONE PLOT 21

2.3 PHOTOVOLTAIC ENERGY FOR THE FUTURE **22**

2.3.1 ELECTRICITY GENERATION FROM THE SUN 22

2.3.2 PHOTOVOLTAIC FUNDAMENTALS 24

2.3.3 SOLAR CELL PARAMETERS 28

2.3.4 SOLAR MODULE (SOLAR PANEL) 30

2.3.5 SOLAR IRRADIATION FOR PV SYSTEM DESIGN [16, pp27] 32

2.3.6 PV SYSTEM CONFIGURATION 33

2.3.7 MPPT TECHNIQUES 36

2.3.8 MAXIMUM POWER TRANSFER CONCEPT IN BRIEF 37

2.3.9 MPPT METHODS 38

2.3.10 ANALYSIS OF MPPT TECHNIQUE FOR SUPERCAPACITOR-BASED ENERGY STORAGE. 42

CHAPTER 3: FUNDAMENTALS OF CAPACITORS AND SUPERCAPACITORS *44*

3.1 FUNDAMENTALS OF CAPACITORS **44**

3.1.1 HISTORICAL BACKGROUND OF CAPACITORS IN BRIEF 44

3.1.2 Electric Capacitor Fundamentals 44

3.1.3 CALCULATING THE CAPACITANCE 46

3.1.4 CAPACITORS IN PARALLEL AND SERIES 47

3.1.5 ENERGY STORED IN A CAPACITOR 49

3.1.6 ENERGY DENSITY 50

3.1.7 Power density 51
3.1.8 CAPACITOR CHARGING AND DISCHARGING 51
3.1.9 Time constant 53
3.2 FUNDAMENTALS OF SUPERCAPACITORS 54
3.2.1 SUPERCAPACITOR STRUCTURE AND PRINCIPLE 54
3.2.2 CLASSIFICATION OF SUPERCAPACITORS 56
3.2.3 SUPERCAPACITOR STRUCTURE. 56
3.2.4 SUPERCAPACITOR PRINCIPLE 57
3.2.5 CELL CONSTRUCTION OF SUPERCAPACITORS 58
3.2.6 PSEUDOCAPACITORS (PC) 60
3.2.7 HYBRID SUPERCAPACITORS (ASYMMETRIC SC) 61
3.2.8 EQUIVALENT CIRCUIT MODEL OF SC 61
3.2.9 SUPERCAPACITOR AS AN ENERGY STORAGE DEVICE 63
3.2.10 Generalized comparison of Supercapacitors against Li-ion batteries 64
3.2.11 COMPARISON OF ADVANTAGES AND DRAWBACKS OF SUPERCAPACITORS 67
3.3 SUPERCAPACITOR MODULES AND APPLICATIONS 67
3.3.1 DIFFERENT TYPES OF SUPERCAPACITORS AND COMMERCIAL SUPERCAPACITOR MODULES 67
3.3.2 SC MODULES (SCM) FOR POWER APPLICATIONS 68
3.3.3 SUPERCAPACITOR MODULE MANAGEMENT 69
3.3.4 PASSIVE BALANCING METHODS 70
3.3.5 ACTIVE BALANCING 71
3.3.6 SUPERCAPACITORS IN ELECTRICAL CIRCUITS 73
CHAPTER 4: EVOLUTION OF NOVEL SUPERCAPACITOR ASSISTED LOSS MANAGEMENT (SCALoM) PRINCIPLE. 75
4.1 SIMPLE R-C LOOP BEHAVIOUR AND CHARGING EFFICIENCY. 75
4.2 LOSS CIRCUMVENTION ANALYSIS OF R-C CIRCUIT 76
4.3 MODIFIED R-C LOOP AND EFFICIENCY 78
4.4 R-C CIRCUIT WITH OVER-RATED DC VOLTAGE SOURCE AND PRE-CHARGED CAPACITOR 79
4.5 R-C CIRCUIT ANALYSIS OF OVER-RATED DC VOLTAGE SOURCE AND PRE-CHARGED CAPACITOR WITH USEFUL LOAD. 82
4.6 SUCCESSFUL APPLICATION OF SUPERCAPACITOR ASSISTED LOSS MANAGEMENT (SCALoM) CONCEPT. 85
4.6.1 Supercapacitor-assisted low-dropout regulator (SCALDO) 85
4.6.2 Supercapacitor-assisted surge absorber (SCASA) 86
4.6.3 Supercapacitor-assisted temperature modification apparatus (SCATMA) 87
4.6.4 Supercapacitor-assisted LED lighting (SCALED) 88
4.6.5 SCA Refrigerator Technique 89
CHAPTER 5: RESIDENTIAL REFRIGERATOR TECHNOLOGY 90
5.1 REFRIGERATION PRINCIPLES AND MAIN COMPONENTS 90
5.1.1 Refrigeration Cycle 90
5.2 COMPRESSOR TECHNOLOGIES FOR DOMESTIC REFRIGERATORS 91
5.3 Functional differences between a regular refrigerator and an inverter refrigerator 92

5.4 COMPARISON OF THE TWO COMPRESSOR MOTOR TYPES (BLDC VS INDUCTION MOTOR) 95

Chapter 6: Supercapacitor-Assisted Refrigerator (SCA-Ref) 96

6.1 Refrigerator Specifications 96

6.2 DC-AC conversion 101

6.3 The Supercapacitor-Assisted DC refrigerator (SCA-ref) concept 101

6.4 SCA-Ref circuit topology and operation 104

6.4.1 Charging phase 105

6.4.2 Discharging phase 105

6.5 Switch selection for main circuit 106

6.6 Control circuit design 108

6.6.1 Non-Inverting Schmitt trigger (Non-symmetrical Schmitt trigger) 109

6.6.2 Regulator for the control circuit 110

6.7 Efficiency of SCA-Ref 111

Chapter 7: Conclusion 118

7.1 Summary of results 118

7.2 Future work 118

References 120

A. Appendix 123

Abstract

Energy efficiency is a prime concern in power generation as well as in usage. Product developers and end users are encouraged to reduce their carbon footprint for help in the fight against climate change. In this effect designing power electronic systems with high end to end efficiency is paramount. Direct DC application with tactical circuit topologies show promising results for improved efficiency gains resulting in increased attention for the DC microgrid concept. DC powered households are developed, where solar photovoltaics on rooftops generate purely DC electricity to power the immediate community. Recent developments have made solar generation quite economical for this to be realized. Unfortunately, solar power is not consistent due to environmental factors, thus needing an alternate DC source or energy storage for uninterrupted supply of power. To meet this demand research into energy storage has ramped up. As a result, supercapacitor technology has advanced considerably with superior characteristics compared to rechargeable batteries. Almost all modern white goods run on DC internally. The inverter-based refrigerator operates using a variable frequency inverter for efficient and smooth operation. The refrigerator has shown to function efficiently within a range around the nominal operating voltage. This has allowed the application of the well matured supercapacitor assisted loss management (SCALoM) technique to develop a power converter to operate the refrigerator with the characteristic DC power supply of a solar photovoltaic (PV) array. The system benefits from the replacement of the battery and Maximum Power Point Tracking (MPPT) Charge controller with supercapacitors for a solar power system with long operation time in between of service intervals. While MPPT charge controller is based on a high frequency switch mode DC-DC converter, the proposed power converter allows for switching frequencies in the mHz region, allowing lower switching losses and reduction in potential electromagnetic interference and radio frequency interference. The concept was proven by using a 24V DC camping fridge and obtaining an efficiency of up to 94%. This work will lead to the development of the converter for a consumer grade 240Vac inverter driven refrigerator where the AC-DC converter is bypassed to achieve improved efficiency. This thesis covers the broader design and technical aspects of the power converter.

Acknowledgements

My Life journey is wonderful. I am fortunate enough to get the best opportunity in my life journey. Therefore, first part of my acknowledgement if to my beloved father and mother to introducing me into this colourful world. Secondly, I cannot thank enough for all my teachers who gave their guidance to broaden my vision through knowledge.

Solving Problems through applying fundamentals is my supervisor Prof. Nihal Kularatna's motto. Without his generous guidance towards me to reach this milestone and submit my Masters thesis. My very special acknowledgement to Prof Nihal Kularatna and Dr. Andrew Lapthron for giving me one of the best opportunities to manipulate electrons in a real working circuit.

My special thanks to Nirashi Gallage, Chamila Naligama and Chamara Dassanayake(PhD candidates at UOW). I would also like to acknowledge the kind support from the technical officers Mr. Benson Chang and Mr. Viking Zhou during my experiment.

List of Figures

Figure 1-1: :End-to-End efficiency:(a) Typical appliance powered by AC. (b) Typical appliance powered by DC [6] 1
Figure 2-1:Schematic of general centralized power network [5,pp2] 4
Figure 2-2 (a): Importance of solar energy for future energy, (b) the mean horizontal irradiation of the world [1] 5
Figure 2-3:Typical block diagram of: (a) AC microgrid system, (b) DC microgrid system. [7] 7
Figure 2-4: A block diagram of AC and DC source-fed traditional residential electrical system 9
Figure 2-5: A block diagram representing a DC microgrid at home based on a solar PV system and alternate AC grid power for emergency DC supply. 10
Figure 2-6: A residential power system with Non-traditional SCA power converter-based, battery-less DC residence with DC appliance 11
Figure 2-7: A block diagram of the flywheel energy storage system [4] 17
Figure 2-8: A schematic of a typical CAES {4} 17
Figure 2-9: A schematic of superconducting magnetic energy storage { 4] 18
Figure 2-10: A structure of a typical hydrogen fuel cell [4] 19
Figure 2-11: A schematic diagram of the Li-ion battery [4] 20
Figure 2-12: A schematic of an SC's system [4] 21
Figure 2-13: Ragone plot comparing different energy storage systems [5, pp 186] 22
Figure 2-14: Solar power field [9] 23
Figure 2-15: Concentrated Solar power:(a)Parabolic trough solar thermal system, (b) A solar power tower system [11, pp366] 24
Figure 2-16: Electron energy bands of metals, insulators, and semiconductors [12] 25
Figure 2-17: A structure of a solar cell, A closeup view of the depletion zone around the p-n junction and built in electric field. [13] 26
Figure 2-18: The equivalent circuit of an ideal solar cell [11, pp109] 27
Figure 2-19: The equivalent circuit of solar cell represented with a series resistance, R_s and parallel resistance, R_P [10, pp109] 28
Figure 2-20: Identifying the shunt resistance and series resistance [14] 28
Figure 2-21: I-V curve of PV panel [11,pp265] 29
Figure 2-22: Solar panel construction: (a) Solar cell, (b) Solar module [15] 31
Figure 2-23: Schematic of three solar cells connected in series [11, pp253] 32
Figure 2-24: Schematic of three solar cells connected in parallel [11, pp253] 32
Figure 2-25: Schematic of stand-alone PV system with storage, power conditioner, DC and AC loads [11, pp220] 34
Figure 2-26: Schematic of a typical grid-connected PV system [11, pp221] 35
Figure 2-27: Schematic of hybrid PV system with backup alternative source [11, pp225] 36
Figure 2-28: Maximum power point variation due to: (a)Irradiance, (b) Temperature [17] 37
Figure 2-29: DC power source: (a) consisting of the voltage source and fixed internal resistance, (b) Closed circuit formed with external load [5, pp41] 37
Figure 2-30: A conceptual flow chart of perturb and observe (P&O) algorithm [18] 39
Figure 2-31: A conceptual flow chart of the incremental conductance (IC) algorithm [18,19] 40
Figure 2-32: A representation of the constant voltage (CV) method flow chart [5, pp348] 41
Figure 2-33: A typical I-V characteristic curve of a solar PV system [21] 42
Figure 3-1: A charged parallel plate electrostatic capacitor 44
Figure 3-2: Different types of capacitors [5, (pp 194)] 46
Figure 3-3: A parallel plate capacitor charged with Q 47

Figure 3-4: Capacitors connected in parallel to the source 48
Figure 3-5: Capacitor connected in series 49
Figure 3-6: A capacitor charging from a voltage source [5, pp 182] 51
Figure 3-7: Voltage-current variation with time during charging [5, pp 183] 52
Figure 3-8: Capacitor discharging through resistor 52
Figure 3-9: Capacitor discharging with time. [5, (pp 183)] 53
Figure 3-10: Measuring time constant 53
Figure 3-11: Cross-section of electrostatic capacitor [24] 55
Figure 3-12: Supercapacitors and electrolytic capacitors of similar geometry [5, pp 243] 55
Figure 3-13: Supercapacitor families [26] 56
Figure 3-14: Schematic of EDLC [24] 57
Figure 3-15: Cross-section of EDLC [28] 58
Figure 3-16: Schematic of pseudocapacitor [27] 61
Figure 3-17: Capacitor equivalent circuit: (a) First order model, (b) Classical model [5, (pp 188), 32] 62
Figure 3-18: Supercapacitor models: (a) Two branch, (b) Three branch [5, pp 222] 62
Figure 3-19: Ragone plot [5, pp 242] 65
Figure 3-20: Variation of life cycle and depth of discharge of supercapacitors and battery [5,pp 96] 67
Figure 3-21: Different types of Supercapacitors: (a) Cells, (b) Modules [24] 68
Figure 3-22:Root causes, modes and effects of supercapacitor module voltage unbalance [28] 69
Figure 3-23: Passive balancing circuit with resistors [5, pp 230] 70
Figure 3-24: Passive balancing circuit with Zener diodes [5, (pp 230)] 71
Figure 3-25: Passive balancing circuit with switch resistor [28] 71
Figure 3-26: Integrated circuit-based active balancing [39] 72
Figure 3-27: Areas of supercapacitor application 74
Figure 4-1: A simple RC circuit connected to a DC voltage source [5,pp 182] 75
Figure 4-2: Basic RC charging loop [41, pp 46] 77
Figure 4-3: Modified RC loop with loss circumvention concept [41, pp 46] 78
Figure 4-4: Capacitor charging circuit [5, pp 256] 79
Figure 4-5: Capacitor charging curve [5, pp 256] 80
Figure 4-6: Variation of charging efficiency with over-rate factor m and pre-charged factor k [41, pp 49] 82
Figure 4-7: Modified circuit with useful resistance R_L inserted [5, pp 262] 83
Figure 4-8: Graphical representation of circuit behaviour in terms of efficiency vs m (over-rated or over-voltage factor) and k (pre-charged factor) [5, pp 256] 85
Figure 4-9: Supercapacitor-assisted Low-dropout regulator [5, pp 283] 86
Figure 4-10: Supercapacitor Assisted Surge Absorber (SCASA) [43] 87
Figure 4-11: Supercapacitor assisted temperature modification apparatus:(a) Block diagram (b) temperature vs time for 15V supercapacitor banks with different changeover delays of S1, S2 and S3 [43] 88
Figure 4-12: Supercapacitor Assisted LED lighting system [5, pp 365] 89
Figure 5-1: Schematic of refrigeration cycle [47] 90
Figure 5-2: A typical reciprocating compressor operation [49] 92
Figure 5-3: Single-phase induction motor refrigerator circuit diagram [50] 93
Figure 5-4: Inverter refrigerator: (a)Block diagram of typical inverter module for motor control, (b) Operational behaviour and power consumption comparison of inverter and non-inverter refrigerator [3, 52] [Your Figure 5-5 (a) is not of good quality. Do you have a possibility to redraw it. Exteranl examiners usually comment (negatively) when complex figures are not easily readable] 94
Figure 6-1: 12V/24V DC refrigerator (a) Reverse panel (b) Compressor and controller (c)Controller module . 97
Figure 6-2: Refrigerator performance : (a) Temperature variation for thermistor setting 2, (b) Current drawn at thermistor setting 2 99

Figure 6-3: Refrigerator performance : (a) Temperature variation for thermistor setting 6, (b) Current drawn at thermistor setting 6 100
Figure 6-4: AC-DC conversion 101
Figure 6-5: Modes of operation: (a) Charging phase (b) Discharging phase 103
Figure 6-6: SCA-ref topology 104
Figure 6-7: Typical output characteristics: (a)P-Channel MOSFET (b) N-Channel MOSFET 107
Figure 6-8:Power stage 108
Figure 6-9: Schmitt trigger waveform 108
Figure 6-10: Schmitt trigger circuit 109
Figure 6-11: Driving P-channel MOSFETs (a) Charging phase (b) Discharging phase 110
Figure 6-12: Experimental set-up: (a) Measurement set-up (b) Prototype circuit board. 111
Figure 6-13: SCA-Ref waveforms for temperature setting 2: (a) Refrigerator voltage vs time, (b) Refrigerator current vs time, (c) Capacitor voltage vs time, (d)Refrigerator power vs time 113
Figure 6-14: SCA-Ref waveforms for thermistor setting 6: (a) Refrigerator voltage vs time, (b) Refrigerator current vs time, (c) Capacitor voltage vs time, (d)Refrigerator power vs time 116
Figure A-1: Control circuit 123
Figure A-2: 9V linear regulator datasheet 124
Figure A-3:9V linear regulator datasheet continued 125
Figure A-4: P-Channel MOSFET datasheet 126
Figure A-5:P-Channel MOSFET datasheet continued 127
Figure A-6:P-Channel MOSFET datasheet continued 128
Figure A-7:P-Channel MOSFET datasheet continued 129
Figure A-8: Diode datasheet 130
Figure A-9:Diode datasheet continued 131

List of Tables

Table 2-1: Key parameters of various ESS technologies 13
Table 2-2: key parameters of various ESS technologies (continued) 14
Table 3-1: Comparision of supercapacitor families [25] 56
Table 3-2: key parameters of supercapacitors and Li-ion battery [26] 64
Table 3-3: Features of supercapacitors [24] 67
Table 3-4: Performance comparison of voltage balancing techniques [40] 72
Table 5-1: BLDC motor vs Induction motor [54] 95
Table 6-1: Refrigerator specifications 100
Table 6-2: Switch states for the different modes 105
Table 6-3:Data collected for SCA-Ref at thermistor setting 2 113
Table 6-4: Efficiency of SCA-Ref at thermistor setting 2 114
Table 6-5: Data collected for SCA-Ref at thermistor setting 6 117
Table 6-6: Efficiency of SCA-Ref at thermistor setting 6 117

Chapter 1: Introduction

There is no argument that energy efficient appliances are making significant savings to mankind. While increasing efficiency provide valuable economic benefits it also leads to the reduction of greenhouse emissions that is invaluable for mitigating the greatest threat to our planet, global warming. The consumer devices around the world are powered by plugging into a power source providing alternating current (AC). Even so, most energy efficient appliances are internally operated by direct current (DC). Therefore, not much modifications to the internal modules are required for them to work on direct DC.

Of the world population 98% received more than 3kWh/m2 of solar irradiation per day [1]. Therefore, solar photovoltaic (PV) has greater potential to generate sufficient electricity for daily needs even in very remote location around the earth. Solar energy is truly renewable and sustainable to meet the global energy demand for more greener future. Solar energy provides a pure DC supply. Due to the possibility of direct DC operation of most household appliances the energy losses in the inherit conversion from DC-AC and back to AC-DC can be avoided straightaway. Therefore, DC home with DC loads is timely and ideal solution for future consumers. Research done by the United States on Energy savings from direct-DC residential buildings [2] shows that the direct DC application could yield significant energy saving. Figure 1-1 below shows clear evident that by eliminating AC-DC conversion stage itself, the end to end efficiency (EETE) can be improved by approximately 4%.

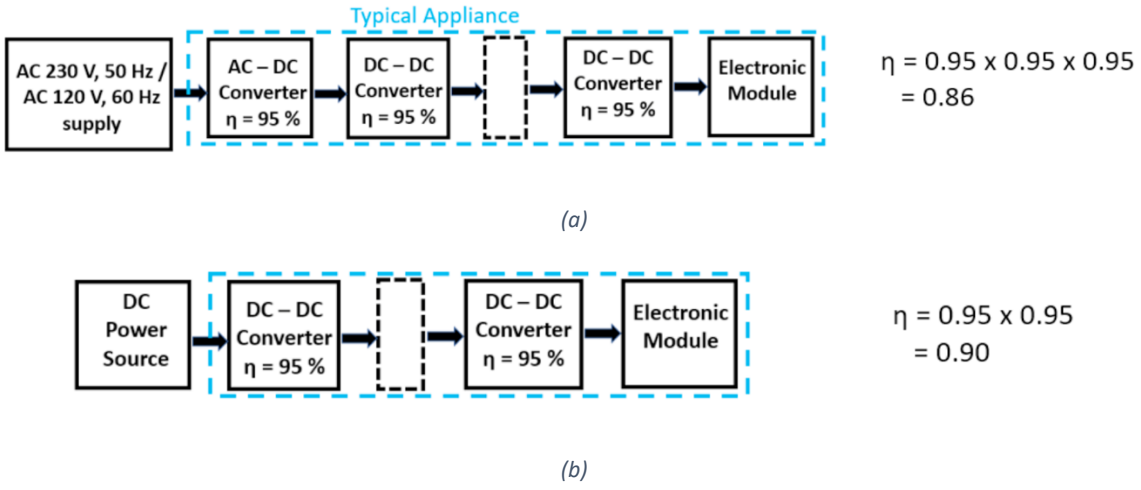

Figure 1-1: :End-to-End efficiency:(a) Typical appliance powered by AC. (b) Typical appliance powered by DC [6]

In 2009, Global energy consumption was about 16 TW (1Terra Watt = 10^12 watts) [1]. Refrigerators are expected to consume about 6% of global electricity generation [3](Negrao and Hermes 2011). Therefore, even fractional improvement resulted huge energy savings in global scale.

1.1 New approach to powering a DC refrigerator

Supercapacitor Assisted (SCA) technique is a unique and tactical new approach, where a loss circumventing method was applied to the fundamental resister- capacitor (the best-known R-C circuit) circuit loop. This is now known as Supercapacitor Assisted Loss Management (SCALoM) principle. This method is now theoretically and experimentally proven to improve the overall efficiency of the R-C loop. At present, there are quite a few successful applications namely supercapacitor assisted low dropout regulator (SCALDO), Supercapacitor assisted surge absorber (SCASA), Supercapacitor assisted temperature modification apparatus (SCATMA) and Supercapacitor assisted LED lighting (SCALED) under this belt.

The aim of this experiment is to extend the SCA principle further and to develop workable supercapacitor assisted DC refrigerator (SCARef) which is driven by renewable energy (Solar energy).

1.2 Project Development and objectives

For the protype power converter a 12/24 V DC refrigerator was obtained, which consisted of a three-phase BLDC motor in the compressor with a motor controller.

The main objectives of the project are,

- To access the viability of SCALoM concept to a DC powered refrigerator
- To develop an effective SCA-Ref converter, with ultra-low switching frequency, to power the refrigerator using a DC power source simulating a solar photovoltaic panel
- For the supercapacitor bank to provide an energy buffer during any power fluctuations due to solar irradiation
- To complete objectives within the time frame of a Master of Engineering programme

1.3 Thesis structure

The preceding chapters explore the technical developments that aided in the development of the supercapacitor assisted bicycle prototype.

Chapter 2	Covers the concepts of power distribution systems, energy storage and photovoltaic systems .
Chapter 3	Explores the fundamentals of capacitors and supercapacitors. This chapter details the important characteristics and applications of capacitor families
Chapter 4	Details the Supercapacitor-Assisted Loss Management (SCALoM) concept, where efficiency improvements is achieved through the fundamental R-C circuit.
Chapter 5	Explores the residential refrigerator technology, showcasing modern developments in the area.
Chapter 6	Combines the technical knowledge explored in the earlier chapters to develop the Supercapacitor-Assisted DC refrigerator concept.
Chapter 7	Reports on the objectives achieved and future areas of development.

Chapter 2: CONCEPTS OF POWER DISTRIBUTION SYSTEMS, ENERGY STORAGE AND PHOTOVOLTAIC FUNDAMENTALS

2.1 POWER SYSTEM ARCHITECTURE

2.1.1 CENTRALIZED GENERATION AND DISTRIBUTED GENERATION

Electricity has become a fundamental need of modern society. To satisfy this need electrical system must be able to provide a continuous supply with adequate power quality at any time and any place. Over the years, with increasing demand, hydroelectric and thermoelectric generation plants were developed and utilized. A power system based on having a central power plant with bulk generation capabilities located away from the end users was preferred. This was achieved by transmission and distribution via the AC grid. This model is known as centralized generation (CG). As depicted in Fig 2-1 large power plants are located at distant locations and connected to end consumers via national transmission and distribution networks.

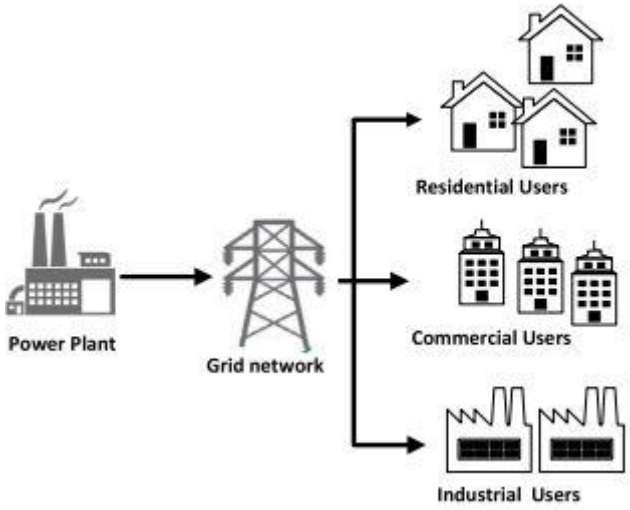

Figure 2-1:Schematic of general centralized power network [5,pp2]

The centralized system has provided an efficient and reliable power delivery network over the years. With the environmental impact and the depletion of fossil-based energy systems, the primary energy source for nearly more than half a century [5, pp3], the present electrical supply system may face significant shortfall to satisfy the energy demand in the future. Through the last two decades, a variety of new energy technologies, such as solar photovoltaics, wind, have been developed as a means to meet this demand. These technologies are posed to challenge the tradition centralized generation model to fully utilize their capabilities. With the cost competitiveness and increased power density of solar and wind based energy systems, a new concept known as distributed generation was developed. This model is defined by the generation and distribution of power at or near the consumers.

All life on earth primarily depend on energy received from the sun. Fossil fuels are understood to have originated from the energy of sun stored in various forms through multiple process over millions of years. The rate at which human civilization is consuming fossil fuels is faster than the rate at which they are regenerated naturally. Hence to fuel the growing demand it is urgently required to generate energy sustainably and direct solar based power generation is posed to be the best technology among the various renewable energy technologies. Figure 2-2 showcases the massive potential of solar energy and the composition of current energy production at a global scale.

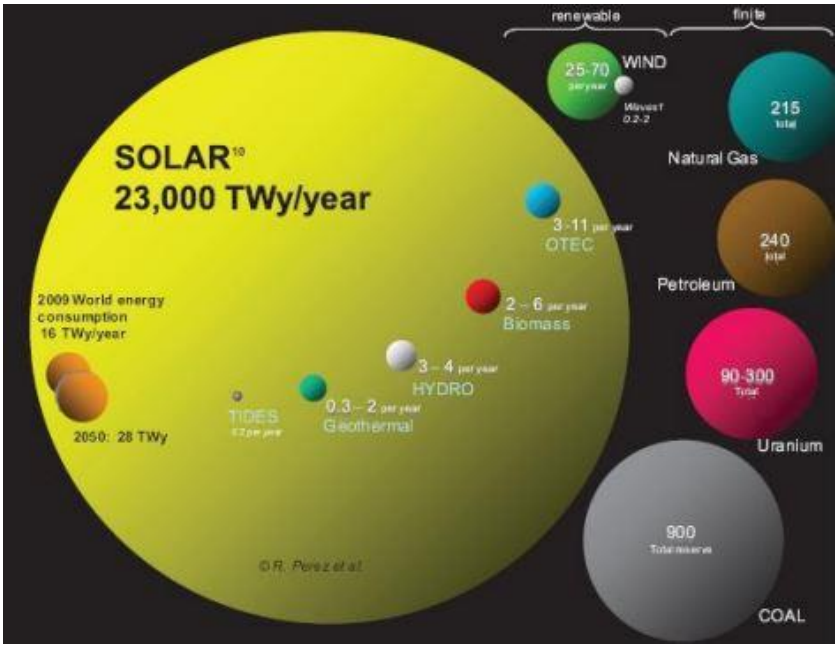

(a)

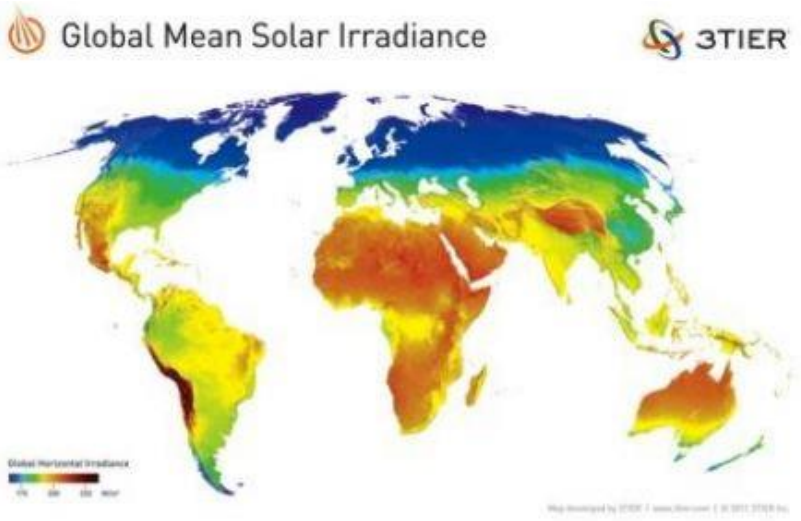

(b)

Figure 2-2 (a): Importance of solar energy for future energy, (b) the mean horizontal irradiation of the world [1]

2.1.2 DC MICROGRID AND DC HOME CONCEPT

2.1.2.1 DC microgrid

The concept of microgrid power systems is fundamentally not a very new idea. At the beginning of the 20th century, there was a famous debate (known as the “current war”) regarding Alternating Current (AC) and Direct Current (DC). Due to the invention of the transformer, facilitating the easy conversion of AC power for long distance transmission, and the induction motor AC power came out on top resulting in becoming the prominent form of generation and transmission of electricity. With new renewable power generation technologies, DC based power systems are due for a renaissance. The concept of local DC generation and consumption was a century old idea developed by Thomas Edison [1] . This means the generation and end-user must be at a minimum distance. Out of renewable electricity generation methods, solar PVs and wind power technologies generate pure DC power. However, due to the centralized power system, most of these are incorporated to the AC grid and therefore follows several conversion stages, as shown in Figure 2-3 (a). As a result, the overall end-to-end efficiency is reduced significantly.

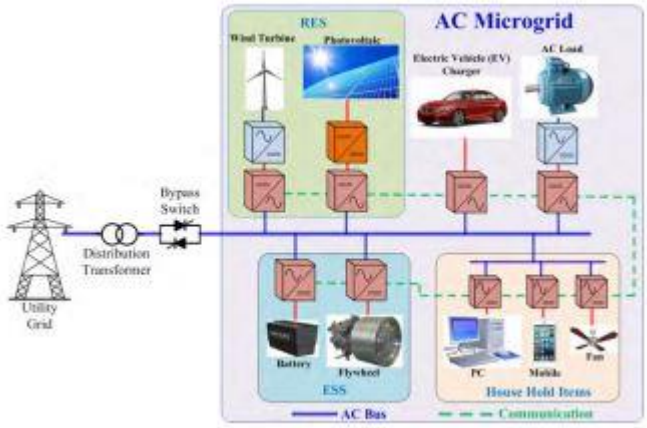

(a)

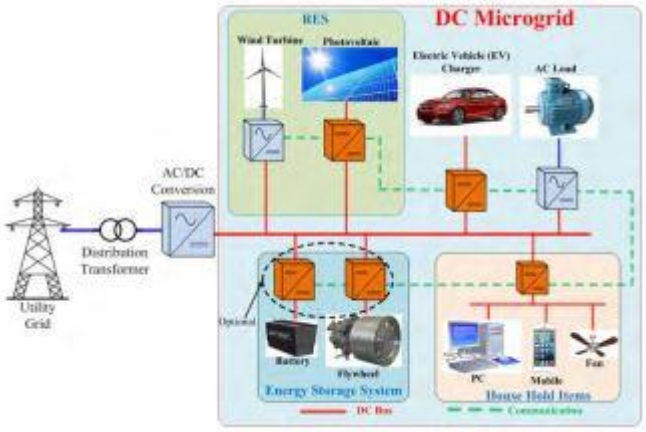

(b)

Figure 2-3:Typical block diagram of: (a) AC microgrid system, (b) DC microgrid system. [7]

Most modern household appliances and some industrial equipment are internally operated by DC power. If these appliances are directly operated by a low-voltage DC distribution system, a significant percentage of the conversion losses can be eliminated. A self-generated power network (for example: a self-sufficient rooftop PV system with or without energy storage) is basically, a smaller version of a larger power grid, known as a DC microgrid. This can be considered the rebirth of Edison's original concept of DC generation and distribution locally [7].

As shown in Figure 2-3 (b), in a DC microgrid system, there are a lesser number of conversion stages while supplying the loads with suitable voltage levels. Hence, power can be delivered with a comparatively higher end-to-end efficiency.

2.1.2.2 Benefits and obstacles of DC microgrid system [1,5(pp29-30),6]

Benefits of a DC microgrid systems are:

(1) PV or wind turbine produces clean and renewable DC power instead of power generated in the main AC grid, most likely using fossil fuel. Therefore, the DC microgrid system is more eco-friendly.

(2) Due to localized power generation, the energy losses in transmission can be minimized.

(3) The source generation is pure DC, therefore, AC-DC or DC-AC conversion is not required when end devices could be powered from a DC power rail . Hence, conversion losses can be eliminated.

(4) DC microgrids are more resilient than the AC infrastructure due to their ability to island. And being a smaller structure, it is more resilient to drastic weather or disaster.

(5) Reactive power management and frequency synchronization are not required.

(6) In the DC system, current flows through the entire conductor. While in AC, it flows along the outer edges. Therefore, there is no skin effect.

There are a few practical obstacles to the implementation of the DC microgrid [7].

(1) Unlike the AC distribution system, there is no zero crossing of the current. Therefore, the protection systems of the DC grid system need more research.

(2) Grounding and corrosion issues need to be addressed.

(3) New standards for products and voltage levels are required.

2.1.2.3 Direct DC home concept

Aiming for a sustainable future with renewed concern for the environment, many renewable energy technologies have been investigated during the last decade. Among them, solar PV generation gained much attention on a residential scale. This is due to the abundance of solar irradiation, which can be installed over rooftops, low maintenance of PV systems, long-term investment, decreasing cost of PV components, development of battery storage systems, state sponsorship, etc.

Currently, the most popular PV system incorporates in residential buildings feeds from both AC and DC generated from the rooftop via a DC-AC converter (inverter). Figure 2-4 shows a block diagram of such a system.

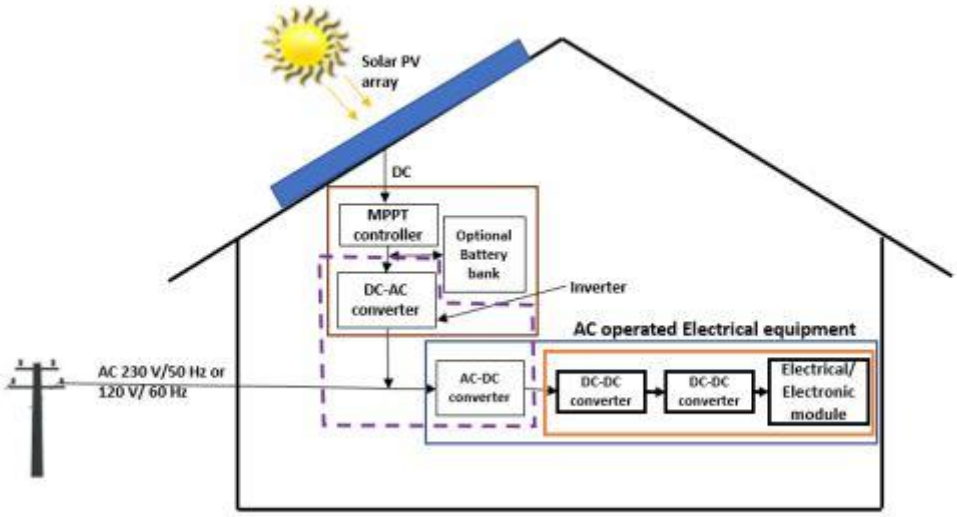

Figure 2-4: A block diagram of AC and DC source-fed traditional residential electrical system

The efficient use of electricity by redesigning the energy management system at the residential level can cause huge energy savings on a global scale. By considering the DC home concept, removal of the initial conversion stage in conventional AC input appliances, the first AC-DC conversion stage, as well as the components required for this can be eliminated. Figure 2-5 outlines a block diagram of the DC home concept.

Studies carried out in several states in the United States, show that there is significant gain in energy efficiency in direct DC residential building compared to conventional AC residential buildings [2].

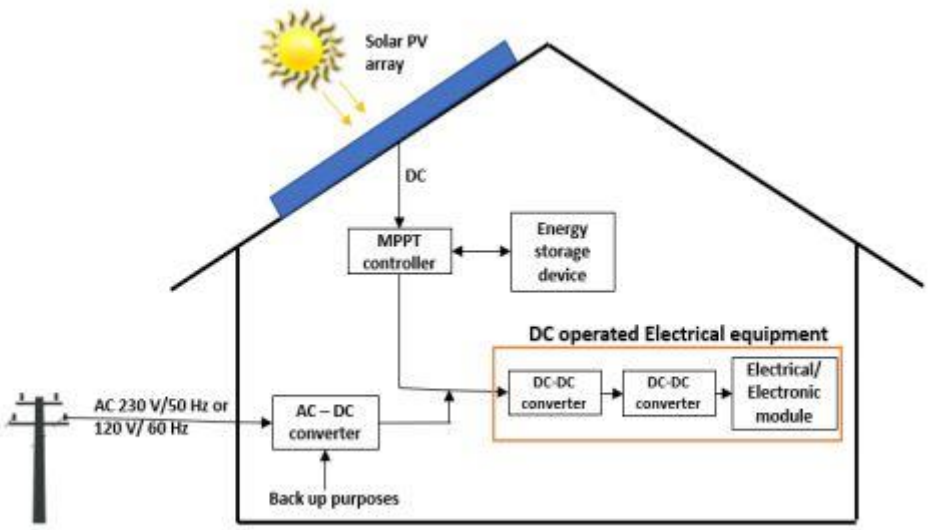

Figure 2-5: A block diagram representing a DC microgrid at home based on a solar PV system and alternate AC grid power for emergency DC supply.

2.1.2.4 Reducing the battery packs for environmental advantage

Renewable energy-based systems, such as solar and wind, are intermittent and cannot provide power reliably on their own. This makes energy storage systems an essential part of the renewable energy-based system. The dominant energy storage for solar PV systems are rechargeable batteries. While having a favourable energy density, they possess much lower cycle life compared to that of supercapacitors. Supercapacitors are also more environmentally friendly than batteries during manufacture. These benefits are the main reason behind the research into DC appliances in DC homes powered with solar energy through supercapacitor-assisted (SCA) converter replacing batteries [46] . Figure 2-6 shows the proposed SCA converter-based DC home block diagram. During insufficient irradiation such as cloudy days and night AC main supply can be fed through a converter to power the DC home.

A more detailed discussion on SCA techniques is provided in Chapter 4

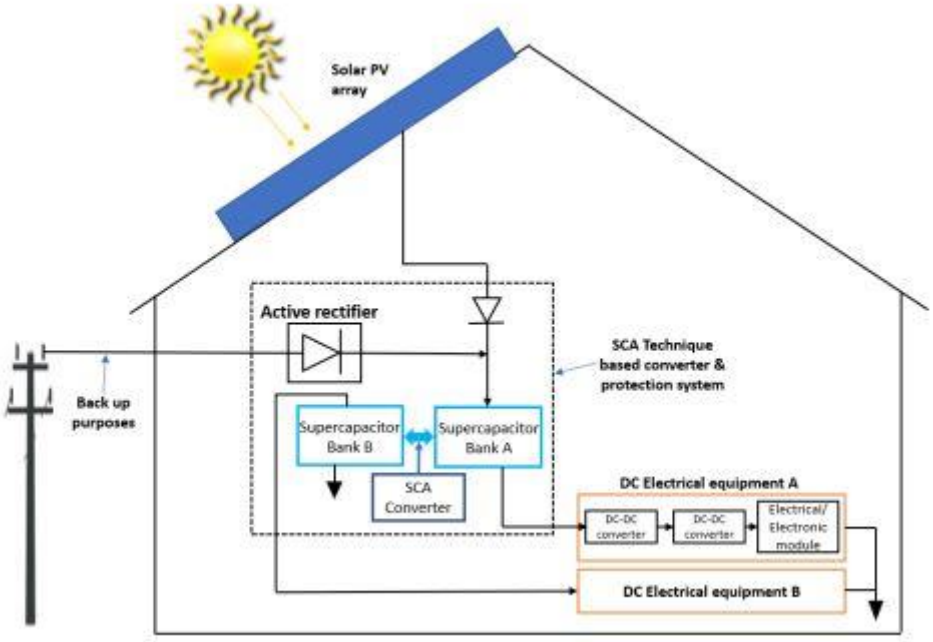

Figure 2-6: A residential power system with Non-traditional SCA power converter-based, battery-less DC residence with DC appliance.

2.2 ENERGY STORAGE TECHNOLOGIES FOR RENEWABLE ENERGY

Due to the intermittent nature of renewable energy, to maintain a real-time balance between generation and load demand and provide uninterrupted and stable power a reliable energy storage system (ESS) is required. Therefore, energy storage systems play an important role in future renewable energy-based power generation.

2.2.1 KEY PARAMETERS FOR ESS [4]

2.2.1.1 Energy Density and power density

Energy density and power density are defined as energy per unit volume and power per unit volume respectively. By definition, volume is a key factor. Therefore, the application of low energy density and power density technologies is not suited for when space is limited.

2.2.1.2 Specific Energy and specific power

Specific energy and specific power are the energy per unit weight and power per unit weight. This indicates the greater the specific energy, the smaller the weight and it is suitable for the application of light duty.

2.2.1.3 Rated energy capacity and Power Rating

Rated energy capacities and power ratings are the total energy available after a full charge. The criteria are the discharge time under the rated power used. ESS characteristics of short-term rapid discharge capability and long-term rated discharge capability are the key consideration for such applications.

2.2.1.4 Cycle efficiency

Cycle efficiency is defined as the percentage of power output and power input during a charge and discharge cycle. This is one of the key important parameters when considering large-scale and commercial applications.

2.2.1.5 Self-discharge rate

The self-discharge rate is the percentage of the energy dissipated in the rated capacity per defined period when the system is not utilized. The lower the self-discharge, the longer the duration and better storage capabilities.

2.2.1.6 Depth of discharge

Depth of discharge (DoD) is defined as a percentage of the available capacity and the rated capacity of the device during discharging. This is a key parameter in rechargeable battery technology.

2.2.1.7 Lifetime

Lifetime is generally defined as the numbers that can be cycled charged and discharged fully. Therefore, lower cycle life ESS increases the maintenance and replacement.

2.2.1.8 Capital cost

The capital cost is the cost per kilowatt or kWh. For ESS technologies that require frequent maintenance and replacement the operational cost should be taken into consideration as well.

Tables 2-1 and Table 2-2 show the comparison of those key parameters of various ESS technologies [4].

Table 2-1: Key parameters of various ESS technologies

Storage type	Rated power (W)	Rated energy capacity (MWh)	Energy density (Wh/L)	Power Density (W/L)	Lifetime (years)
PHS	100-5000	500-8000	1-2	1-1.5	30-60
CAES	5-300	600-3000	3-6	1-2	30-40
FES	0.01-20	0.75	20-80	1000-2000	15-20
Li-ion	0.1-100	0.024-10	200-500	1500-10,000	5-15
Lead-acid battery	0-40	0.001-40	50-90	10-400	5-15
NaS battery	0.15-10	0.4-240	150-300	140-180	15-20
NiCd battery	0-40	6.75	15-150	80-600	10-20
Zn-air battery	0-10	0.05-5	150-3000	100	0.17-30
ZEBRA	0-0.3	0.1-10	150-180	220-300	10-20
VRB	0.3-15	<60	25-35	<2	5-20
ZnBr battery	0.05-10	0.05-4	30-65	<25	5-20
PSB	0.1-15	0.06-12	20-30	<2	10-15
SCs	0.01-1	0.0005	10-30	>100,000	10-20
SMES	0.1-10	0.0008-0.0015	0.2-6	1000-4000	20-30
TES	0.1-300	-	80-500	-	5-20
HFC	0.001-50	-	500-3000	>500	5-20

Table 2-2: key parameters of various ESS technologies (continued)

Storage type	Efficiency (%)	Capital Cost ($/kW)	Capital Cost ($/kWh)	Self-discharge rate (%/day)	Discharge time	Respond time
PHS	70-85	2500-4600	5-430	0.01	Hour-day	Min
CAES	70	400-800	2-120	0.5	Hour-day	Sec-min
FES	90-95	250-330	1000-5000	100	Sec-min	Sec
Li-ion battery	90-97	1200-4000	600-3800	0.1-0.3	Sec-hour	<5ms
Lead-acid battery	75-85	300-600	100-400	<0.1	Sec-hour	<5ms
NaS battery	75-90	1000-3000	300-500	0.05	Sec-hour	<5ms
NiCd battery	60-80	500-1500	800-2400	0.2-0.6	Sec-hour	<5ms
Zn-air battery	60-65	700-1900	10-150	0.005-0.01	Sec-1 day	<5ms
ZEBRA	75-85	150-300	100-200	5	Sec-hour	<5ms
VRB	75-85	600-1500	150-600	0.15	Sec-10 hours	<5ms
ZnBr battery	65-80	400-2500	340-1350	Almost 0	Sec-10 hours	<5ms

PSB	60-75	700-2500	150-1000	Almost 0	Sec-10 hours	20ms
SCs	90-98	100-300	300-2000	5-10	Sec-min	<5ms
SMES	95-97	200-300	1000-10,000	10-15	Sec-30 min	5ms
TES	30-60	100-400	30-60	0.05-1	Hour	Not for rapid
HFC	30-50	1500-3000	2-15	Almost 0	Min-hour	<5ms

2.2.2 ENERGY STORAGE SYSTEM CLASSIFICATIONS

Further to the above key parameters, ESSs can be subdivided into three categories based on the technical requirements [4].

2.2.2.1 Short-term applications

In this category, ESS requires a fast response time. Applications such as frequency regulation, voltage control over fluctuations, emergency backup power to the critical user and maintaining the power quality.

2.2.2.2 Medium-term applications

This category requires fast response and considerable capacity to discharge over a few hours. Such applications are operating reserve, black-start, and uninterruptable power supply.

2.2.2.3 long term applications

In this category, require the discharge duration of the stored energy for several days. Applications such as integration of renewable energy, time shifting, seasonal energy storage and T&D upgrade deferral (this refers to delaying the upgrade of transmission and distribution lines).

2.2.3 ENERGY STORAGE SYSTEMS (ESS)

We require some form of energy storage system to keep the expected reliability level of electrical and electronic systems when utilizing power systems with fluctuation in nature. Few options are summarised here.

2.2.3.1 Flywheel energy system (FES) [4,5 pp51]

FES stores energy in the form of kinetic energy. The inertia of the rotating mass and angular velocity quantify the stored energy. The kinetic energy stored in the rotor Ek is given by,

$$E_k = \frac{1}{2} J\omega \tag{2.1}$$

J – moment of inertia ω – angular velocity

FES consists of a large cylindrical flywheel and magnetic suspension bearing. Additionally, it consists of a reversible generator, vacuum chamber, power converter and low-voltage housing. A typical FES system is shown in Figure 2-7.

In FES energy density can be maximized by enhancing the strength of the flywheel material and energy loss can be minimized by placing the Flywheel in a vacuum environment with non-contact magnetic bearing. There are two basic categories of FES based on rotational speed. Generally, speeds of 10^5 rpm are high speed and specific energy of 100Wh/kg. The low speed once is 6 x 10^3 rpm and the energy density of 6 Wh/kg.

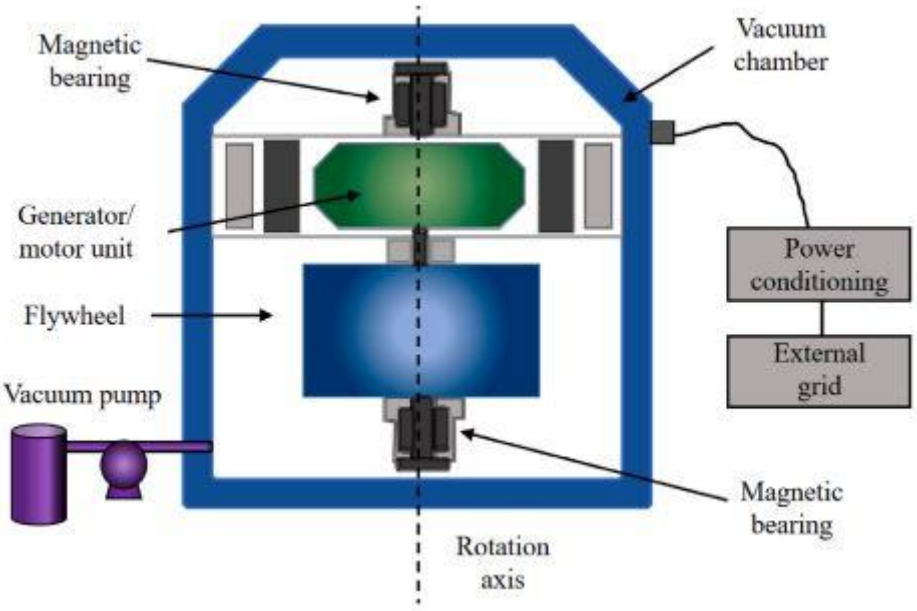

Figure 2-7: A block diagram of the flywheel energy storage system [4]

2.2.3.2 Compressed air energy system (CAES)

This ESS stores energy in the form of compressed air. The compressed air is stored during the period of lower grid demand and when required the stored energy is converted back to electricity. CAES consists of an air compressor, generator, and high-pressure turbine. A schematic of a typical CAES is shown in Figure 2-8. In comparison to commercial ESSs, CAES is second only to pump hydro system. Long energy storage time, long asset time, low environmental impact, short response time, high efficiency and flexible capacity range are some advantages [4].

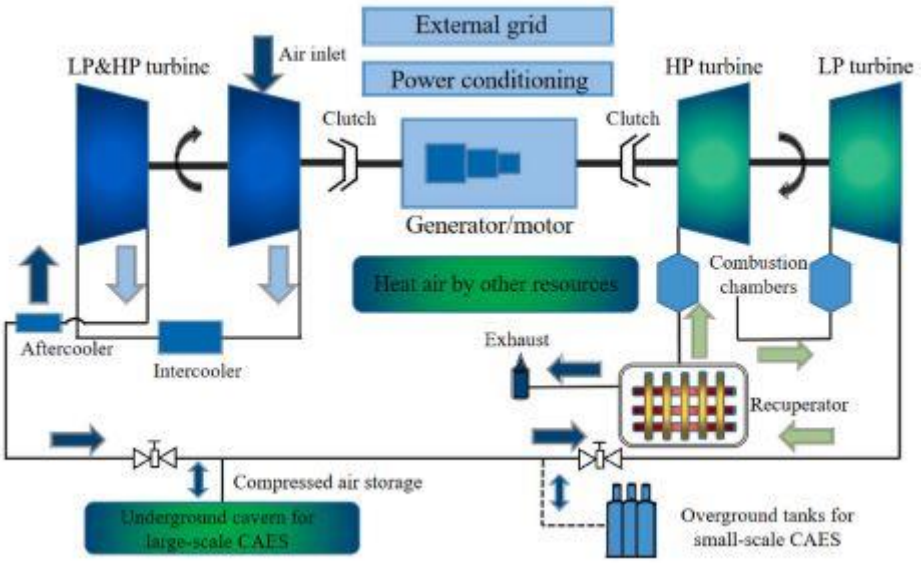

Figure 2-8: A schematic of a typical CAES {4]

2.2.3.3 Superconductive magnetic energy storage (SMES)

The energy stored in the SMES system is accomplished by a superconductive coil kept in an extremely low-temperature environment (liquid Nitrogen or liquid Helium container). The energy is stored in a DC magnetic field generated by a direct current through the coil. Due to the properties of extreme conductivity and no resistive losses the DC fed inductor can be used as fast-acting ESD. The specific energy stored (E) in the system can be determined,

$$E = \frac{1}{2}LI^2 \tag{2.2}$$

L – self-inductance of the coil I – current in the coil

The advantages of SMES are fast response, high power density, high efficiency, unlimited charge/ discharge, and long lifecycle [4]. Figure 2-9 shows a schematic of a SMES system.

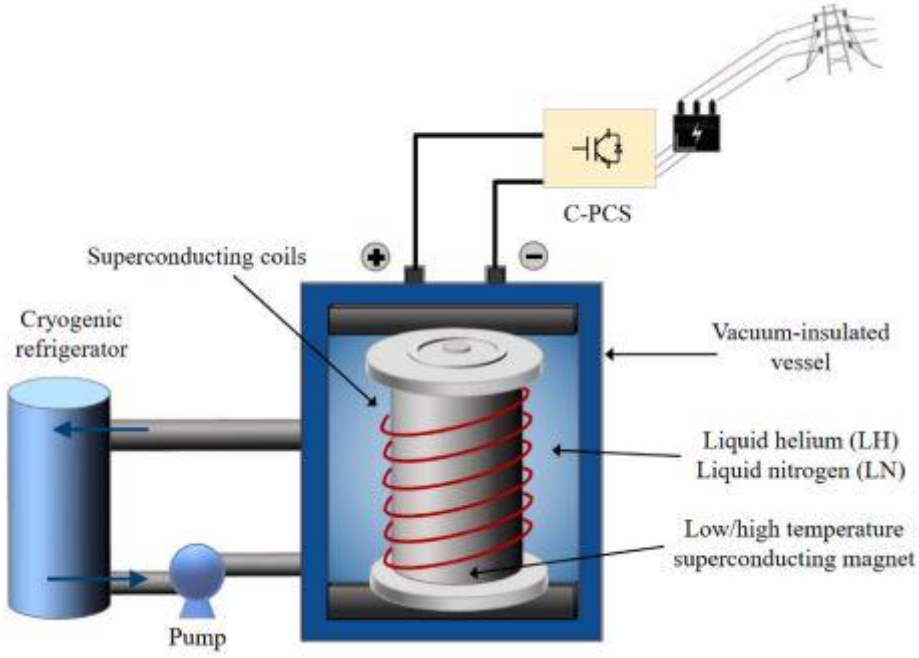

Figure 2-9: A schematic of superconducting magnetic energy storage { 4]

2.2.3.4 Fuel cells (FC)

FC converts the chemical energy in Hydrogen-rich fuel and air into electrical energy [4]. A fuel cell is very close to a galvanic cell. The structure of a typical fuel cell is shown in Figure 2-10. The fuel and oxidizing agent are supplied separately by an external process. In a FC, the whole system is confined to itself. The FC generally, consists of electrodes, electrolytic cell unit and energy conversion unit. The fuel is supplied to the anode, where electrons are released from the fuel under the catalyst. The electron under the potential difference between the anode and cathode flow through the external

circuit to the cathode. FC technology is a fast developing and mature technology. There are many types of FC with different power capabilities available today. The most commonly used FC is Hydrogen based FC (HFC) [4].

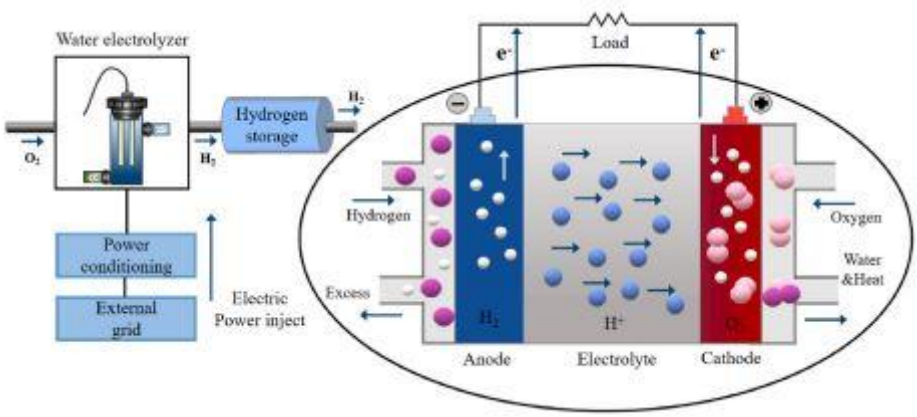

Figure 2-10: A structure of a typical hydrogen fuel cell [4]

2.2.3.5 Electrochemical Systems (EC)

EC batteries are the most widely used ESS technology. Battery chemistries come in two different forms. Namely, primary batteries (disposable batteries) and secondary batteries (rechargeable batteries). Mature rechargeable battery chemistries start from commonly used lead-acid to modern Lithium-ion batteries. There is a huge demand for the development of batteries with higher energy density, superior cycle life, being environmentally friendly and safe. In rechargeable battery chemistries, the anode provides electrons, and the cathode receives electrons. The electrolyte is responsible for transporting electrons between them, and the separator guarantees the insulating relationship between electrodes. Figure 2-11 shows the structure of a rechargeable battery (Lithium-ion battery) [4].

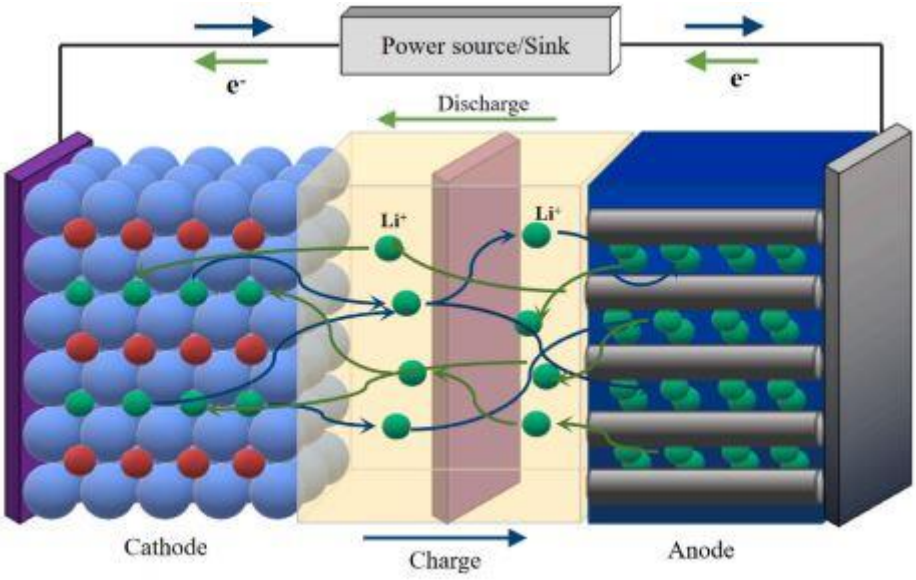

Figure 2-11: A schematic diagram of the Li-ion battery [4]

2.2.3.6 Supercapacitors (SCs)

The capacitor is one of the most critical passive circuit elements used in electronic circuits. Capacitors are considered as a short-term energy storage devices. The common capacitor seen in the electronic circuit does not have capacitance beyond several hundred thousand microfarads. But they have voltage ratings from a few volts to even several kilovolts. When considering energy storage requirements equivalent to batteries, there is a newer family of capacitors called electrochemical capacitors that can fit in. These electrochemical capacitors are now commonly known as supercapacitors (SC), Ultracapacitors (UC), or electrochemical double-layer capacitors (EDLC).

These devices have much higher capacitance and can store much larger amounts of energy. Due to these superior characteristics, SC is now used in many areas. At present, commercially available SC devices are relatively low-voltage cells with less than 5VDC. To achieve higher voltage rating SC need to connected in series to make modules. Figure 2-12 shows a schematic of an SC system. More detail about SC and its characteristics are included in chapter 3.

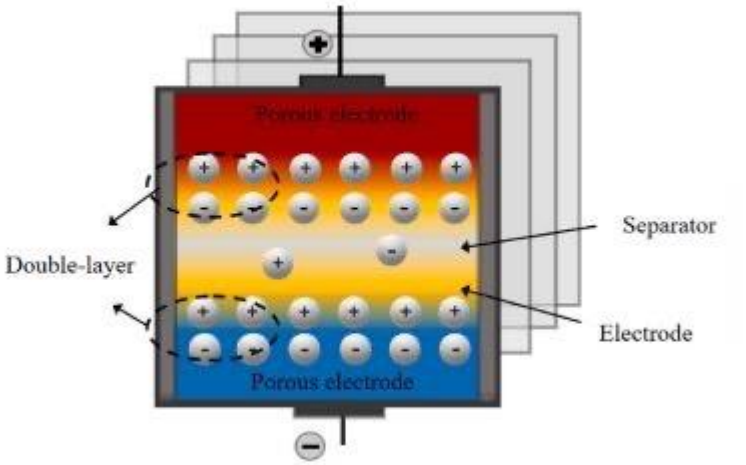

Figure 2-12: A schematic of an SC's system [4]

2.2.4 RAGONE PLOT

When analysing ESS in different sizes, their specifications are largely varied. To compare the performance of ESS, key parameters such as energy density and power density are used. American metallurgist David V Ragone developed a graphical presentation to compare energy storage and power delivery capabilities. This graphical presentation is called the "Ragone plot "and is shown in Figure 2-13. The Ragone plot interprets specific energy density (Wh/kg) Vs specific density (W/kg) or energy density (Wh/l) Vs power density (W/l). Both axis are presented in logarithmic scale and the sloping line indicates the relative time taken to charge or discharge of the devices. The Ragone plot illustrates that longer runtime applications need devices with higher energy densities such as batteries. On the other hand, capacitors, have higher power densities and are most suited for high-power applications but shorter time applications. The Ragone plot is useful for showcasing the characteristics of new and existing energy storage devices [1].

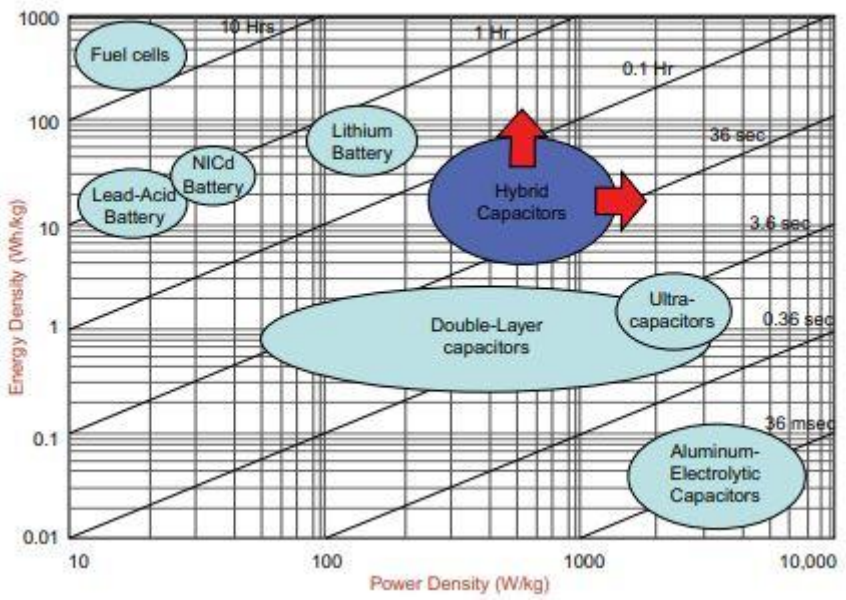

Figure 2-13: Ragone plot comparing different energy storage systems [5, pp 186]

2.3 PHOTOVOLTAIC ENERGY FOR THE FUTURE

2.3.1 ELECTRICITY GENERATION FROM THE SUN

Providing sustainable and more environmentally friendly energy solutions have received greater attention for future energy demand. Hydro, biomass and geothermal are renewable, but not totally sustainable [1]. Solar and wind energy sources are the only available sustainable energy sources.

The Sun is about 4.6 billion years old. It is estimated that the Hydrogen fuel in the sun will survive another 5 billion years [8]. This will not run out anytime soon. Solar energy is a clean energy source and essentially unlimited. Therefore, to satisfy the future energy demand solar energy become the best solution and it is predicted that by 2050, a major portion of electricity generation will be from solar energy [8].

In the last three decades, solar energy became a very popular energy source for generating electricity. Solar power generation is achieved by mainly following two methods.

2.3.1.1 Solar photo voltaic (PV)

In this method, solar energy converts directly into electricity by using electronic devices. This is the most popular fast-growing technology around the world. Figure 2-14 shows a typical solar photovoltaic system. In the past decade, the declining manufacturing cost, research directions, favorable energy policies, and manufacturing innovations influenced solar energy to become more cost competitive and will improve further. According to an International Renewable Energy Agency (IRENA) report, the capacity of solar photovoltaics reached 710 GW by the end of 2020 globally. Alongside, the price of a solar module dropped by 93% between 2010 to 2020 [9].

According to the International Energy Agency (IEA) forecast, 5% of global electricity consumption will be generated by solar photovoltaics by 2030 and is likely to increase by 4600 GW by 2050 [8].

When compared to other renewable energy sources, solar energy is more uniformly distributed and 98% of the world population receives a solar irradiation of 3 kWh/m^2 [1]. Due to the intrinsic cost advantage of photovoltaics over other solar technologies available, photovoltaics became the primary interest in solar energy generation.

Figure 2-14: Solar power field [9]

2.3.1.2 Concentrated solar power (CSP)

In this method, steam is created by heating a fluid by concentrating solar rays with the help of mirrors. This steam is used to drive turbines which generate electricity. Figure 2-15 shows a solar thermal system. By the end of 2020, CSP generation was about 7 GW in globally [9]. CSP is classified into two groups based on the principle of solar collector concentration, namely linear concentrators and point concentrators. Linear concentrators used parabolic trough collectors and solar towers, or power towers are used as point concentrators.

When comparing PV and CSP technologies, the latter can store heat to be used during night-time power generation. The CSP also shows a significant role in future renewable energy technologies.

(a)

(b)

Figure 2-15: Concentrated Solar power:(a)Parabolic trough solar thermal system, (b) A solar power tower system [11, pp366]

2.3.2 PHOTOVOLTAIC FUNDAMENTALS

2.3.2.1 History of Photovoltaic

In 1839, the French physicist Alexander Becquerel discovered the photovoltaic effect. In 1884, Charles Fritts made the first solar cell using the gold-selenium junction. But it had quite a low efficiency at around 1%. In 1954, Calvin Southern and Gerald Pearson of Bell Laboratories produced the first practical photovoltaic cell that convert light energy into electricity by the photovoltaic effect with a recorded efficiency of about 6% [8].

The first silicon solar cell was developed to power space satellites in early 1960 [8]. During the 1970s, after the first oil crisis, photovoltaic generation received greater attention as an alternative energy generation technique for terrestrial use. The National Renewable Energy Laboratory (NREL) based in the state of Colorado, USA, developed a PV cell made on indium-gallium-phosphide/gallium-arsenide tandem junction exceeding 30% efficiency in 1994, [8]. In 2016

Yoshikawa et.al from Kaneka Cooperation built an interdigitated back contact (IBC) crystalline silicon (c-Si) solar cell with a conversion efficiency of 26.33% [8].

Each of these innovations contributed vastly to the development and growth of photovoltaic technology around the world.

2.3.2.2 General Theory of photovoltaic cell [12]

A PV cell is an electrical device, made out of semiconductor material. The most common semiconductor material used for solar cells is silicon. The electron energy levels in the atomic structure of semiconductors can convert light energy into electricity. Now let us look at the general theory of photovoltaic generation.

There are two electron energy levels in atomic structure. The valance band: the highest electron energy level (more energy is required to remove an electron from this level). The conduction band: the lowest electron energy level (less energy is required to remove electrons from this level). The energy difference between the top of the valance band and the bottom of the conduction band is called the “band gap” (Eg).

As shown in Figure 2-16, in conductor materials, the valance band is not completely filled and as such these electrons are free to move through the metallic structure resulting in no band gap. In contrast, in insulator materials, the band gap is extremely large and inhibits the electron moving from the valance band to the conduction band. In semiconductor materials, the band gap is relatively small and a small amount of energy is sufficient to move some electrons to the conduction band.

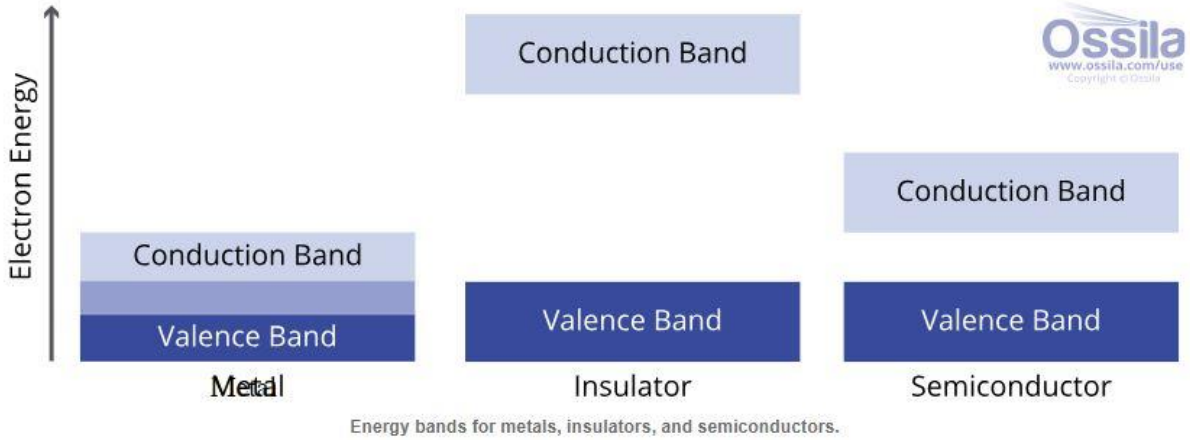

Figure 2-16: Electron energy bands of metals, insulators, and semiconductors [12]

When solar energy (photon energy) is incident on semiconductor material, the atom becomes excited thus releasing electrons to the conduction band by creating a “hole” (equivalent positive charge). These excited electron and hole pair are bounded by coulomb force. This state is known as “exciton”. In order to collect these charge carriers, a mechanism is needed to break the exciton. This is known as “dissociation”. This action can be done by a built-in electric field by creating a junction with doping (adding) high (n-type) and low (p-type) electron density semiconductor materials (p-n junction). Due to that, it is now creating a depletion region as shown in Figure 2-17, where there are no free electrons or holes established in an electric field within the depletion zone. This electric field is directed from the n-type to the p-type as indicated in Figure 2-17.

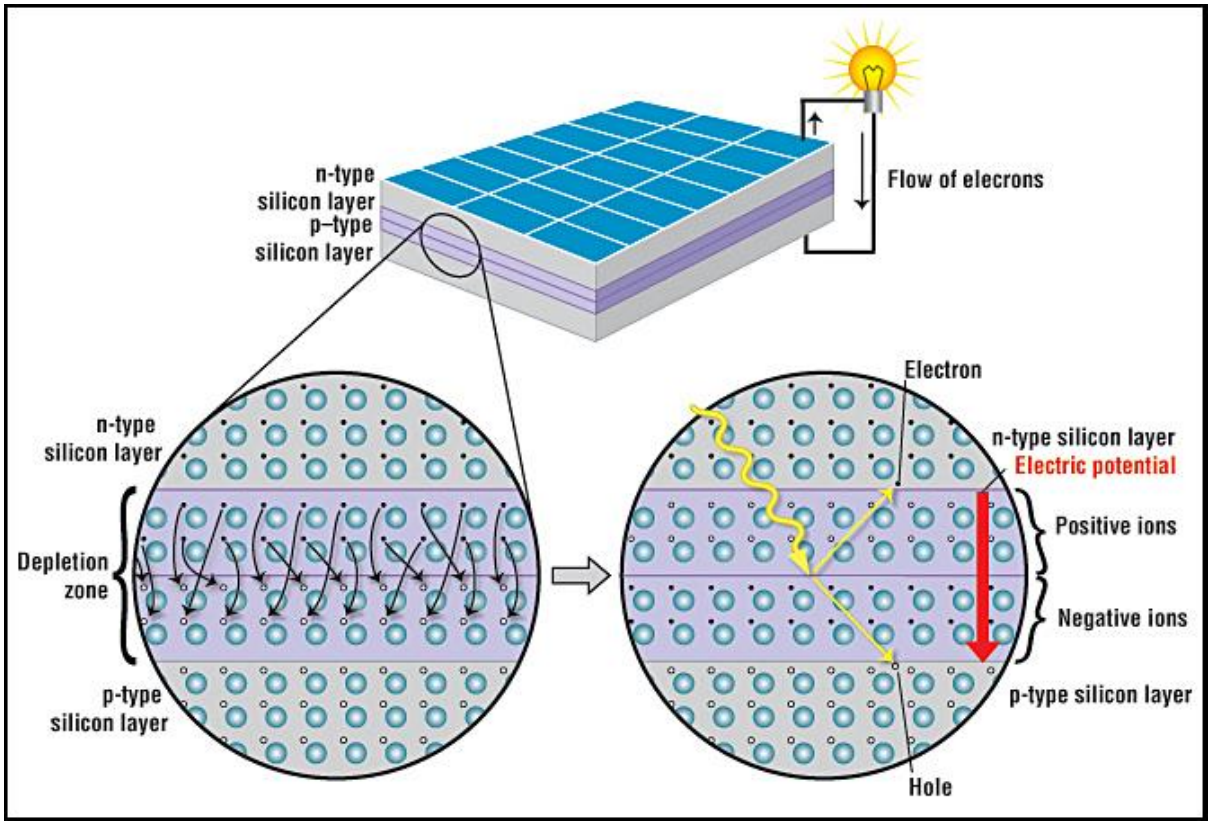

Figure 2-17: A structure of a solar cell, A closeup view of the depletion zone around the p-n junction and built in electric field. [13]

When the p-n junction (solar cell) is exposed to solar irradiation (sunlight), due to the built electric field of the p-n junction, electrons move to the n-type side and holes to the p-type side terminal, thus creating an electric current when this terminal connected externally.

2.3.2.3 Photovoltaic cell model

To understand the electrical characteristics of a solar cell, the electrically equivalent circuit model is useful. The one-diode model is the most practical model widely used to analyse the performance of PV cells.

2.3.2.4 Ideal solar cell model

The ideal solar cell can be modelled by a current source and a diode as shown in Figure 2-18. The ideal solar cell does not consist of resistance. Therefore, in this model, there are no power losses. The characteristics equation of solar cell is given by,

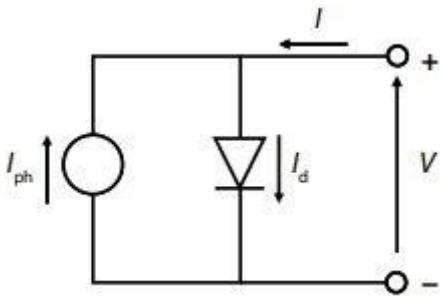

Figure 2-18: The equivalent circuit of an ideal solar cell [11, pp109]

$$I = I_{Ph} - I_O\left(e^{\frac{qV}{akT}} - 1\right) \tag{2.3}$$

$$V_T = \frac{kT}{q} \tag{2.4}$$

Combining equations (2.3) and (2.4), load current (I) can be calculated as shown in equation (2.5)

$$I = I_{Ph} - I_O\left(e^{\frac{V}{aV_T}} - 1\right) \tag{2.5}$$

V_T- is called thermal voltage.

I_{Ph}- is the photocurrent generated at given irradiation and temperature.

I_O- Dark current or saturation current of the diode. This is represented by the electron-hole recombination that exists in the solar cell.

2.3.2.5 Practical solar cell model

All solar cells are not ideal. There are some losses due to parasitic resistive components. The practical solar cell model shown in Figure 2-19 consists of a series resistance and parallel resistance. This is the basic model of solar cells generally known as one diode model. A series resistance (R_s) represents the combined resistance due to the metal grid and the p-n junction. The parallel resistance or shunt resistance (R_p) represents the resistance due to the leakage current through the P-N junction.

The crystal defects, pinholes, and impurity precipitation cause the leakage current. Typically, this resistance should be large as possible otherwise it will reduce the power to the load.

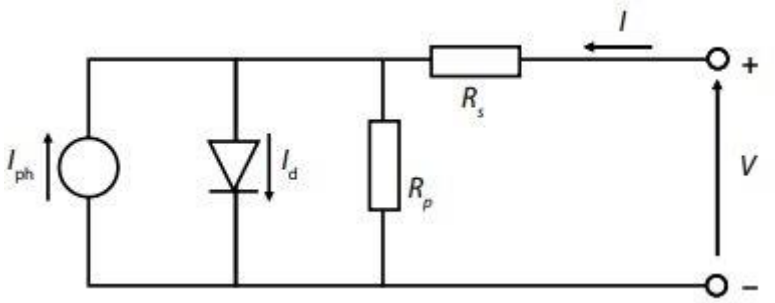

Figure 2-19: The equivalent circuit of solar cell represented with a series resistance, R_s and parallel resistance, R_P [10, pp109]

The slope of the curve from I_{sc} to V_{max} in the characteristic I-V curve, Figure 2-20 implies the shunt resistance, and the slope of the curve from V_{max} to V_{oc} implies the series resistance at the terminal [14].

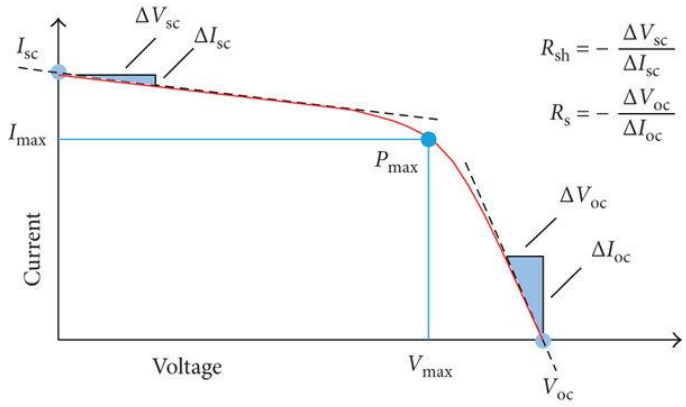

Figure 2-20: Identifying the shunt resistance and series resistance [14]

2.3.3 SOLAR CELL PARAMETERS

2.3.3.1 I-V curve

The I-V characteristics curve of a solar cell is a graphical presentation of the current and voltage variation for a given irradiation and temperature. Increasing irradiation leads to an increased current and a slight increase in voltage. It is the superposition of a current source and diode characteristics.

From the I-V characteristics curve, the important parameters of solar cells can be determined.

Figure 2-21 shows the I-V characteristics curve and important parameters of solar cells.

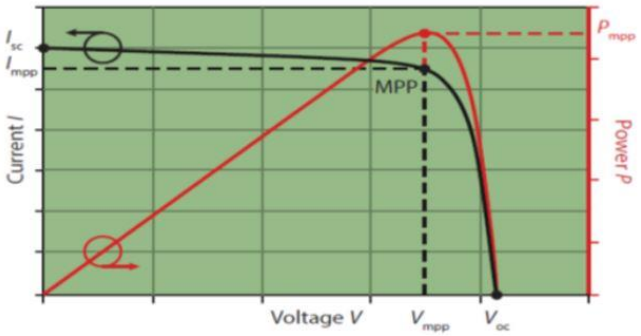

Figure 2-21: I-V curve of PV panel [11,pp265]

2.3.3.2 Short circuit current (Isc)

This is the maximum current that a solar cell can generate without damaging its structure. This current is due to the generation and collection of photo-generated carriers. The short circuit current depends on the following factors [11, pp101].

(1) the area of the solar cell

(2) light intensity (the number of photons of the incident light)

(3) the spectrum of light

(4) absorption and reflection properties of the cell

(5) the probability of minority carrier collection

$$J_{SC} = \frac{I_{SC}}{A} \tag{2.6}$$

Where I_{sc}- short circuit current, J_{sc}- maximum current density, A- area of the solar cell

2.3.3.3 Open circuit voltage (V_{oc})

This is the maximum voltage that solar cells can deliver when the current is at zero. This corresponds to the amount of forward bias on the cell due to the bias of the cell junction with the light-generated current. V_{oc} is a function of the band gap, and the open circuit voltage increases as the band gap increases.

$$V_{OC} = \frac{nKT}{q} ln\left(\frac{I_L}{I_O} - 1\right) \tag{2.7}$$

This voltage depends on temperature. Typical value close to 0.5 - 0.6 volts.

I_0 – reverse saturation current, K – Boltzmann constant n – diode ideality factor

q – elementary charge T – absolute temperature I_L- photo generated current

2.3.3.4 Fill factor (FF)

The fill factor is defined as the ratio of maximum power from a solar cell and the product of open circuit voltage and short circuit current. This parameter indicates the quality of the cell. The typical commercially available solar cell fill factor is in the range of 0.83 to 0.85, where higher is better.

$$FF = \frac{V_{MP} I_{MP}}{V_{OC} I_{SC}}$$

$$FF = \frac{P_{MP}}{V_{OC} I_{SC}} \tag{2.8}$$

2.3.3.5 Conversion efficiency (%)

The conversion efficiency is defined as the ratio between the maximum power generated by the cell to the incident power of the cell. The standard for this measurement is irradiation of 1000 W/m^2 for AM 1.5 spectrum and the temperature at 25 C. This parameter is important when a performance comparison of different cells is needed [11, pp104].

The typical conversion efficiency of crystalline silicon solar cells is in the range of 17 – 18%.

$$\eta = \frac{P_{max}}{P_{in}} \tag{2.9}$$

2.3.3.6 Maximum power point (MPP)

This is where the power delivered by the cell is at maximum value. At a certain current and voltage value the power output of a solar cell becomes maximum. This point is the ideal current-voltage combination for extracting maximum power and is known as maximum power point (MPP).

The MPP is not a constant point. It varies with irradiation conditions and ambient temperature. Hence, to obtain maximum power output, the shift of MPP due to changes in ambient conditions has to be tracked. This process is called maximum power point tracking and it is an integral part of modern PV installations.

2.3.4 SOLAR MODULE (SOLAR PANEL)

The solar cell is the building block of a PV system. A single solar cell is very small. Typically able to produce about one or two Watts of power. Solar cells are connected like a chain to form a larger unit

for increased power output. Such an assembly is framed in an aluminium structure making a PV module. Figure 2-22 shows a typical solar cell and commercially available solar module.

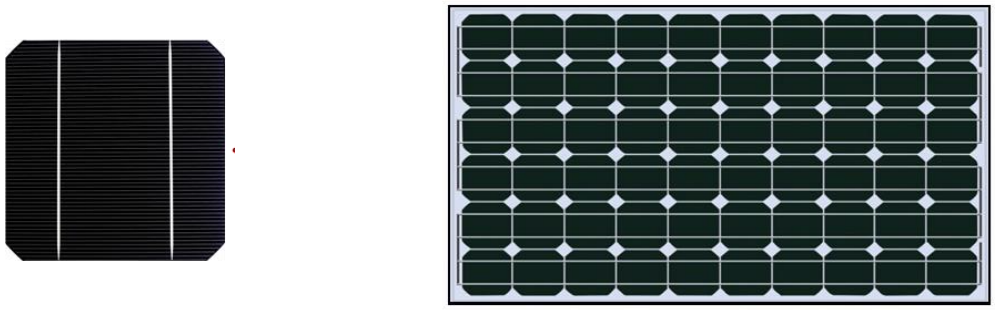

(a) *(b)*

Figure 2-22: Solar panel construction: (a) Solar cell, (b) Solar module [15]

2.3.4.1 Solar Module Strings

There are three ways of solar modules are connected in general.

(1) Series connections

(2) Parallel connections

(3) Series – parallel connections

2.3.4.2 Solar modules in series

PV modules consist of positive and negative terminals. A solar PV string is made by connecting the solar module's positive terminal to the negative terminal. By wiring solar modules in series, the output voltage can be increased. The total voltage of each panel is summed together, but the electric current is limited to the maximum current capacity of the least powerful panel. Wiring in series, simplifies the installation and lower the cost of linking component. But a significant drawback is if one module generation drops(Ex. due to shade) the overall current of the string reduces due to underperforming module. Regulatory limitation have to be observed when making series PV strings for residential installation (Example – in the US, the maximum voltage of PV string is 600 volts – article 690 section 7 of the national electrical code NEC 690.7)

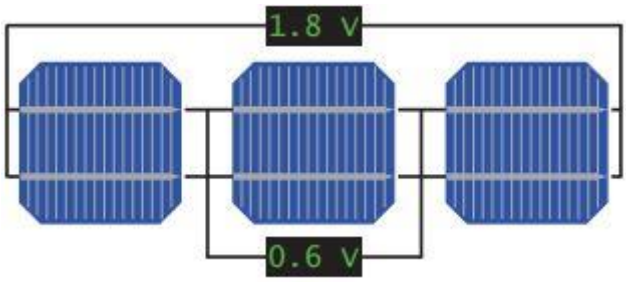

Figure 2-23: Schematic of three solar cells connected in series [11, pp253]

2.3.4.3 Modules in Parallel

In a parallel connection, the positive and negative terminals of each solar module are connected. In this type of connection, the output voltage stays the same and electrical currents are summed up together. Figure 2-23 shows a parallel connected PV string. Parallel connections also have some installation limitations such as conductor size and over current devices. (Ex. NEC regulation 680.8(A)(1) and NEC 690.8(A)(2) applicable in US).

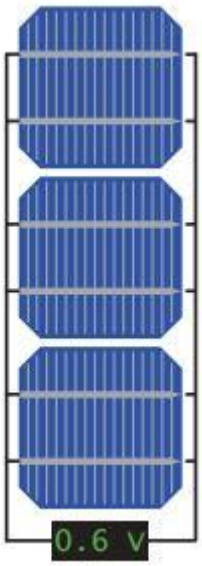

Figure 2-24: Schematic of three solar cells connected in parallel [11, pp253]

2.3.4.4 Series-Parallel connection

In this type of system, PV modules are connected in series as before and these strings are connected in parallel. To obtain optimum performance, all modules need to be of the same model.

2.3.5 SOLAR IRRADIATION FOR PV SYSTEM DESIGN [16, pp27]

Though PV energy is sustainable and clean energy, the solar irradiation variability needs to be considered when designing a PV system. The evaluation of the following factors is very important for designing a practical and successful PV system.

2.3.5.1 *Daily and hourly variations*

Daily variation of irradiation behaviour is very important for designing a self-sufficient system. In general, the output power of the PV cells and the system is not linearly proportional to solar irradiation. This means for example, for a given period one hour irradiation of 2kW/m^2 and one hour zero irradiation would not generate the same electrical energy for two hours of 1 kW/m^2 irradiation. Due to this uncertainty, when designing storage capacity for a self-sufficient system, a statistical data-based technique is more practical.

2.3.5.2 *Monthly variations*

The effect of seasonal changes and weather, in other words cloudiness resulted in the monthly variation. Data based on expected monthly electricity demand and average monthly sunshine must be taken into consideration for a PV system design.

2.3.5.3 *Yearly variations*

The average solar irradiation varies from the mean yearly values by less than 10%. This data is generally used to evaluate the average cost and estimate the energy payback time.

2.3.6 PV SYSTEM CONFIGURATION

There are three different types of PV systems based on its system configuration.

(1) Stand-alone configuration

(2) Grid-connected configuration

(3) Hybrid configuration

2.3.6.1 *Stand-alone configuration*

This configuration relies only on solar power. It consists of only the PV modules and the load or they can include energy storage (Eg. Batteries). Energy storage must be of large enough capacity to store required energy for the night and solar fluctuations. Figure 2-25 shows a schematic of the stand-alone configuration of the PV system.

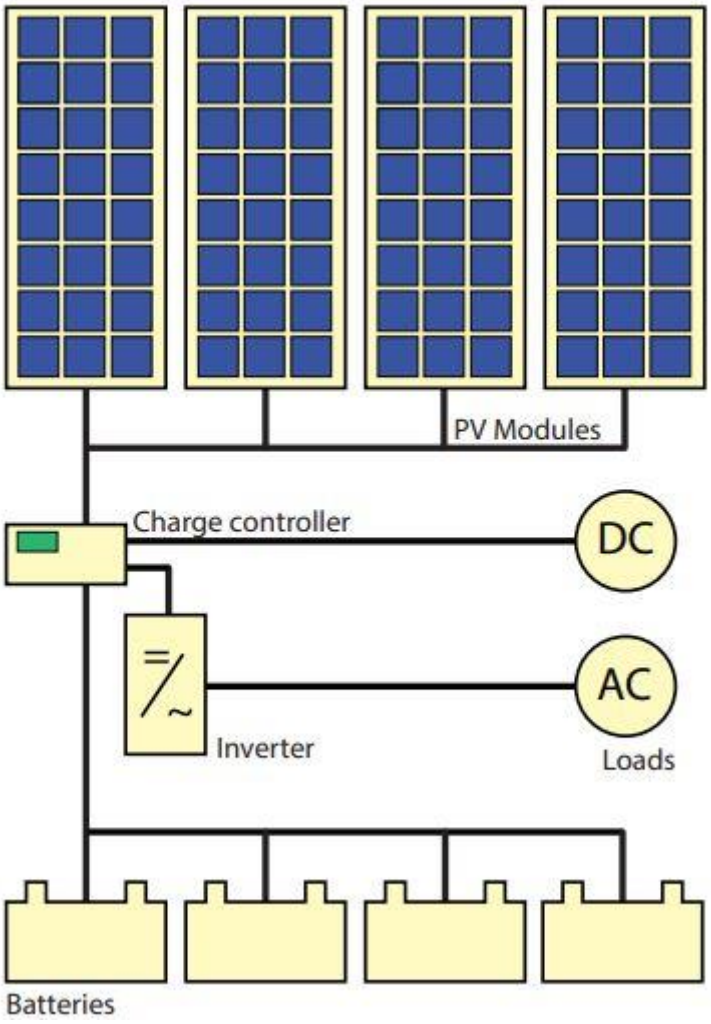

Figure 2-25: Schematic of stand-alone PV system with storage, power conditioner, DC and AC loads [11, pp220]

2.3.6.2 Grid-connected configuration

In this configuration, the PV system is connected to the grid via an inverter. This is the most popular residential PV application. The PV-generated DC power is converted to AC and transferred to the electricity grid or AC appliances in the house. This system does not require a storage device. The excess PV generation is transported to the grid and at the time of insufficient PV generation, energy is taken from the grid to power residential AC loads. Figure 2-26 shows a schematic of a grid-connected PV system.

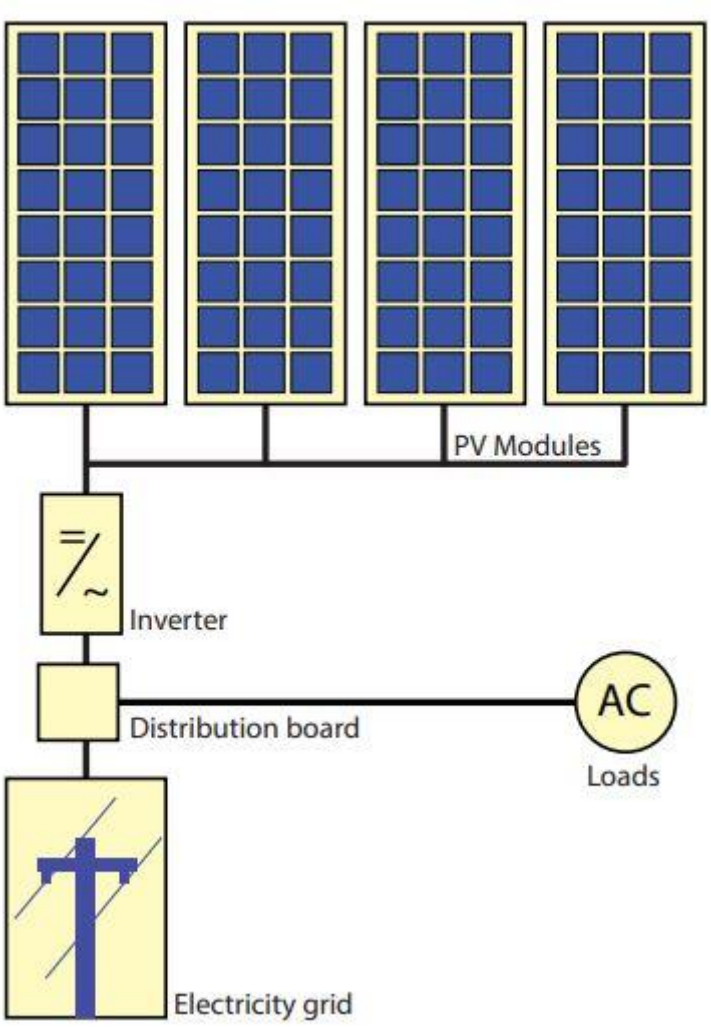

Figure 2-26: Schematic of a typical grid-connected PV system [11, pp221]

2.3.6.3 Hybrid Configuration

The configuration shown in Figure 2-27 consists of PV modules and a complimentary method of power generation system. Hybrid systems typically require more advanced control than stand-alone and grid-connected systems. Hybrid systems provide a high level of energy security by optimizing the power generation of the combined system.

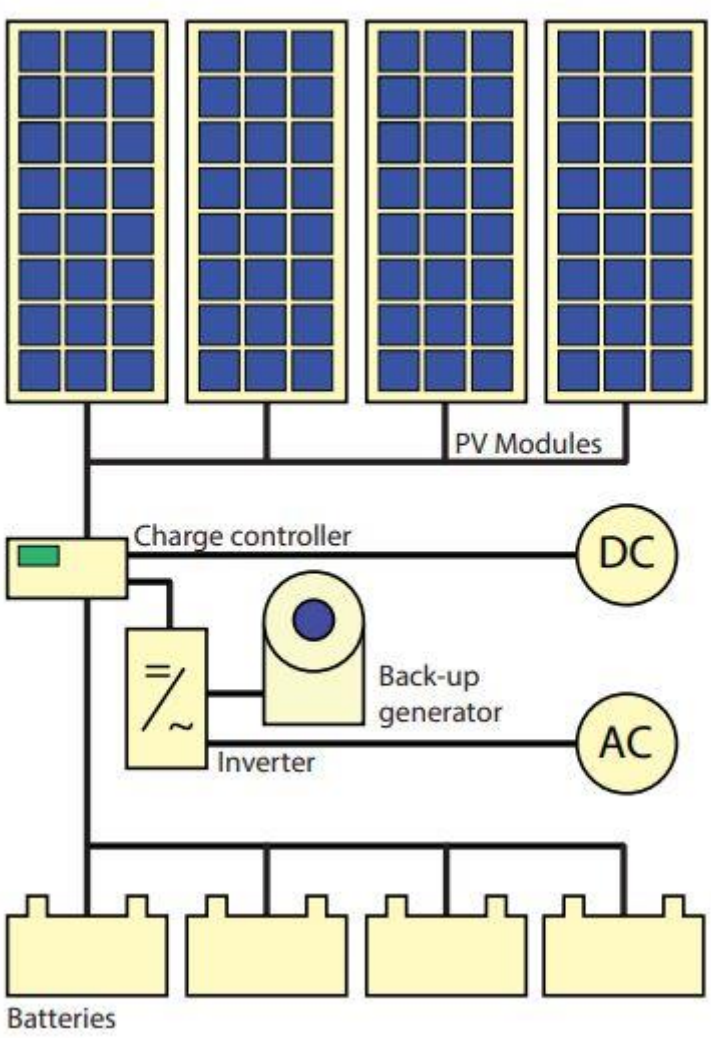

Figure 2-27: Schematic of hybrid PV system with backup alternative source [11, pp225]

2.3.7 MPPT TECHNIQUES

Solar PV energy generation has many advantages. But still, the energy conversion efficiency of solar modules is at a low value. It is still in the range of 15 – 20%. Therefore, maximizing efficiency of the PV system is very important.

In the I-V characteristics curve under specific irradiation conditions, the peak power occurs at the knee of the I-V curve. Where at the point of Imp and V_{mp}. The maximum power point is fundamentally dependent on irradiation level, temperature, and load. Figure 2-28 shows the maximum power point variation of different irradiation conditions and different temperatures. Maximum power point tracking (MPPT) is the process used to obtain maximum power from a solar module by tracking the voltage and current of the solar module.

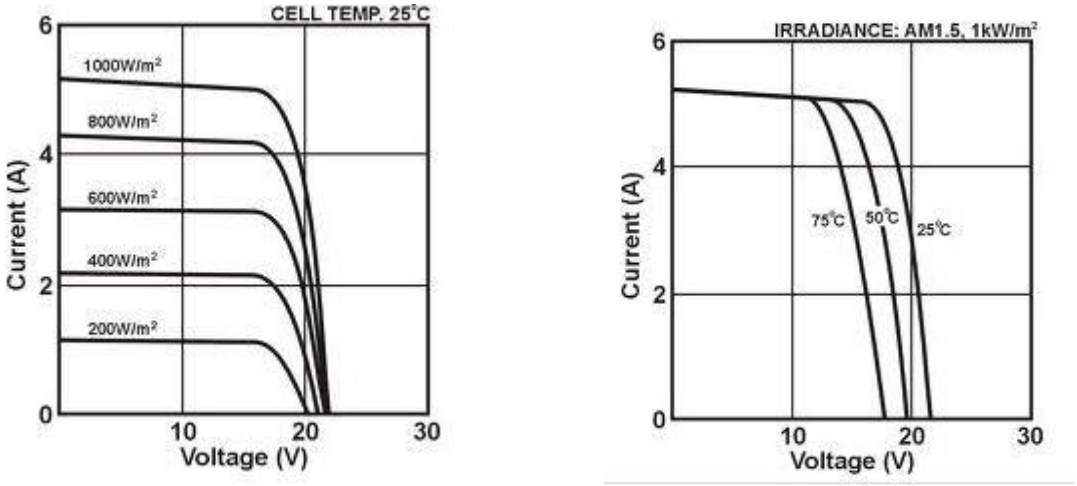

(a) *(b)*

Figure 2-28: Maximum power point variation due to: (a)Irradiance, (b) Temperature [17]

Therefore, the extraction of maximum power and delivery to the external load needs a technique. The method commonly used for this purpose is called the MPPT technique and the electronic device does this function is called the MPPT controller. This is an integral part of modern PV systems.

Theoretically, the maximum power transfer can be achieved when the source resistance matches the load resistance [5, pp42].

2.3.8 MAXIMUM POWER TRANSFER CONCEPT IN BRIEF

Let us consider the circuit shown in Figure 2-29.

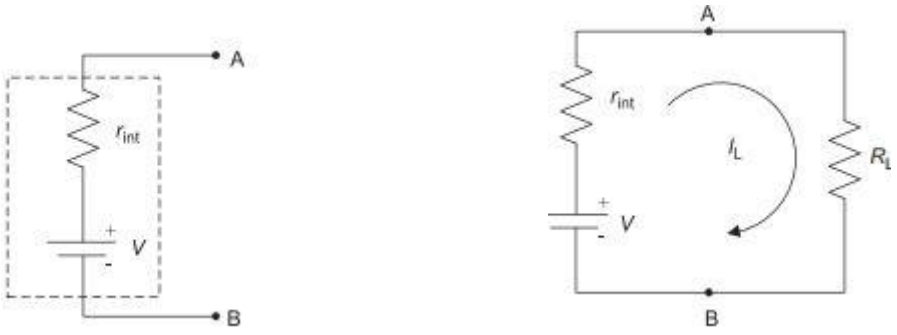

(a) *(b)*

Figure 2-29: DC power source: (a) consisting of the voltage source and fixed internal resistance, (b) Closed circuit formed with external load [5, pp41]

Applying Ohm's law to this circuit

$$i_O = \frac{V_{in}}{V_{in} + R_L} \tag{2.10}$$

The voltage across the load can be written as

$$V_L = \frac{V_{in} R_L}{r_{in} + R_L} \tag{2.11}$$

From the equation (2.10) and (2.11), the power delivered to the load can be written as

$$P_L = V_L i_O = \frac{V_{in}^2}{R_L}\left[\frac{1}{\left(1 + \frac{r_{in}}{R_L}\right)^2}\right] \tag{2.12}$$

Differentiating the above equation with respect to R_L , we can show that the maximum power delivered to the load occurred at $r_{in} = R_L$

Therefore, when this condition, the maximum power possible $P_{L(max)}$ is as shown in equation (2.13)

$$P_{L(\max)} = \frac{V^2}{4R_L} \tag{2.13}$$

Every technique used in MPPT is based on above mention maximum power transfer theory. To deliver maximum power to the load, the impedance of the PV module must be matched with the load connected.

MPPT can be achieved in several ways. In general, this is accomplished by using an algorithm. There are various MPPT techniques that are used in the PV industry. A few such methods discussed briefly are the perturbed and observe method (P&O), incremental conductance method (IC), constant voltage method (CV), beta method and temperature method.

2.3.9 MPPT METHODS

2.3.9.1 Perturb and Observe Method (P&O)

This method is the most widely used and discussed MPPT algorithm. The fundamental concept of P&O, the increasing voltage left of the MPP increases power, and on the right side of the MPP

decreasing the voltage, increases power. This algorithm compares the power of the previous power reading (P_{k-1}) with the current power reading (P_k). In response to this, the switch-mode DC-DC converter increases or decreases the reference voltage by modifying its duty cycle. This process is continued at each MPP tracking step until the correct MPP is achieved. The flowchart of this method is shown in Figure 2-30 [5, (pp349), 18].

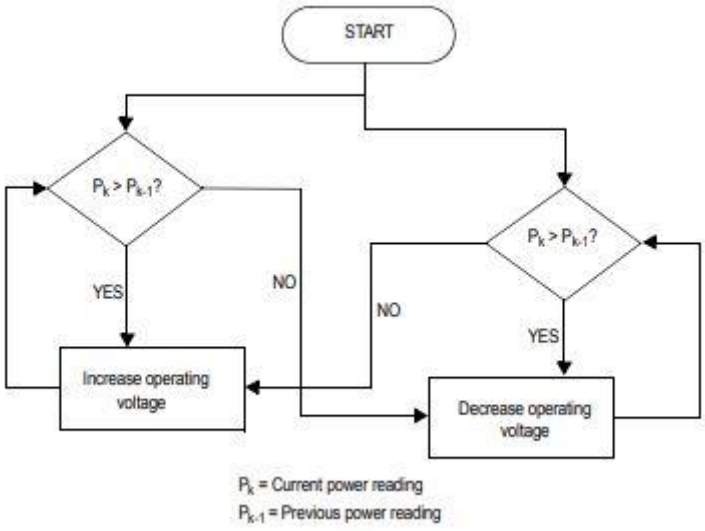

Figure 2-30: A conceptual flow chart of perturb and observe (P&O) algorithm [18]

This algorithm uses a fixed step of voltage increment or decrement. After achieving the MPP, the algorithm naturally oscillates around the MPP value. If the size of the step is larger the greater the oscillation but reaches MPP much quicker. However, the power loss will increase due to this oscillation.

2.3.9.2 Incremental conductance method (IC)

IC algorithm is based on characteristics of the PV module power curve derivative (or slope) is zero at MPP$\left(\frac{dp}{dv} = 0\right)$.

$$\frac{dp}{dv} = 0, \qquad at\ MPP$$

$$\frac{dp}{dv} > 0, \qquad left\ of\ MPP$$

$$\frac{dp}{dv} < 0, \qquad right\ of\ MPP$$

The above power derivatives can be written as,

$$\frac{\Delta I}{\Delta V} = -\frac{1}{V}, \qquad at\ MPP$$

$$\frac{\Delta I}{\Delta V} > -\frac{1}{V}, \qquad left\ of\ MPP$$

$$\frac{\Delta I}{\Delta V} < -\frac{1}{V}, \qquad right\ of\ MPP$$

The fundamental concept is comparing incremental conductance and instantaneous conductance of the PV module. The flowchart of this algorithm is shown in Figure 2-31. Based on the comparison the module voltage either increases or decreases by changing the duty cycle of the switch-mode DC-DC converter. After reaching the correct MPP the incremental conductance stops further modification of voltage. This method does not create any voltage oscillation unlike in the P&O method. But both P&O and incremental conductance algorithms are using a fixed voltage steps size. Similar to P&O, using large voltage steps results in quicker MPP tracking and may result in the algorithm oscillating around the MPP instead of locking on [5,(pp349), 18].

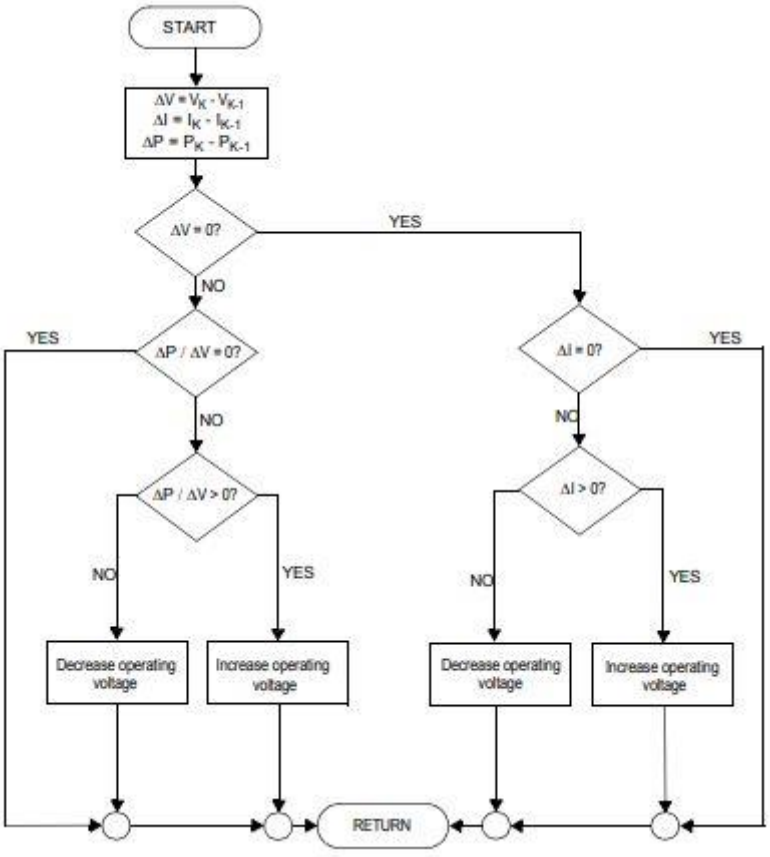

Figure 2-31: A conceptual flow chart of the incremental conductance (IC) algorithm [18,19]

2.3.9.3 Constant Voltage Method (CV)

This method is very simple and used the linear dependency of maximum power-point voltage (V_{mmp}) on the open circuit voltage (V_{oc}) at standard test conditions. The constant voltage method assumed that,

$$V_{mmp} = k.V_{OC} \quad (2.14)$$

Where k is dependent on the type and configuration of the PV module. The open circuit voltage of the PV module varies significantly with temperature. Therefore, this method is not suitable for places where the temperature changes are large. Also, this method will not give a proper MPP due to disconnecting the load periodically to measure the V_{oc} to calculate the operating voltage. The temporary loss of power is inherited from this method. The flowchart which represents the CV method is shown in Figure 2-32 [5, pp348].

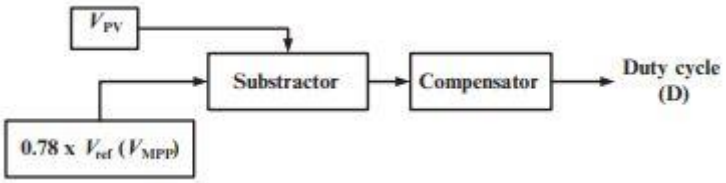

Figure 2-32: A representation of the constant voltage (CV) method flow chart [5, pp348]

2.3.9.4 Beta Method (B)

This method is one of the fastest MPP tracking algorithms which provides better tracking and fewer oscillations along the MPP [20]. The following equation is used to calculate the variable coefficient β , using the voltage and current values of the PV module.

$$\beta(V_{PV}, I_{PV}) = ln\left(\frac{I_{PV}}{V_{PV}}\right) - cV_{PV} \quad (2.15)$$

The constant *c* is depending on, temperature(T), electron charge (q), Boltzmann constant(K_b), number of series cells(N_s) and quality factor(n) [5, pp352].

2.3.9.5 Temperature method

This method measures the temperature of the solar module using a low-cost temperature sensor and compares it with the reference temperature and modify the MPP algorithm. Equation 2.16 is used to calculate MPP voltage. The effect of irradiation changes does not significantly affect the MPP voltage. Therefore, the influence of irradiation changes is considered negligible and the MPP algorithm assumed the MPP voltage varied linearly with temperature [5, (pp353), 20].

$$V_{mpp}(T) = V_{mpp}(T_{ref}) + T_{kVoc}(T - T_{ref}) \quad (2.166)$$

T – panel temperature, T_{kvoc} = temperature coefficient of V_{mpp} (available in the datasheet)

T_{ref} – standard test condition temperature

From a real application point of view, the calculated $V_{mpp}(T)$ is greatly affected by the PV module's irregular temperature distribution.

2.3.10 ANALYSIS OF MPPT TECHNIQUE FOR SUPERCAPACITOR-BASED ENERGY STORAGE.

The maximum power transfer theorem dictates that the maximum possible load power occurs when the source resistance matches the load resistance [5, pp42]. For a modern grid-connected, and off-grid-connected PV system with energy storage as a 'battery bank", the MPPT controller is an integral part to achieve the maximum efficiency of the overall system. The MPPT controller does this vital impedance balancing by changing the duty cycle of its switch-mode DC-DC converter.

The advancement of new energy storage technologies such as supercapacitors, due to their superior characteristics has gained much attention as an energy storage device in electronic systems.

In a comparison of a solar-powered DC microgrid system with a battery bank charged by an MPPT charge controller and replacing the same capacitor bank as energy storage, the capacitor bank act as a near-ideal characteristic, the MPPT controller does not see a constant resistive load in this case. Therefore, the nonexistence of impedance matching, the typical MPPT technique will not work efficiently with a capacitor bank.

Analysing the non-linearity of a solar module's characteristic curve, shown in Figure 2-33, it cannot be represented by a simple DC voltage source with open circuit voltage and constant internal resistance. The I-V characteristics curve for lower voltages behaves as a constant current source (A→B). At the higher voltage, it behaves as a constant voltage source with constant internal resistance (C→D) [21].

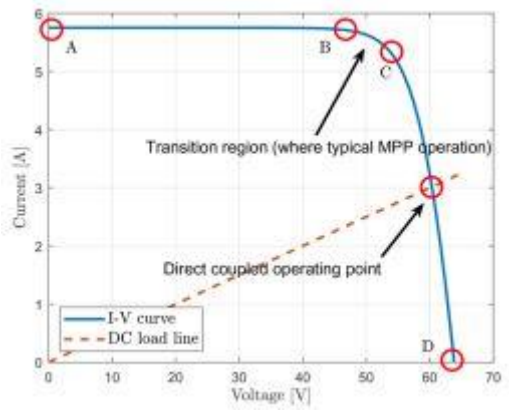

Figure 2-33: A typical I-V characteristic curve of a solar PV system [21]

Theoretical analysis of each energy storage device connected to the output of the MPPT switch-mode DC-DC converter shows that in the case of the battery, the input impedance of the DC-DC converter is a function of the duty cycle. But in the case of capacitors, both parallel and series connected, the input resistance is not only a function of the duty cycle but also a function of the state of charge of the capacitor.

The result of this theoretical analysis proves that the existing MPPT technique cannot be implemented for when a supercapacitor bank is used as the only energy storage device for a PV system. Therefore, to get the full benefit of supercapacitor technology a completely different, efficient power converter technique is essential [21].

CHAPTER 3: FUNDAMENTALS OF CAPACITORS AND SUPERCAPACITORS

3.1 FUNDAMENTALS OF CAPACITORS

Three fundamental components rule the world of electronics. They are resistors, capacitors and inductors. Resistors dissipate energy while capacitors and inductors are considered as short-term energy storage devices in electrical circuits. Capacitors store electrical energy by means of an electric field and similarly, inductors do that by a magnetic field. Other components such as diodes and transistors are non-linear versions of resistors made with help of semiconductors.

3.1.1 HISTORICAL BACKGROUND OF CAPACITORS IN BRIEF

The capacitor is a simple device, where an insulator is in between two conductors.

The birth of the capacitor can be attributed to the invention of the Laden jar, in 1745, by the German Ewald Georg von Kleist [22]. By combining foil electrodes with a sheet of glass, inventor Benjamin Franklin was able to make a flat capacitor[23]. Further developments led to the first practical fixed and variable capacitor introducing dielectric materials was invented by Michel Faraday [22]. The unit of capacitance farad (F) is named for recognizing his work in capacitor technology.

In 1957, General Electric patented the supercapacitor based on double-layer charge storage. This concept was introduced by German physicist Hermann Von Helmholtz in 1853. [5, (pp 199)] Electric double-layer capacitor technology became very popular in the last two decades due to the increasing demand for environmentally friendly devices for modern energy storage applications.

3.1.2 Electric Capacitor Fundamentals

The basic element of any electric capacitor is two isolated conductors, no matter what their geometry is. A more conventional arrangement is a parallel plate capacitor. It consists of two parallel conducting plates of area (A) separated by a distance (d).

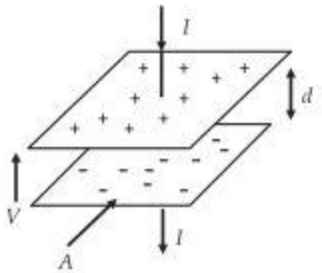

Figure 3-1: A charged parallel plate electrostatic capacitor

When a capacitor is charged, its plates have equal but opposite charges of +q and -q. We define this state as the capacitor has been charged by q. But the net charge on the capacitor is zero. The capacitor plates are made up of conductors, therefore all points on a plate are at the same electric potential. The absolute potential difference (V) is proportional to charge quantity q.

$$q \propto V$$

$$q = CV \tag{2.17}$$

Where C is capacitance, which is a constant. The capacitance is a measure of how much charge must be put on the plate to produce a given potential difference. An important feature of capacitance is that the value of capacitance depends only on the geometry of the plate, but not the charge quantity or potential difference. From equation 2.1 the unit of capacitance becomes coulomb per volt. The SI unit is farad (F). One coulomb (1C) is equal to the electrical charge of approximately 6.24 x 10^{18} electrons or protons. Therefore, the numerical value of one farad is very large. Most capacitors used in electrical circuits are in the range of microfarad (1uF = 10^{-6} F) or picofarad (1pF = 10^{-12} F).

With the advancement of electrochemistry and various manufacturing technologies, scientists were able to develop capacitors with a capacitance ranging from 1 F to 100,000 F. These are called supercapacitors (SC) or ultracapacitors. Figure 3-2 shows some commercially available capacitors in different capacity and size.

More details of Supercapacitors will be discussed in a later part of this chapter.

Figure 3-2: Different types of capacitors [5, (pp 194)]

Coulomb's law is the governing law in electrostatics. Charles Augustin Coulomb, with his experiment in 1785, led to the formulation and derivation of the equation for the electrostatic force between charged (point charge) particles.

Two charged particles having a magnitude of q_1 and q_2 separated by a distance r, the electrostatic force of attraction or repulsion has the magnitude F

$$F = \frac{k\,|q_1||q_2|}{r^2} \tag{2.18}$$

Where k is a constant (electrostatic constant). Whether the force is an attraction or repulsion one depends on the polarity of the two charges (+) or (-).

3.1.3 CALCULATING THE CAPACITANCE

As mentioned earlier, the capacitance depends only on geometry. The most common geometry, illustrated in Figure 3-3, is a parallel plate capacitor.

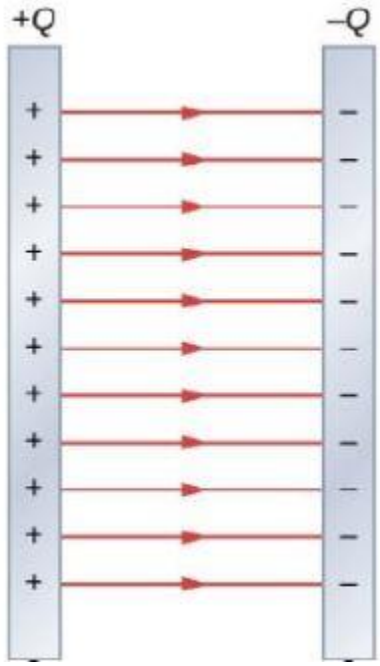

Figure 3-3: A parallel plate capacitor charged with Q

Capacitance can be calculated by taking the electric field between the plates (E) to be constant with an area of the plate A as shown in equation 2.5. This does however neglect the fringing of the electric field at the edge of the plate.

$$Q = \varepsilon_0 EA \tag{2.19}$$

$$V = Ed \tag{2.20}$$

From equation 2.3 and 2.4,

$$C = \varepsilon_0 \frac{A}{d} \tag{2.21}$$

E -Electric field between the plates

ε_0 – Permittivity constant

3.1.4 CAPACITORS IN PARALLEL AND SERIES

When there is a combination of capacitors in a circuit, they can be replaced with an equivalent capacitor.

3.1.4.1 Capacitors in Parallel

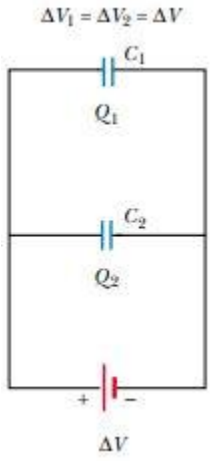

Figure 3-4: Capacitors connected in parallel to the source

A potential difference ΔV applied across several capacitors connected in parallel, as shown in Figure 3-4, will have the same potential ΔV appeared across each capacitor. The charge stored in each capacitor will depend on its capacitance. The total charge stored in the string is the sum of individual capacitors. Therefore, this string can be replaced by one equivalent capacitor with the same potential difference ΔV and the total charge in the string.

$$Q_{TOTAL} = Q_1 + Q_2 + \cdots + Q_n$$

$$Q = C\Delta V$$

Hence,

$$C_{eq} = C_1 + C_2 + \cdots + C_n$$

$$C_{eq} = \sum_{z=1}^{n} C_i \qquad (2.22)$$

3.1.4.2 Capacitors in Series

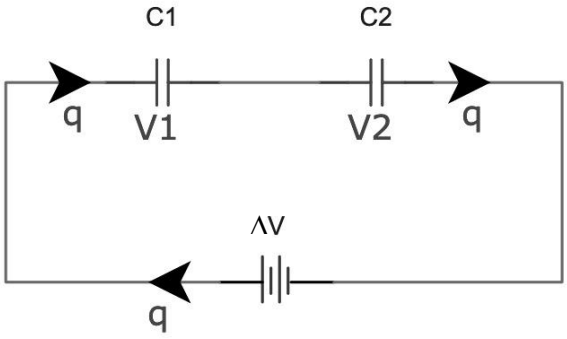

Figure 3-5: Capacitor connected in series

When the capacitor is connected in series, as shown in Figure 3-5, the potential difference ΔV is the sum of the potential difference in each individual capacitor. Each capacitor is charged with same current and therefore each capacitor stores the same amount of charge

$$V = V_1 + V_2 + \cdots + V_n$$

$$V = \frac{q}{C}$$

$$\frac{1}{C_{eq}} = \frac{1}{C_1} + \frac{1}{C_2} + \cdots + \frac{1}{C_n}$$

$$\frac{1}{C_{eq}} = \sum_{z=1}^{n} \frac{1}{C_i} \tag{2.23}$$

3.1.5 ENERGY STORED IN A CAPACITOR

Energy is stored in a capacitor as an electric field between plates can be considered as being an electric potential energy. This stored energy can be recovered by discharging the capacitor in a circuit.

Assume at a given instance a charge q' has been transferred from one plate to another of a capacitor. The potential difference V' at that instant between the plates.

Therefore,

$$V' = \frac{q'}{C} \tag{2.24}$$

In this instant a further increment of dq' is transferred, the work done required is dw,

$$dw = V'dq'$$

$$dw = \frac{q'}{C}dq'$$

The total work required to bring the charge up to the final value q is,

$$W = \int_0^q dw = \int_0^q \frac{1}{C}q'dq'$$

$$W = \frac{q^2}{2C} \tag{2.25}$$

This work is then stored as potential energy in the capacitor (U)

$$U = \frac{q^2}{2C}$$

$$U = \frac{1}{2}CV^2 \tag{2.26}$$

3.1.6 ENERGY DENSITY

The energy density (U) is the electric potential energy per unit volume between the capacitor plates. Neglecting the electric field at the end of the plates, the electric field is the same at all points between the plates,

$$U = \frac{stored\ potential\ energy}{Volume\ (space\ between\ the\ plates)}$$

$$U = \frac{\frac{1}{2}CV^2}{Ad}$$

A – area of the plate, d – distance between the plates.

From equation (2.3)

$$C = \varepsilon_0 \frac{A}{d}$$

$$U = \frac{1}{2}\varepsilon_0 E^2 \tag{2.27}$$

ε_0 – permeability of the material between the parallel plate

E – magnitude of electric field

3.1.7 Power density

The power density is the measure of power output per unit volume. Maximum Power output of any energy storage device depends on its terminal voltage and effective internal resistance of the device.

$$Power\ Density\ = \frac{Maximum\ Power\ output}{Volume}$$

$$Maximum\ Power\ Output\ = \frac{V^2}{4r_{int}}$$

Where,

V – Terminal voltage, r_{int} - Internal resistance of the device

$$Power\ Density\ = \frac{V^2}{4r_{int}Volume} \tag{2.28}$$

3.1.8 CAPACITOR CHARGING AND DISCHARGING

A capacitor is a fundamental electrical component that stores electrical energy and released it when required by the circuit.

3.1.8.1 Capacitor charging.

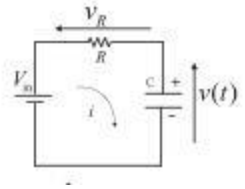

Figure 3-6: A capacitor charging from a voltage source [5, pp 182]

A simple charging circuit of a capacitor is shown in Figure 3-6. A constant DC voltage V(in) and resistance R, which represents the equivalent series resistance of the capacitor, the resistance of external leads, the resistance of connecting wire and any extra resistance introduce to the path, etc.

Assume the initial voltage of the capacitor V_0,

Using Kirchhoff's voltage law,

$$V_{in} = i(t)R + \frac{1}{C}\int_0^T i(t)\,dt \tag{2.29}$$

Solving the above equation for current,

$$i(t) = \frac{V_{in}}{R} e^{\frac{-t}{RC}} \tag{2.30}$$

The capacitor voltage at any given time,

$$V(t) = V_{in}\left[1 - e^{\frac{-t}{RC}}\right] \tag{2.31}$$

The charge time of the capacitor depends on the product of R and C.
This is usually called the time constant, τ= RC. It takes more than 5-time constants for a capacitor to fully charge or discharge. The Figure 3-7 shows the voltage and current variation with time during charging a capacitor.

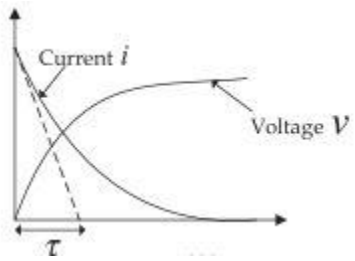

Figure 3-7: Voltage-current variation with time during charging [5, pp 183]

3.1.8.2 Capacitor discharging.

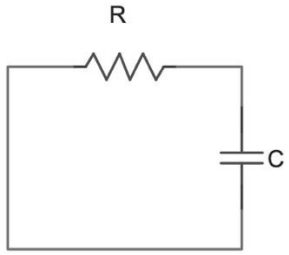

Figure 3-8: Capacitor discharging through resistor

After charging the capacitor, the DC source is replaced and the capacitor is discharged through a load resistance R as shown in the Figure 3-8. The voltage across the capacitor will decrease exponentially with the current decreasing the same way but in opposite direction.

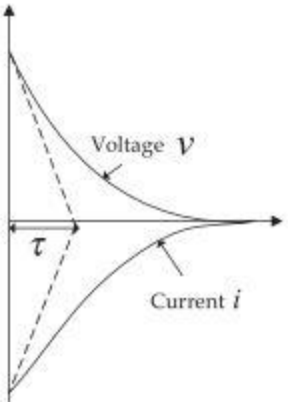

Figure 3-9: Capacitor discharging with time. [5, (pp 183)]

The equation for the capacitor voltage at any given time t is,

$$V(t) = V_f e^{\frac{-t}{RC}} \tag{2.32}$$

And current at any given time t, i(t)

$$i(t) = \frac{V_f}{R} e^{\frac{-t}{RC}} \tag{2.33}$$

V_f- Voltage at the start of the discharge process.

3.1.9 Time constant

Consider a simple circuit containing only a capacitor and resistor as shown in Figure 3-10. Assume the capacitance is C F and charged to a non-zero voltage V_0 resulting in some charge q_0 on the capacitor.

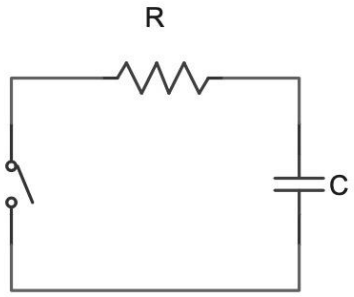

Figure 3-10: Measuring time constant

When the switch is closed (on), current will flow through the circuit from the positive plate to the negative plate of the capacitor. Due to this current flow, the voltage across the capacitor and charge of the capacitor changes with time.

The voltage over capacitor V is,

$$V = \frac{q}{C}$$

So, the current through the circuit I,

$$I = \frac{V}{R} = \frac{Q}{RC}$$

And

$$I = \frac{dq}{dt}$$

In this situation, net charges on either side of the capacitor decrease. Therefore,

$$\frac{dq}{dt} = -\frac{q}{RC}$$

By solving the above differential equation

$$q(t) = q_o e^{-\frac{t}{RC}}$$

The factor RC tells us how fast this charge-balancing process occurs. If t= RC (seconds)

$$q(t) = \frac{1}{e} q_o$$

During time t, (RC) the charge decreases with the factor of e or 36.8%. Similarly, charging a capacitor charge increases by ($1-e^{-1}$) or 63.2%.

It usually takes about 5 time constants for a capacitor to fully charge or discharge.

3.2 FUNDAMENTALS OF SUPERCAPACITORS

3.2.1 SUPERCAPACITOR STRUCTURE AND PRINCIPLE

Supercapacitors (SC) also known as ultracapacitors (UC) or electric double-layer capacitors (EDLC), are based on the same fundamental principles that are applicable to the common electrostatic capacitor, as shown in Figure 3-11. The capacitance depends on the area of the plate and the distance between them.

The electrostatic capacitor's capacitance is represented by Equation 2.18.

$$C = \frac{\varepsilon_o \varepsilon_r A}{d} \qquad (2.34)$$

Where ε_o – permittivity of air, ε_r– relative permittivity of dielectric material, A – the surface area, d – the distance between two electrodes.

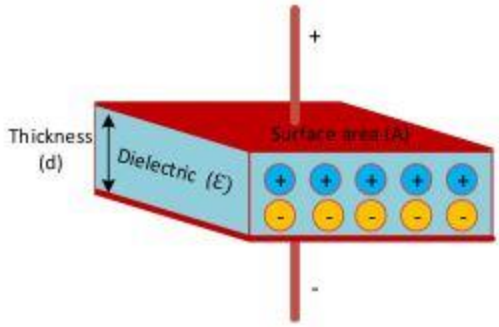

Figure 3-11: Cross-section of electrostatic capacitor [24]

Figure 3-12 shows a comparison of electrolytic and film capacitors with commonly available supercapacitors (SC), highlighting their canister size and the amount of energy that can be stored. Newer supercapacitor cells come with a relatively low equivalent series resistance (ESR) value, which can offer very high charge/discharge capability without excessive heat dissipation.

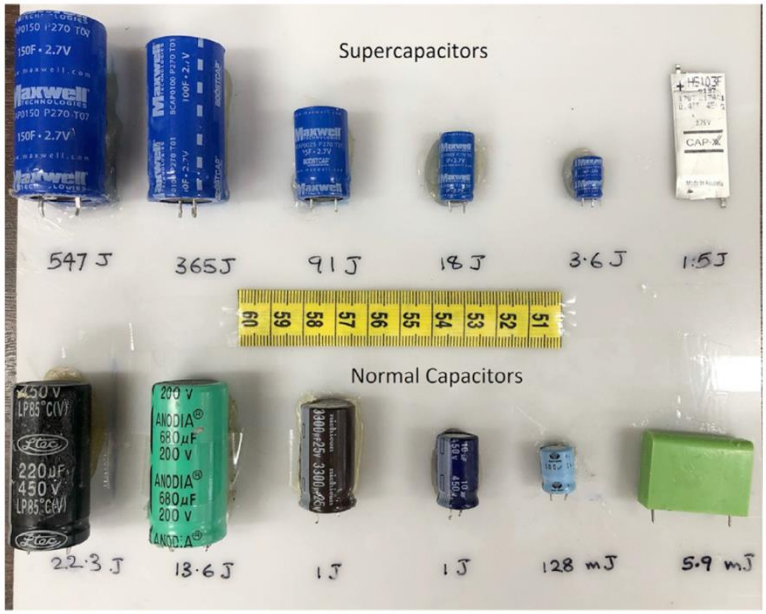

Figure 3-12: Supercapacitors and electrolytic capacitors of similar geometry [5, pp 243]

There are three different SC families commercially available in the market. These are namely EDLC, Hybrid supercapacitors (HSC) and battery capacitors with individual cell voltage ratings less than 5 VDC and capacitances ranging from 1F to 100,000F. Table 3-1 shows a comparison of these devices commercially available.

Table 3-1: Comparision of supercapacitor families [25]

Parameter	EDLCs	Hybrid SCs	CAPAbatteries
Energy density, Wh/L	5-8	10-14	50-120
Power density, W/L	8000	2500-4000	1600-3200
Cycle life, cycles	1,000,000	40,000-50,000	15,000-20,000
Rated voltage, V	2.7	2.7	2.8
Capacitance, F	1-3000	200-7500	1000-70,000
ESR, DC (mΩ)	13-0.29	19-0.8	18-0.7

3.2.2 CLASSIFICATION OF SUPERCAPACITORS

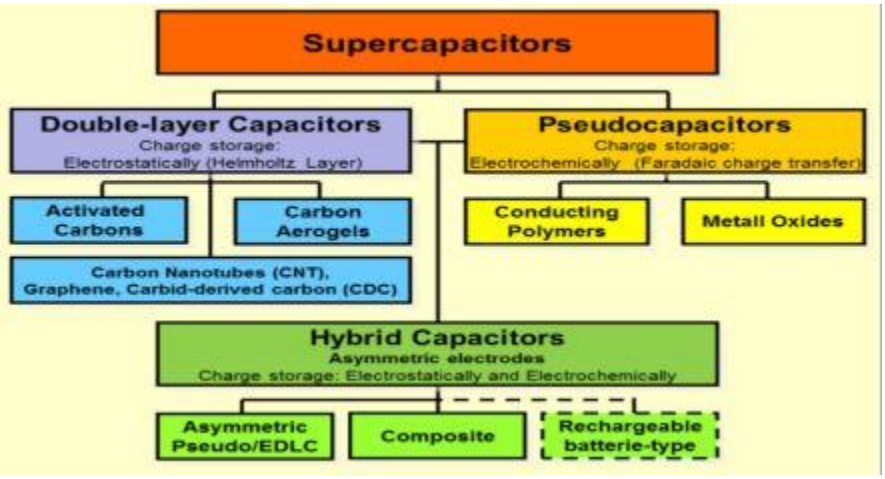

Figure 3-13: Supercapacitor families [26]

3.2.3 SUPERCAPACITOR STRUCTURE.

Th structure of EDLC consists of an electrolyte, two carbon-based electrodes and a non-conductive separator. In an EDLC, there is no charge transported between electrodes and electrolytes [5, (pp 202)]. Figure 3-14 shows the structure of SC.

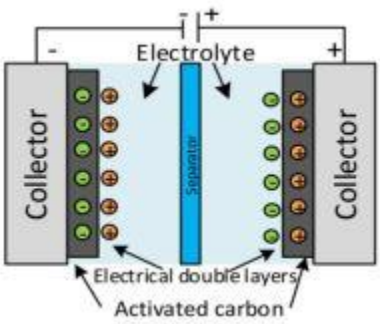

Figure 3-14: Schematic of EDLC [24]

3.2.4 SUPERCAPACITOR PRINCIPLE

The energy storage principle behind the electrochemical cell is the electron transfer caused by the oxidation or reduction process, commonly known as the “Faradaic process”. But in electrochemical capacitors, the positive and negative charges physically exist through the adsorption and desorption process. The structure of the electrode-solution interface can change with changing potential or composition of the solution. This process is called the “non-faradaic process”.

Hermann Von Helmholtz, a German physicist, first described the idea that a charged electrode immersed in an electrolyte solution repels similarly charged ions and attracts oppositely charged ions to electrodes. This resulted in the formation of two layers of opposite polarity at the interface between the electrode and electrolyte. He showed that an electric double layer is essentially a molecular dielectric and stores charge electrostatically [5, 24,27].

The electric double layer formed next to a large area electrode and an electrolyte is effectively used and this is called an electrical double layer capacitor (EDLC) [5, pp 203].

3.2.5 CELL CONSTRUCTION OF SUPERCAPACITORS

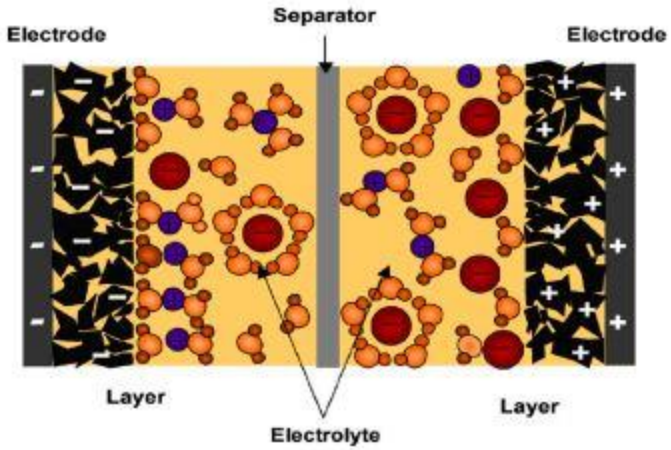

Figure 3-15: Cross-section of EDLC [28]

A supercapacitor consists of two metallic electrodes attached to the current collector. The inner surface of the electrode is padded with active material, such as activated porous carbon, which produces a high specific surface area (SSA -surface area per square millimeter) that is about 100,000 times larger than an ordinary electrostatic capacitor [5, pp 204]. These electrodes are soaked in electrolytes which are separated by a membrane, allowing the mobility of the charge ions and forbidding electronic conduction [29]. Due to the high surface area and very small distance separation between opposite charges, the capacitance of an EDLC can reach thousands of farads. Figure 3-15 shows a sketch of a cross-section of the SC cell.

3.2.5.1 Electrodes

The capacitance depends on the surface area. Therefore, the electrode material is a key property for high capacitance. To form a double layer with the maximum number of electrolyte ions, electrochemical inert materials with the highest specific area are necessary. Other properties related to electrical characteristics such as high conductivity, low resistance and thermal stability, high cycle stability, mechanical strength, and cost-effectiveness are vital when selecting electrode material. Carbon-based materials such as activated carbon, aerogels, xerogels, carbon nanotubes, nanofibers, mesocarbon microbeads, expanded graphite and other mesoporous carbons are experimented with for prospective electrode materials [5, pp 206]. Metal oxides and conducting polymers are used as electrode materials in supercapacitors with high-specific capacitance and such high-performance supercapacitors fall under pseudo capacitance (PS) and hybrid supercapacitors (HSC).

In capacitors used for high-energy applications, activated carbon electrodes are commonly used. The best carbon electrode has a surface area as high as 3000 m^2 per gram [29]. By making a shorter distance between opposite charge layers, it is possible to achieve very high capacitance. Since charge separation takes place by a non-faradaic process, these supercapacitors are capable of fairly high charge and discharge cycles compared to other energy storage devices [24,27].

As mentioned earlier, metal oxides and conducting polymer materials exhibits high specific capacitance. With metal oxides electrode, the electric double-layer effect is combined with a faradaic process as found in batteries to obtain high energy densities. The major disadvantage is that metal oxides are expensive, toxic, and environmentally unfriendly. As a result there are ongoing research and development of electrode materials with higher stability, that are more safe and more environmentally friendly [5, (pp 210)].

Electronically conducting polymer (ECP) electrode materials are used for SCs-based pseudo capacitance. ECP are an excellent electrode materials for high-performance SCs. Their charge and discharge processes are generally fast, have low ESR, high specific energy and power.

3.2.5.2 Electrolyte

Electrolytes determine key characteristics of SC, such as ESR, operating temperature range and voltage capability [30]. More ions in the electrolyte results in better conductivity. However, another important property to consider is that they must be chemically inert in order to ensure the long stable behaviour of electrical parameters. Different kinds of electrolytes are used in EDLC with activated carbon electrodes. Aqueous, organic, and ionic liquid electrolytes are used at present [30].

Aqueous electrolytes are cost-effective and have a high ionic conductivity. SC with aqueous electrolytes show high specific power and low specific energy density [5, pp 211].

Major disadvantages are low maximum applied voltage and corrosiveness at high temperatures. These affect the lifetime and life cycle limitation of EDLC [5, pp 211].

Organic electrolytes show higher maximum applied voltages and better temperature ranges but are more expensive. Organic electrolyte-based EDLC shows moderately high maximum applied voltages, very high life cycle and higher operating temperature ranges. Due to their low thermal stability, flammability, and toxicity, it is limited in high-performance SC applications [5, pp 211].

Ionic liquid (IL) consists of liquid salt. They have lower ionic conductivity when compared to other electrolytes [31]. Due to the properties of ionic liquids, the performance of SC can be improved. Nonflammability, higher thermal and electrochemical stability and high voltage window are important characteristics. Ionic liquid-based EDLCs have high energy density [5, pp 212].

3.2.5.3 Separators

Separators are used to prevent short circuits of electrodes by direct contact while allowing charged ions to transfer [32]. Poorly designed separators negatively affect the performance of supercapacitors [32]. They must be chemically inert. The separator must be very thin and must be porous to minimize ESR. Polymer-based or paper separators can be used for organic electrolytes. With aqueous electrolytes glass fibre separators are possible. In general, low cost, high flexibility, and porosity are important aspects to consider when selecting separators [31].

3.2.6 PSEUDOCAPACITORS (PC)

Pseudocapacitor or faradaic supercapacitors are different from EDLC. Pseudocapacitance depends upon the faradaic reaction that takes place on the electrode surface. The materials used are metal oxides. These electrodes can undergo the required redox reactions. The whole process involves potential induced adsorption on charge electrodes, redox reactions and intercalation process. PCs exhibit higher capacitance and higher energy density but relatively lower power density. The faradaic process being relatively slower than the non-faradaic process accounts for the decrease in power density. As redox reaction takes place at the electrode PCs often lack cyclic stability, resulting in lower charge-discharge cycles compared to EDLCs. [5, pp 214] Figure 3-16 shows a cross-sectional view of a pseudocapacitor.

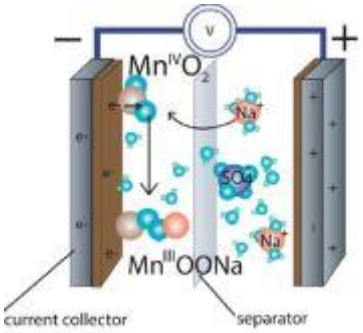

Figure 3-16: Schematic of pseudocapacitor [27]

3.2.7 HYBRID SUPERCAPACITORS (ASYMMETRIC SC)

Rechargeable batteries have high specific energy and low specific power compared to SCs, which have low specific energy but high specific power. A major challenge in the past decade was to develop a high energy – high power capable devices to meet new energy storage goals. For that effect, research has been undertaken to combine the best characteristics of electrochemical capacitors and rechargeable batteries.

Asymmetric electrochemical capacitors or now commonly known as hybrid capacitors were developed on the principles of hybridization at the electrode level. The capacitor-type electrode stored charges by the non-faradaic process while the battery-type electrode stored charges by reversible faradaic process, where this electrode undergoes a phase transition during charging and discharging [5, pp 215].

HSC has one electrode like that of a rechargeable battery while the other electrode is a standard SC electrode. This results in an energy density closer to the conventional rechargeable battery and it's about ten times higher than EDLCs. In comparison with EDLCs, HSCs have a higher operating voltage, much higher capacitance, and much lower self-discharge. Traditional SC has higher power capability due to low ESR, wider operating temperature range and can be discharged fully [33].

3.2.8 EQUIVALENT CIRCUIT MODEL OF SC

The simplest capacitor model can be represented with two lumped parameter elements as shown in Figure 3-17 (a). In this simplest version, ESR and the capacitance are in series with the assumption of a constant capacitance and constant resistance. But the experimental

results indicate that this is only the very first approximation and does not consider the leakage of the capacitor.

(a) *(b)*

Figure 3-17: Capacitor equivalent circuit: (a) First order model, (b) Classical model [5, (pp 188), 32]

Therefore, there are several SC equivalent circuit models are proposed. The classical capacitor model as shown in Figure 3-17 (b), is mostly used [34]. The equivalent series resistance (Rs) represents the internal resistance that occurs during charging and discharging. The parallel resistance (Rp) represents the resistance estimated due to leakage current in long-term effects. Cd represents the total capacitance of SC.

Most theoretical models are very complicated to apply when designing circuits using SCs. For circuit designing, the practical model is the two or three-branch series model and the voltage-dependent ladder model [5, pp 222] as shown in Figure 3-18.

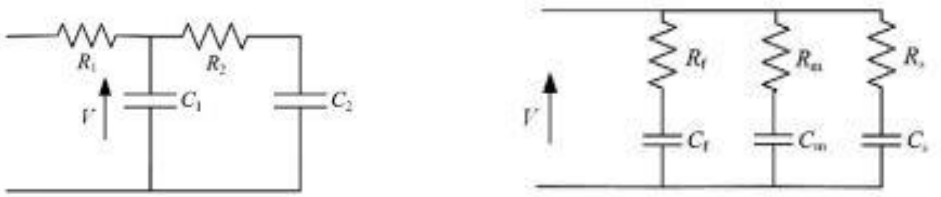

(a) *(b)*

Figure 3-18: Supercapacitor models: (a) Two branch, (b) Three branch [5, pp 222]

3.2.9 SUPERCAPACITOR AS AN ENERGY STORAGE DEVICE

Due to the intermittent nature of true renewable energy, such as solar photovoltaic and wind, those systems must have energy storage devices to provide consistent energy over time. Supercapacitor technology proves to be increasingly promising and one of the emerging technologies to complement batteries in meeting the demand for both power and energy.

Fundamentally, batteries are made of two electrodes that act as an anode and cathode immersed in an electrolyte solution. When these electrodes are in contact with electrolytes, a certain potential is developed between electrodes. This potential creates a flow of current and delivers power when these electrodes are connected to the electronic circuit. In batteries the oxidization and reduction of the electrochemical reaction agents results in a flow of charge between the electrode and electrolyte, commonly referred to as faradaic processes. Therefore, the charge that flows through the interface is proportional to the amount of chemical change of electrode-electrolysis.

Supercapacitors bridges the gap between electrolytic capacitor and rechargeable batteries. Supercapacitors are also composed of electrodes and electrolytes but the charge accumulation is accomplished by the electrical double-layer effect, where oppositely charged ions are adsorbed at the electrode surface separated only by the Helmholtz layer. SCs can charge and discharge much faster than a battery and is capable of very high charge and discharge cycles. Internal resistance is also of an extremely low value and remains fairly constant throughout its life.

When comparing supercapacitors and batteries, the fundamental difference is that batteries store charge in bulk, while supercapacitors stores charge on the surface. This fundamental difference in the internal working principle leads to significant differences in their operational characteristics. This can be analysed by key parameters of energy storage.

The important performance comparison of Supercapacitors and rechargeable battery (Lithium-ion) chemistries is summarised in the Table 3-2.

Table 3-2: key parameters of supercapacitors and Li-ion battery [26]

Function	Supercapacitor	Lithium-ion (general)
Charge time	1-10 seconds	10-60 minutes
Cycle life	1 million or 30,000 hours	500 and higher
Cell voltage	2.3-2.75 V	3.6-3.7 V
Specific energy (Wh/kg)	5 (typical)	100-200
Specific Power (W/kg)	Upto 10,000	1,000-3,000
Cost per Wh	$20 (typical)	$0.50-$1.00 (large system)
Service life (in vehicle)	10-50 years	5-10 years
Charge temperature	-40 to 65°C (-40 to 149°F)	0 to 45°C (32 to 113°F)
Discharge temperature	-40 to 65°C (-40 to 149°F)	-20 to 60°C (-4 to 140°F)

3.2.10 Generalized comparison of Supercapacitors against Li-ion batteries

3.2.10.1 ENERGY DENSITY

For fuel cells and battery chemistries the energy density is well above supercapacitors. But Over the last decade, with the advancement of manufacturing technologies and the success of new electrode and electrolyte materials, more advanced supercapacitor devices have entered to the market. Among those, the capa-batteries have reached significantly close to the energy density of lead-acid chemistries [5, pp 95]. This can be evident in the Ragone plot shown in Figure 3-19.

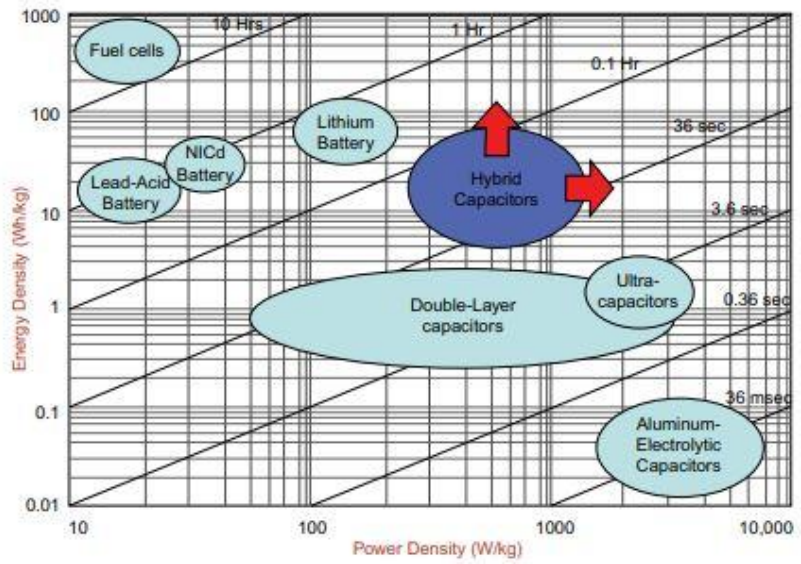

Figure 3-19: Ragone plot [5, pp 242]

3.2.10.2 POWER DENSITY, CHARGE RATE/DISCHARGE TIME

The power density of energy storage technology directly relates to charge rate and discharge time [34]. For power applications where quick delivery of power is required power density is preferred over energy density. Supercapacitors show excellent charge rates which is hundreds of times compared to rechargeable battery chemistries and discharge time in the order of seconds and minutes, whereas most rechargeable batteries take hours.

Due to design optimization, impurities, and material imperfections, the onloaded capacitors lose a portion of charge due to self-discharge and leakage current. In comparison with supercapacitors and rechargeable batteries, SC loses nearly 30% of stored energy but the latter loses only about 10% [35]. However, SCs have extremely high recharge capability, they can be recharged as fast as they discharge.

Another advantage is multiple charging methods of SCs over batteries such as constant current, constant voltage, constant power or paralleling an energy source [35].

3.2.10.3 CYCLE LIFE

Unlike rechargeable batteries, SCs have less chemical changes and phase changes during charging and discharging. Since the charge storage occurs by the non-faradaic process there are no significant failure points to affect its long cycle life. But in rechargeable battery chemistries, due to the faradaic process, the cyclic stresses on charging and discharging leads to the decomposition of both solvent and solute characteristics and degrade the electrode, such as cracking of electrodes, affecting the reversible reaction causing a reduction in capacity and power density over time. [35]

3.2.10.4 OPERATING TEMPERATURE

Rechargeable batteries are impacted by two different degradations because of temperature. At low temperature it is observed that the chemical reaction capability and charge transfer velocity resulted in lower ionic conductivity. On the other hand, at higher storage temperatures or high power/current applications, the defects in electrodes due to manufacturing may lead to extreme heat generation and consequently result in thermal runaway.

During the charge transfer in a battery, entopic heat is generated due to a chemical reaction due to charging and discharging. Furthermore, the resistance of the electrode and electrolyte during charge transfer creates ohmic heat generation. Therefore, heat generation is inherent in rechargeable battery chemistries.

However, since the SC has a very low internal resistance power lost as heat is kept to a minimum within the SC reducing the likelihood of thermal runaway. As mentioned earlier, charge storage and electron transfer are mainly due to non-faradaic processes. At low temperatures the effect of decomposition of electrode and electrolyte is even slower. Hence typical operating temperature range of SCs are much wider than batteries. [35]

3.2.10.5 MANAGEMENT SYSTEMS

Maintaining the nominal performance of the batteries needs a carefully designed battery management system (BMS). The function of the BMS is to monitor, control, and optimize the parameters such as temperature, voltage, current, overcurrent/over voltage protections, state of discharge (SoC), depth of discharge (DoD), relay actuation to disconnect faulty cells, etc. Therefore, a rechargeable battery storage system needs a complex external monitoring system.

SCs however only need to maintain their voltage within their maximum to achieve their long lifetimes. To achieve the inherent long life cycles of SCs, a SC module (SCM) only needs cell balancing.

The main two methods used in voltage balancing in SC modules are passive balancing and active balancing. More details of these methods will be discussed later in the chapter. Unlike BMS, SC voltage balancing does not require complex external control and monitoring [35].

3.2.10.6 INTERNAL RESISTANCE

SC internal resistance, also called equivalent series resistance (ESR), is in the milliohms range. Unlike batteries, the internal resistance and cycle life are independent of the depth of

discharge (DoD) [5, (pp 96)]. Figure 3-20 is showing the DoD against the life cycle of the battery and three different SC technologies.

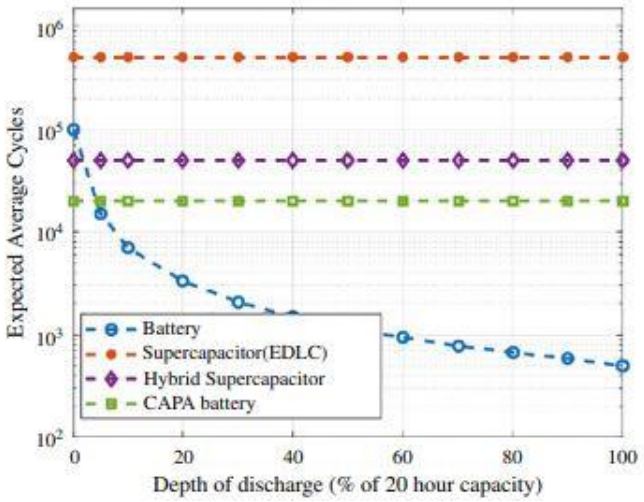

Figure 3-20: Variation of life cycle and depth of discharge of supercapacitors and battery [5,pp 96]

3.2.11 COMPARISON OF ADVANTAGES AND DRAWBACKS OF SUPERCAPACITORS

Supercapacitors show some superior characteristics over other energy storage devices in many ways, but it has a few drawbacks as well, shown in Table 3-3

Table 3-3: Features of supercapacitors [24]

Advantages:	**Drawbacks**
High specific power density	Low specific energy density
Extremely small ESR	Need balancing circuit for SC modules
Rapid charge-discharge ability	Terminal voltage and SOC are proportional
Long shelf life and extended lifetime	Price and market delivery challenges
Environmentally safe	
Wider operating Temperatures	

3.3 SUPERCAPACITOR MODULES AND APPLICATIONS

3.3.1 DIFFERENT TYPES OF SUPERCAPACITORS AND COMMERCIAL SUPERCAPACITOR MODULES

(a)

(b)

Figure 3-21: Different types of Supercapacitors: (a) Cells, (b) Modules [24]

3.3.2 SC MODULES (SCM) FOR POWER APPLICATIONS

SC applications are an emerging technology and has gained interest from product designers due to their unique features such as high-power density, low ESR, long lifespan, wider operating temperature range and much lower environmental impact in comparison to battery chemistries. However current available SC cells in the market are in the low voltage ranges, typically in ranges up to about 4V. To obtain the required voltage levels for different applications series cell connections are needed. Both series and parallel configurations can also be employed to get the full benefits of both topologies [35].

However, due to the variation in process materials used during mass-scale production, the individual cell properties may not be identical. The industrial standard of tolerance is in the range of $\pm$20% [36]. Therefore, the existence of intrinsic and extrinsic variation between each SC cell will encounter a significant problem with unequal distribution among those SC cells. This will consequently lead to some cells being exposed to over-voltage conditions. The over voltage condition is highly unfavourable to SC cells and will lead to permanent damage such as loss of capacitance, increase ESR, electrolyte decomposition, gas generation, bulging possible venting and ultimately losing its important aspect lifespan [37]. For a long lasting system it is vital to apply voltage balancing (voltage equalization) when SC cells are

connected in series. Therefore, when making SC modules (SC strings) it requires an effective voltage management system to monitor and control the cells within the safe and operational limitations. Figure 3-22 summarised the root cause, modes and effect of SC unbalance.

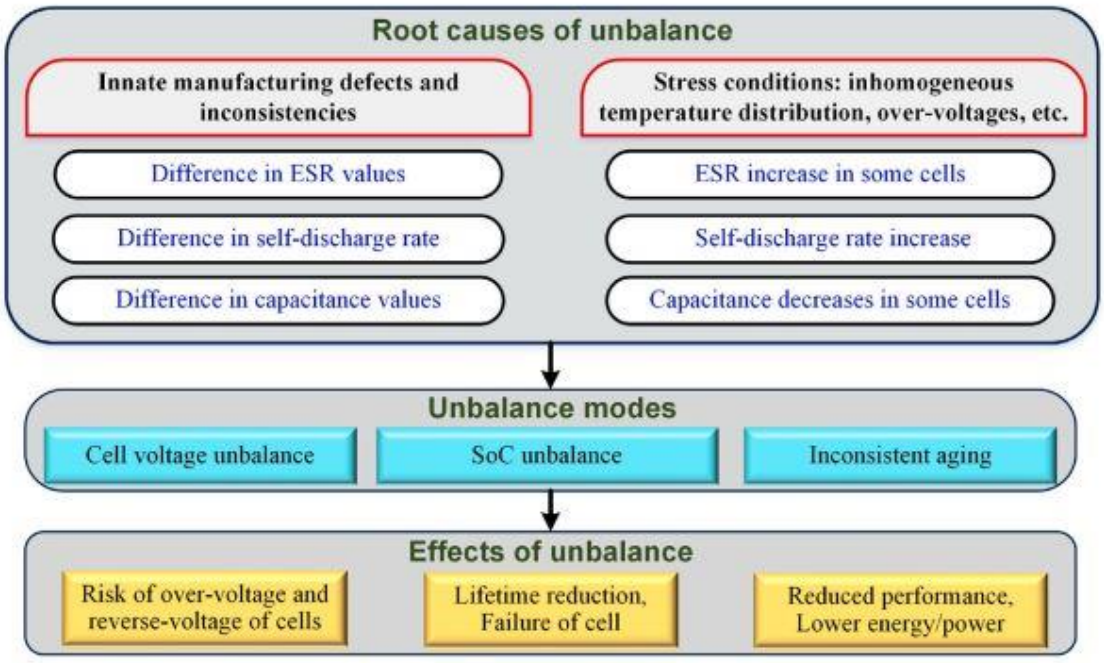

Figure 3-22:Root causes, modes and effects of supercapacitor module voltage unbalance [28]

3.3.3 SUPERCAPACITOR MODULE MANAGEMENT

Prior to choosing a voltage management system the following important strategies needs to be considered [38].

Categories of balancing strategies,

1. Energy dissipative behaviour
2. Balancing speed
3. Type of technology
4. Cost

It's important to know the key parameters and limitations of specific applications when choosing the right balancing strategy.

There are two common topologies in cell balancing in SC modules.

(a) Passive balancing

(b) Active balancing

Passive balancing involves the use of a shunt or voltage-dependent resistor to reduce the overvoltage. This method is relatively slow and increases charge losses, but is less expensive.

Active balancing involves the use of active control switches or amplifying systems [38]. This method is usually energy efficient and fast, but expensive while being slightly complex. They required several switches/ transistors, several capacitors, and inductors [28].

3.3.4 PASSIVE BALANCING METHODS

3.3.4.1 Resister Balancing

This method is the simplest approach to equalize the SCM and the most cost-effective strategy.

Each SC is connected to a bypass resistor in parallel as shown in Figure 3-23. In this method, the amount of current drawn by the resistor is proportional to the cell voltage. As cell voltage decreases it will result in less current being passed through the resistor [5, pp 231]. Similarly higher voltage cells will discharge faster by the resistor connected. The major drawback is the permanently connected resistor across SC dissipates the energy of the module and will be continuous.

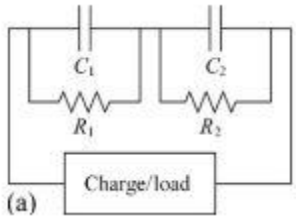

Figure 3-23: Passive balancing circuit with resistors [5, pp 230]

3.3.4.2 Zener diode balancing

In this method, the Zener diode is connected parallel to the capacitor instead of the resistor as shown in Figure 3-24. The diode limits the maximum charging voltage of the capacitor due to its clamping voltage. Zener diode clamping has an advantage over resistive balancing as there is no energy loss before the capacitor has reached the rated voltage. The main disadvantage of the balancing circuit is the lack of dynamic voltage balance due to the temperature dependency of the Zener diode. To achieve this dynamic voltage balancing, it also needs a high power clamping diode. High power high current Zener diodes are not available in the voltage range of SC. Overall the amount of energy loss is minimized through this method, and the balancing time is better than linear resistor [38].

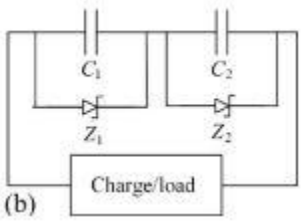

Figure 3-24: Passive balancing circuit with Zener diodes [5, (pp 230)]

3.3.4.3 Switch resistor balancing

This is another passive balancing method that will perform automatic voltage balance and avoid over-voltage conditions while maintaining the current of the SC module. Figure 3-25 shows the circuit topology for this method. In this method, capacitor voltages are monitored by pre-set voltage threshold setting and control of the respective switch. When the capacitor voltage is stabilized the switch will be turned off. In this method, there is power loss associated with the resistor when current passes through it. In comparison to the previous two methods, better voltage balancing can be achieved. A bandgap reference circuit can be used as the required voltage reference and power transistors can be used as bypass switches in this method. Due to inherent power dissipation, this method is best suited for low-power or low-current charge/discharge rate applications. [28]

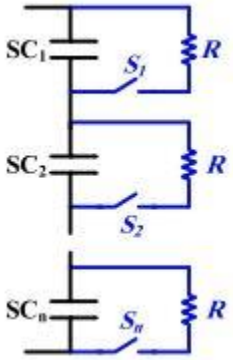

Figure 3-25: Passive balancing circuit with switch resistor [28]

3.3.5 ACTIVE BALANCING

Any application that needs a shorter balance time with limited energy loss will have to apply an active balancing method. Active balancing always involves integrated circuits [38]. Figure 3-26 shows an active balancing circuit diagram. Active balancing consumes less power and can handle large currents when capacitor voltages are not out of balance.

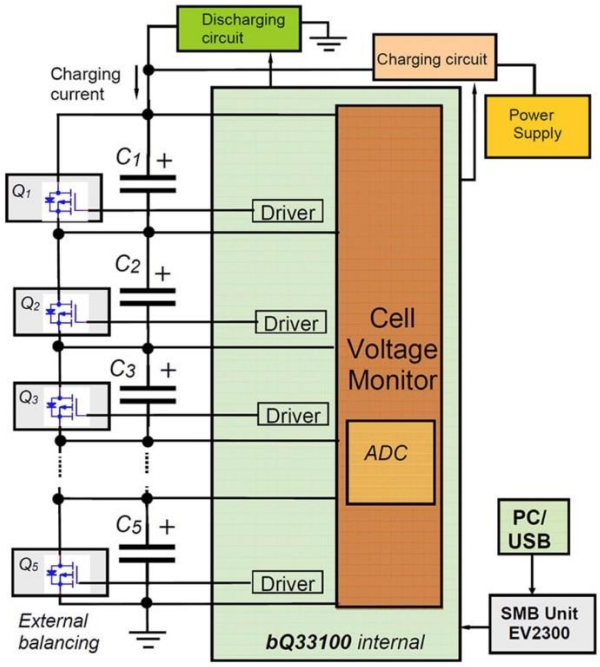

Figure 3-26: Integrated circuit-based active balancing [39]

With the development of new generation SCs, SC modules have become a more popular choice for energy storage systems. Therefore, leading electronic manufacturers develop IC-based supercapacitor auto-balancing MOSFET arrays that can serve as active balancing circuits for SC. These MOSFET arrays provide one shop solution offering self-balancing of SCM with nearly eliminating power losses. [ref; Analog device application note]
Table 3-4 shows the performance comparison of the voltage balancing technique.

Table 3-4: Performance comparison of voltage balancing techniques [40]

Parameter	Resistor circuit	Dedicated IC
Circuit cost	Low	High
Voltage balance performance	Medium	Good
Power consumption	High	Low
Operating voltage unit	No limit	Limited
Component count	2	1
Implementation	Easy	Easy

3.3.6 SUPERCAPACITORS IN ELECTRICAL CIRCUITS

Supercapacitors are used in a wide range of applications. SC can charge and discharge much faster than batteries and has a very large number of charge and discharge cycles compared to rechargeable batteries. Therefore, SCs are used in applications that require rapid power delivery and short-term energy storage.

3.3.6.1 Traditional applications [24]

(a) Electric cars, buses, aircraft, and other vehicles
(b) Portable devices
(c) Automotive tasks including the eco-mode, start-stop function, and regenerative breaking in the automotive industry.
(d) Utility voltage stabilizer system
(e) Battery-less uninterruptable power system (UPS)
(f) Military Industry
(g) Medical equipment
(h) Microgrid system and grid power buffer

Figure 3-27: Areas of supercapacitor application

3.3.6.2 Non-traditional applications

More than a decade of research by the power electronic research team at the University of Waikato (UOW) has led to the development of SC applications in a non-traditional way. These applications are currently known as Supercapacitor assisted (SCA) circuits. Following are the successful applications of the SCA technique.

(a) Supercapacitor-assisted low dropout regulator (SCALDO)

(b) Supercapacitor-assisted surge absorber (SCASA)

(c) Supercapacitor-assisted temperature-modification apparatus (SCATMA)

(d) Supercapacitor-assisted LED luminaries (SCALED)

CHAPTER 4: EVOLUTION OF NOVEL SUPERCAPACITOR ASSISTED LOSS MANAGEMENT (SCALoM) PRINCIPLE.

This chapter describes the innovative method of efficiency improvement through a fundamental circuit commonly known as the R-C loop. The power electronic research team at the University of Waikato first documented this new concept now commonly referred to as supercapacitor assisted loss management principle (SCALoM) [5,pp 251]. This novel concept is now well established and opens new avenues for supercapacitor (SC) based circuit design with high efficiency.

4.1 SIMPLE R-C LOOP BEHAVIOUR AND CHARGING EFFICIENCY.

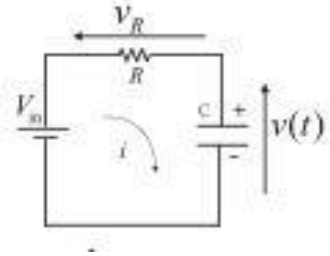

Figure 4-1: A simple RC circuit connected to a DC voltage source [5,pp 182]

Consider a typical R-C circuit connected to a DC source as shown in Figure 4-1. Assume that the capacitor is fully discharged and initial voltage is zero. When the switch is closed (on), there is zero voltage across the capacitor while the resistor takes on the rest.

The energy stored on the capacitor can be expressed in terms of the work done by the source. The voltage represented the energy per unit charge, so the work done to move charge quantity dq from the negative plate to the positive plate can be expressed by

$$dw = Vdq = \frac{q}{C}dq \tag{4.35}$$

V – voltage of the capacitor C- Capacitance of the capacitor

If Q is the amount of charge stored at the equilibrium state, at that time the full supply voltage appears across the capacitor. The total energy stored can be obtained by solving the integral equation below.

$$E = \int_0^Q \frac{q}{c}dq = \frac{1}{2}\frac{Q^2}{C} \tag{4.36}$$

Equation 4.2 can be expressed as,

$$E = \frac{1}{2}\frac{Q^2}{C} = \frac{1}{2}CV^2 \tag{4.37}$$

By the definition of capacitance

$$C = \frac{q}{V} \tag{4.38}$$

The energy supplied by the source is E,

$$E = QV = CV^2 \tag{4.39}$$

This result shows that, when charging the capacitor, ONLY half of the energy supplied is stored in the capacitor and the other half is dissipated as heat by the resistive path. It is important to note that the total energy stored is independent of the resistive element in the circuit. Therefore, it can be observed, no matter the resistance in the loop only 50% of energy is stored when charging a capacitor.

If we analyse this further, the first quantity of charge dq onto the capacitor takes much less work because at that stage most of the source voltage appears across the resistance in the pathway. Therefore, resistive losses (I^2R) are greatest at the beginning and exponentially decrease towards the end of the charging cycle. But considering a full charging cycle 50% of energy is anyway lost as heat. Therefore, the charging efficiency of a simple resister capacitor circuit can expect only 50% efficiency when charging a completely discharged capacitor.

4.2 LOSS CIRCUMVENTION ANALYSIS OF R-C CIRCUIT

The previous discussion observed that the typical R-C circuit shown in Figure 4-2 connected to a constant voltage source V (volts) the stored energy can be quantified as E_c

$$E_C = \frac{1}{2}CV^2 = \frac{1}{2}QV \tag{4.40}$$

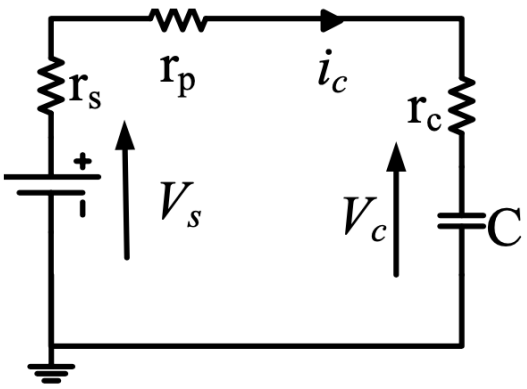

Figure 4-2: Basic RC charging loop [41, pp 46]

Instantaneous current in the loop i_c, shown in Figure 4-2, can be written as,

$$i_c = \frac{V_s}{r_p + r_c + r_s} e^{\frac{-t}{C(r_{p+r_c+r_s})}} \tag{4.41}$$

Where r_c is the equivalent resistance (ESR) of the capacitor, r_p is the path resistance and r_s is the internal resistance of the DC source.

The total energy loss in the loop E_{loss} is due to the total resistive element in the circuit loop. Which can be equated to the energy stored in the capacitor.

$$E_{loss} = \int_0^t i_c^2 (r_p + r_c + r_s)\, dt = \frac{CV^2}{2} = \frac{QV}{2} \tag{4.42}$$

The charging efficiency (η) of the loop in Figure 4-2 can be estimated by,

$$\eta = \frac{E_C}{E_C + E_{loss}} \tag{4.43}$$

The total loss is purely due to the resistive component in the loop. Therefore, the energy loss contributed by each resistive element can be expressed as a fraction of the total loss as follows.

$$E_{SL} = \left(\frac{r_s}{r_p + r_c + r_s}\right) E_{loss} \tag{4.44}$$

$$E_{PL} = \left(\frac{r_p}{r_p + r_c + r_s}\right) E_{loss} \tag{4.45}$$

$$E_{CL} = \left(\frac{r_c}{r_p + r_c + r_s}\right) E_{loss} \tag{4.46}$$

Analysing the individual losses indicates very valuable and impactful conceptual information about the R-C loop. This indicates that if we insert a useful resistive load into the loop, it can make use of the lost energy through the load. This revolutionary idea was developed by the power electronic research team of the University of Waikato (UoW) and now it is known as the Supercapacitor Assisted Loss Management (SCALoM) concept for R-C charging loop.

4.3 MODIFIED R-C LOOP AND EFFICIENCY

Let us consider the circuit in Figure 4-3. This circuit is similar R-C circuit loop before, but we modify the circuit by inserting useful resistive load (R_L) in series.

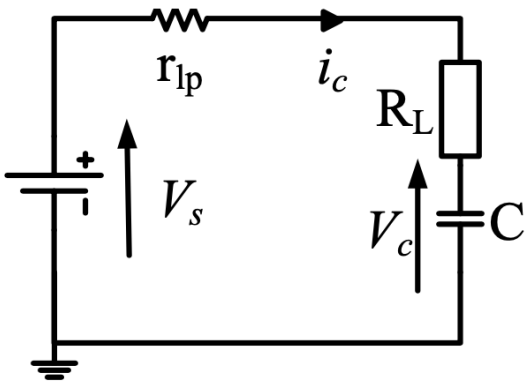

Figure 4-3: Modified RC loop with loss circumvention concept [41, pp 46]

To simplify the quantitative formula, let us take

$$r_{lp} = r_p + r_c + r_s \tag{4.47}$$

Where r_c is the equivalent resistance (ESR) of the capacitor, r_p is the path resistance and r_s is the internal resistance of the DC source.

Similar to the previous section, to quantify the individual losses corresponding to each resistive element, when charging a capacitor from 0 to V_s can be written as,

$$E_{rlp} = \left(\frac{r_{lp}}{r_{lp} + R_L}\right) E_{loss} \tag{4.48}$$

$$E_{RL} = \left(\frac{R_L}{r_{lp} + R_L}\right) E_{loss} \tag{4.49}$$

By inserting a useful load (R_L) into the circuit, this load now consumes a fraction of energy which was previously considered as lost. In other words, we have consumed some lost energy in a useful manner resulting in the efficiency of this circuit increased beyond 50%. The overall efficiency can be interpreted as efficiency η,

$$\eta = \frac{E_C + E_{RL}}{E_C + E_{RL} + E_{rlp}} > 50\% \tag{4.50}$$

4.4 R-C CIRCUIT WITH OVER-RATED DC VOLTAGE SOURCE AND PRE-CHARGED CAPACITOR

As shown in Figure 4-4, consider the scenario where a pre-charged supercapacitor is introduced to the circuit, where the rated DC voltage of the supercapacitor is V_w and the DC source voltage of m times the working voltage of the capacitor (V_w). Where $m \geq 1$. The capacitor is pre-charged to a factor k ($0<k\leq1$)

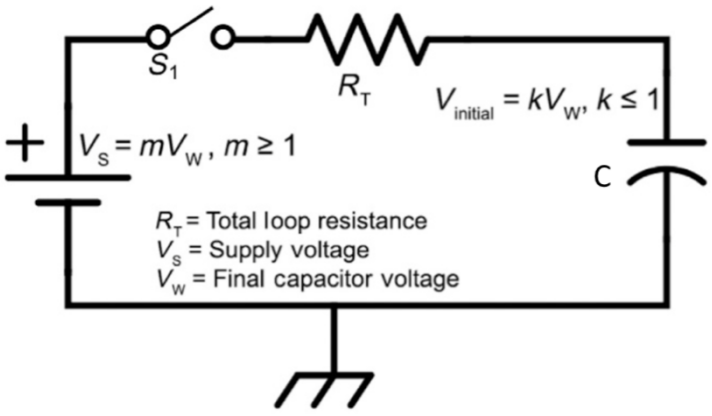

Figure 4-4: Capacitor charging circuit [5, pp 256]

When the capacitor is charged from 0 to V_w from the DC supply of mV_w, the capacitor voltage at any given time t is,

$$V(t) = mV_w\left(1 - e^{-\frac{t}{R_T C}}\right) \tag{4.51}$$

As shown in Figure 4-5, let time t_1 and t_2 be the times the capacitor charges from voltage kV_w and V_w respectively.

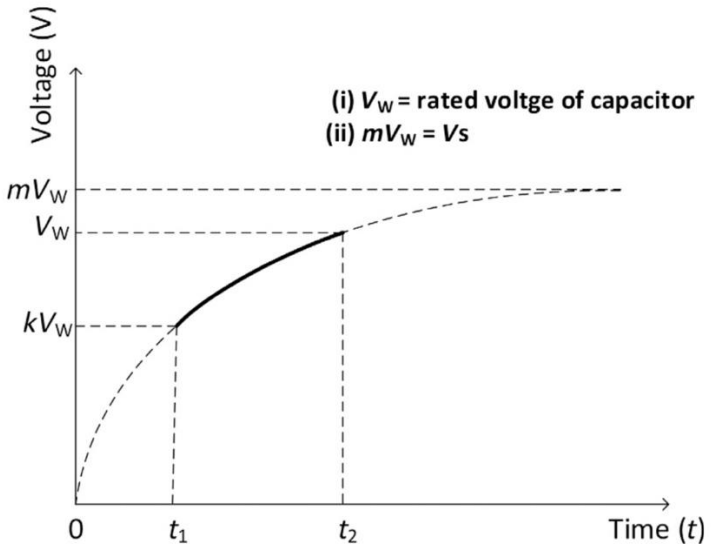

Figure 4-5: Capacitor charging curve [5, pp 256]

Using Equation 4.17 at time t_1,

$$kV_w = mV_w\left(1 - e^{-\frac{t_1}{RC}}\right)$$

$$e^{-\frac{t_1}{RC}} = \frac{m-k}{m} \tag{4.52}$$

similarly at time t_2,

$$V_w = mV_w\left(1 - e^{-\frac{t_2}{RC}}\right)$$

$$e^{-\frac{t_2}{RC}} = \frac{m-k}{m} \tag{4.53}$$

The energy stored in the capacitor between time t_1 and t_2 is,

$$E_C(t_1, t_2) = \frac{1}{2}CV_w^2 - \frac{1}{2}C(kV_w^2)$$

$$E_C(t_1, t_2) = \frac{1}{2}CV_w^2(1 - k^2) \tag{4.54}$$

The total energy loss through the resistive element in the path over this period is,

$$E_R(t_1, t_2) = \int_{t_1}^{t_2} i^2(t)R\, dt \tag{4.55}$$

Applying Kirchhoff's law, the instantaneous current at any given time t is,

$$i(t) = \frac{mV_w e^{-\frac{t}{RC}}}{R} \tag{4.56}$$

The charging efficiency for this configuration becomes,

$$\eta = \frac{E_C}{E_C + E_R} \tag{4.57}$$

Solving equation 4.21 with equation 4.22 provides,

$$E_R(t_2, t_1) = \frac{V_w^2 C}{2}[k^2 - 2mk + 2m - 1] \tag{4.58}$$

By substituting Equation 4.20 and equation 4.24 efficiency becomes,

$$\eta = \frac{1 + k}{m} \tag{4.59}$$

This result shows that the charging efficiency of the R-C loop can be varied by the m and k factors.

m and k factors are considered over-rating factor of the DC voltage source and the pre-charged factor of the supercapacitor respectively. It is worth noting that the capacitor is never exposed to a working voltage above its rated voltage during this process.

Analysing the relationship in Equation 4.25 shows that if, the capacitor has no initial charge (k→0) and the DC power source is not over-rated (m→1) the above relationship reduces to n→1/2. (The usual 50% efficiency case). It proves that the above generic relationship for the R-C circuit can be enhanced.

The overall charging efficiency can be enhanced when the capacitor pre-charge level is close to the higher end and when the over-rated factor is towards the lower end.

The graphical presentation in Figure 4-6 shows that the best theoretical efficiency can be achieved when (k,m) → (1,1)

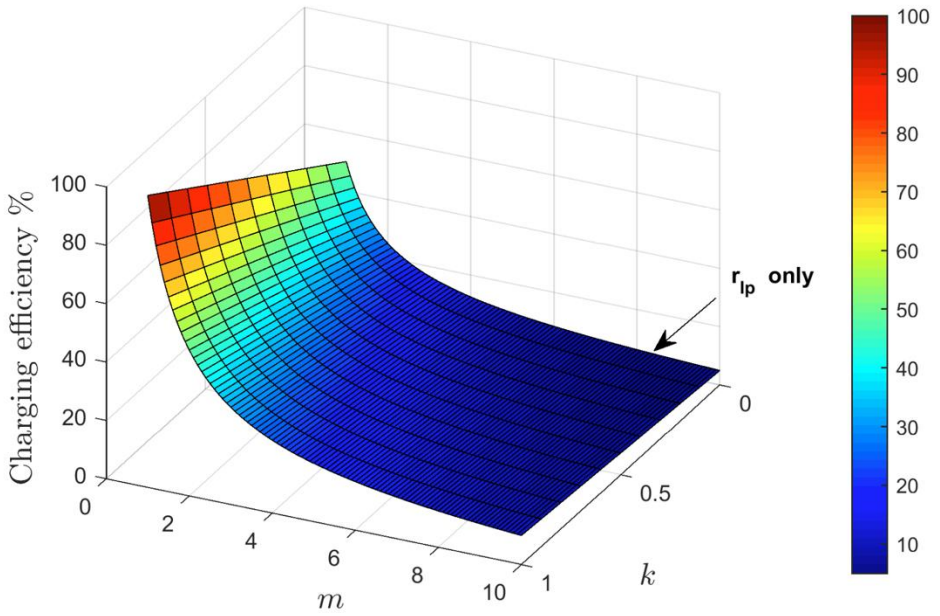

Figure 4-6: Variation of charging efficiency with over-rate factor m and pre-charged factor k [41, pp 49]

4.5 R-C CIRCUIT ANALYSIS OF OVER-RATED DC VOLTAGE SOURCE AND PRE-CHARGED CAPACITOR WITH USEFUL LOAD.

Consider a R-C circuit as shown in Figure 4-7 with useful resistive load R_L connected in series.

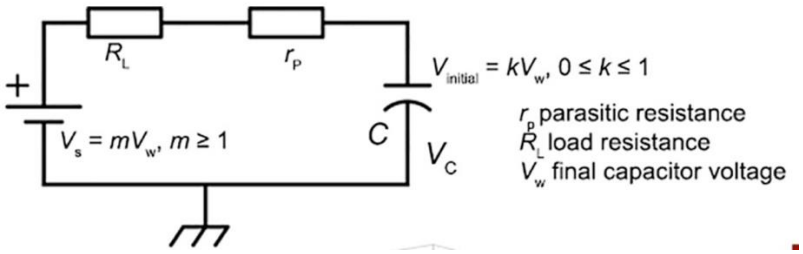

Figure 4-7: Modified circuit with useful resistance R_L inserted [5, pp 262]

It was observed before when a useful load is inserted into an R-C charging loop, the "useful "load does some work while consuming some losses in the loop during the charging process.

In the previous section, we derived the energy losses through the resistive path $E_R(t_2,t_1)$

$$E_R(t_2,t_1) = \frac{V_w^2 C}{2}(1-k)(2m-k-1)$$

Hence,

$$E_{R_L+r_{lp}} = \frac{V_w^2 C}{2}(1-k)(2m-k-1) = x \tag{4.60}$$

Now let us look at energy losses related to each resistive component as before.

The consumed usefully through R_L is

$$E_{R_L} = \frac{R_L}{R_L + r_{lp}}x \tag{4.61}$$

The energy loss component through resistance in the path is,

$$E_{r_{lp}} = \frac{r_{lp}}{R_L + r_{lp}}x \tag{4.62}$$

Let us define $\frac{R_L}{r_{lp}} = A$ and we can write equation (4.27) and equation (4.28) as,

$$E_{R_L} = \frac{Ax}{A+1}$$

$$E_{r_{lp}} = \frac{x}{A+1}$$

The total energy supplied by the DC source can be written as,

$$E_s = E_C + E_{R_L + r_{lp}} \tag{4.63}$$

By substituting relevant components, E_s can be simplified to,

$$E_s = CV^2 m(1-k) \tag{4.64}$$

Substituting equation (4.20), equation (4.27) and equation 4.30 to efficiency formula provides,

$$\eta = \frac{E_C + E_{R_L}}{E_S}$$

$$\eta = \frac{1}{A+1}\left[A + \frac{(1+k)}{2m}\right] \tag{4.65}$$

Where A is the ratio of load resistance to path resistance (parasitic resistance). $A = \frac{R_L}{r_{lp}}$

When A→0, This equation reduced to the relationship derived earlier.

For numerical values of A=0,1,9 the charging efficiencies are illustrated in the graphs, shown in figure 4-8, for varying m and k factors.

These graphical presentations show evidence that the overall efficiency of the R-C charging loop can be increased by inserting a useful resistive load.

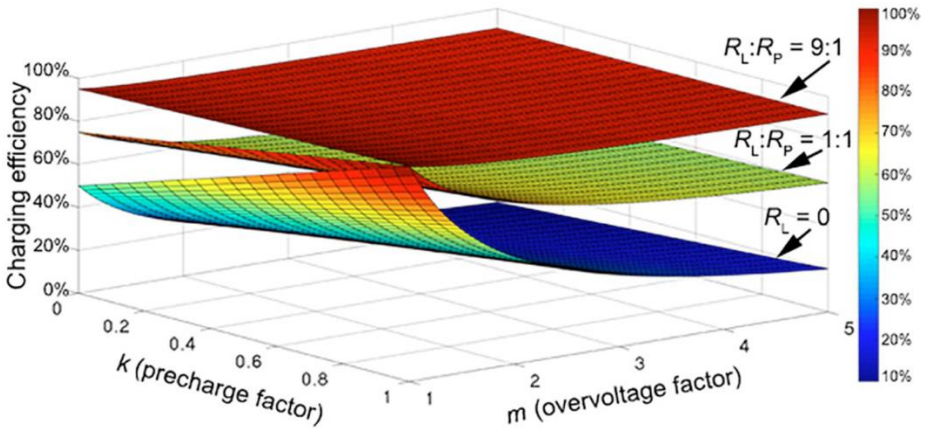

Figure 4-8: Graphical representation of circuit behaviour in terms of efficiency vs m (over-rated or over-voltage factor) and k (pre-charged factor) [5, pp 256]

4.6 SUCCESSFUL APPLICATION OF SUPERCAPACITOR ASSISTED LOSS MANAGEMENT (SCALoM) CONCEPT.

4.6.1 Supercapacitor-assisted low-dropout regulator (SCALDO)

Consumer electronic products are found in every corner of the world. All those products use single or multiple DC-DC converters in their power management system. Commonly used converters are linear regulators, switch-mode converters or switched capacitor converters. Linear DC-DC converters are able to provide high-quality output with less noise sensitivity and high current capability. It does however come with a big drawback of lower efficiency. Inductor-based switch-mode converter is operated at a high frequency and circuits are more complex. The high speed switching also require the need to address RFI/RMI issues. However, they provide much high efficiency at a very small form factor. Similarly, the switched capacitor converters provide very high efficiencies while also operating at high frequency. They do however have considerably low current capabilities. Sometimes they require additional voltage regulators to obtain a precise DC voltage required by the load.

Low-dropout regulators (LDOs) are a special category of linear regulators used in most portable products. As its name suggests the difference between the input voltage and regulated output voltage is small. Therefore, the end-to-end efficiency (ETEE) is very high.

The SCALDO circuit topology was developed based on the SCALoM concept, where a lossless voltage dropper element, an ideal supercapacitor, is introduced into the path of the series pass element. In this concept, the loaded LDO was inserted as a useful load. Figure 4-9 shows the circuit topology implemented in the SCALDO concept.

In doing so, the resistive losses are replaced by useful power in the LDO while charging the supercapacitor and making large time-constant R-C circuits slowing down the charging cycle. Due to the very low equivalent resistance (ESR) of the supercapacitor, it acts as a lossless voltage dropper. Once the supercapacitor (SC) reaches the required voltage, using the switching system the supercapacitor is set into discharging mode while disconnecting the system from the DC source. The stored energy of the supercapacitor is now fed to the LDO. Due to the large time constant created with the useful load, the switching cycles take place at very low frequencies. Therefore, EMI/RMI issues are not applicable. Application of the novel SC proves that the end-to-end efficiency can be increased by a multiplication factor of more than one. SCALDO is the first application under the SCALoM concept which was patented {5,(pp 293-309)] in 2011.

More detail of the SCALDO converter technique is available in [5, (pp 273-309), 41, 43]

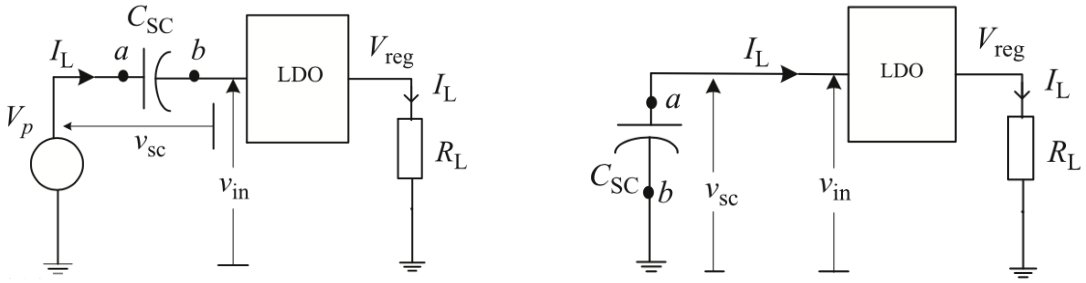

(a) *(b)*

Figure 4-9: Supercapacitor-assisted Low-dropout regulator [5, pp 283]

4.6.2 Supercapacitor-assisted surge absorber (SCASA)

A traditional surge protector design is made with technologies based on non-linear devices (NLD), such as metal oxide varistors (MOVs) and bidirectional break-over diodes (BBDs). These devices are capable of absorbing surge energy within a short period. If these non-linear devices are exposed to repeated surges before dissipating their previously generated heat, they will not be able to withstand further surge energy and the device will fail. But supercapacitors, due to their high energy storage capability within a very short time, can absorb energy by several second-order transient surges without failure of the device.

University of Waikato supercapacitor researchers were able to develop a unique patented surge absorber design based on an R-C circuit where resistors were inserted as an energy dissipative element with a supercapacitor and inductive element in the path. Figure 4-10 shows the unique

circuit configuration that was implemented in the patented SCASA concept. More details are available in the following references [5, (pp 377-394), 43, 44].

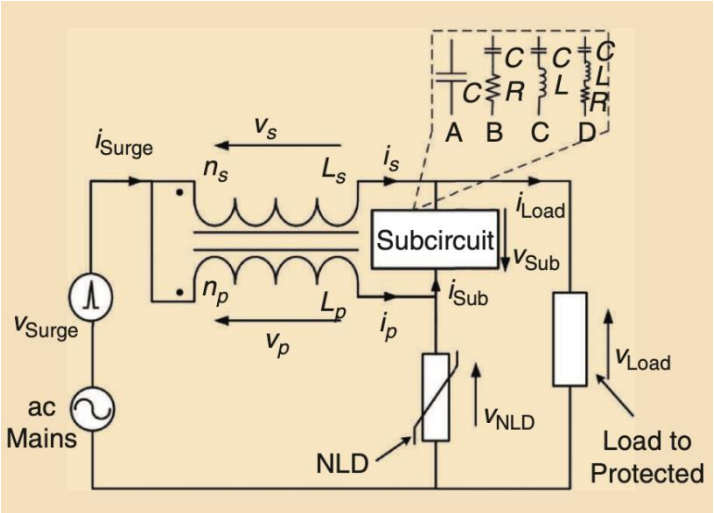

Figure 4-10: Supercapacitor Assisted Surge Absorber (SCASA) [43]

4.6.3 Supercapacitor-assisted temperature modification apparatus (SCATMA)

This application is a timely solution for the world we are facing today. Hot water supply is considered essential for everyday needs especially in countries of cold climates. But in typical designs, the hot water supply units are placed in a central location and distributed through small pipes to the individual faucets. Therefore, it is unavoidable that the water trapped in between the faucet and the hot water system outlet becomes cold. Whenever the faucet opens after a period of unuse the initial water is cold for the user. Therefore, there is a considerable amount of clean water that gets wasted. A rapid heating method is the ultimate solution to overcome this practical problem of every household.

University of Waikato SC researchers developed a solution to overcome the above practical issue. It is called the supercapacitor-assisted temperature modification apparatus (SCATMA).

The total energy requirement for rapid heat of water flowing at a domestic water supply within a short period (in seconds) cannot be achieved by the power through a domestic wall socket (230VAC, 50HZ, 10A). But paying attention to supercapacitor characteristics, the quick power delivery capability due to its very low ESR, very high short circuit current capabilities and very large cycle life encouraged the development of the SCATMA application.

This application utilizes a set of high-power low voltage inline heater coils with temperature sensors and flow measurement sensors that are controlled by a power electronic control unit. Figure 4-11

shows the implementation block diagram of SCATMA. More details of this application are available in reference [5, (pp 265-267), 43, 45].

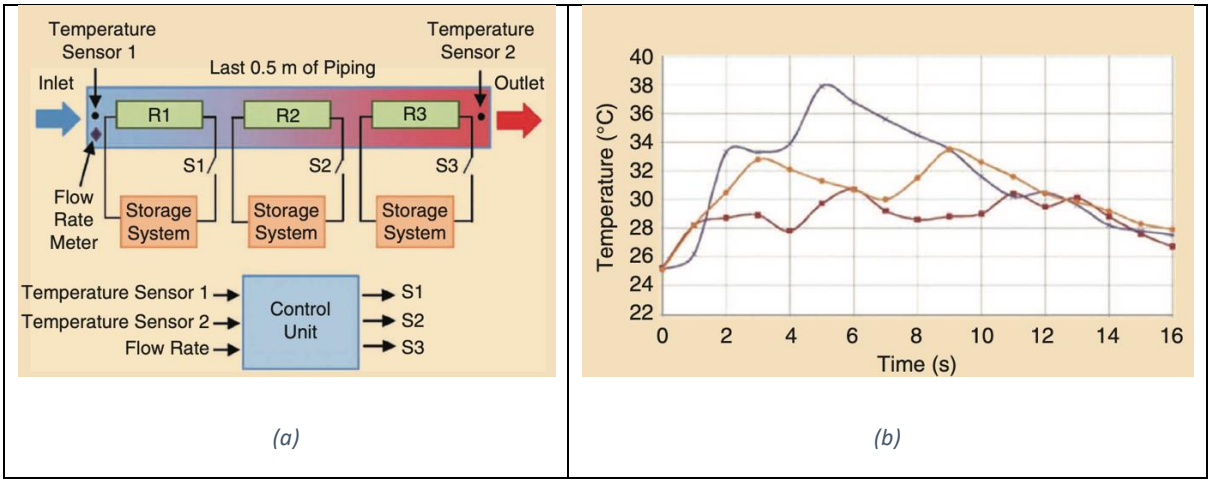

Figure 4-11: Supercapacitor assisted temperature modification apparatus:(a) Block diagram (b) temperature vs time for 15V supercapacitor banks with different changeover delays of S1, S2 and S3 [43]

4.6.4 Supercapacitor-assisted LED lighting (SCALED)

Renewable energy sources are getting more attention for the growing demand of a sustainable future. Solar photovoltaic and wind energy solutions are leading the way and have greater potential for future energy demand. These renewable energy sources generate a purely DC energy. DC powered appliances can greatly benefit by eliminating the inverter requirements to achieve high end-to-end efficiency (ETEE). As a result there is a growing interest in DC-powered goods around the world. LED lighting is a prime application that benefits from DC power generation.

University of Waikato SC researchers have developed another SC-based application by modifying the R-C circuit through the introduction of a DC operable LED lamp system as a useful resistive load. The SCALED system consists of two identical supercapacitor modules and two identical LED light assemblies while being powered by a photovoltaic system. Figure 4-12 shows the circuit topology implemented in the SCALED system. The switching control system operates in such a way that the fully charged SCM supplies one LED assembly while the other partially charged SCM is charging through the other LED assembly which is connected in series with a DC power source. This power converter system switching frequency occurs at an extra low frequency and therefore provides the advantage of a power converter system that is free from EMI/RFI. The most common problem associated with solar photovoltaics is the daily energy fluctuation which can be addressed by properly sizing the SCM to accommodate such variation. More detail about the SCALED lighting system can be found in these references [5, (pp 359-373), 43, 46] .

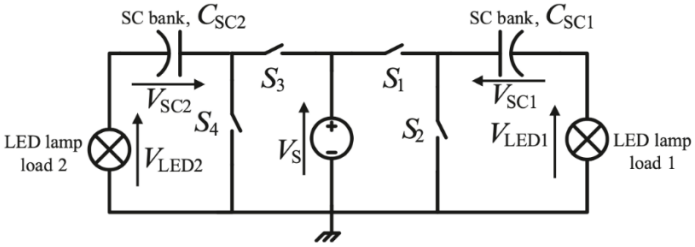

Figure 4-12: Supercapacitor Assisted LED lighting system [5, pp 365]

4.6.5 SCA Refrigerator Technique

Given these few SCA techniques, we see that SCALoM concept is a very valuable concept to develop high performance power electronic building blocks (PEBB) such as low frequency DC-DC converters, surge protectors and others. Extending these experiences, currently the research team works on several other applications of SCALoM concept. In the next few chapters, how the SCALOM concept is applied to a (renewable energy based) DC powered refrigerator is detailed.

CHAPTER 5: RESIDENTIAL REFRIGERATOR TECHNOLOGY

5.1 REFRIGERATION PRINCIPLES AND MAIN COMPONENTS

A refrigerator is one of the common home appliances used in most houses. Undoubtedly a refrigerator is one such appliance that consumes a considerable amount of energy. Unlike other appliances, it operates 24*7, year around. Therefore, refrigerator manufacturers make a constant efforts to design the most energy-efficient product for the consumer market.

The refrigerator is a thermally insulated cabinet designed to store and preserved food. It is equipped with a mechanism that takes the thermal energy out from the inside compartment and keeps the temperature low inside within defined limits. It is designed to compensate for the thermal losses through leakage by thermal insulation and adding energy due to losses through opening of refrigerator door. The general heat-transferring mechanism employed in domestic refrigerators is called a sealed system. This is essentially comprised of a compressor, evaporator, condenser, flow control valve and a refrigerant (gas). The characteristics of each element depends on the type of system and the specific requirements. More sophisticated devices such as multi-compartment systems increase the complexity.

5.1.1 Refrigeration Cycle

Many literatures explain the refrigeration cycle as a process where the working fluid, called the refrigerant, absorbs the heat from the enclosed surrounding providing an environment of low temperature and releasing that heat to the atmosphere. Figure 5-1 shows the process that takes place in a typical refrigeration cycle.

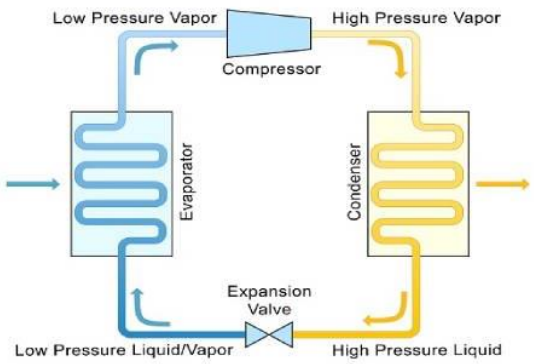

Figure 5-1: Schematic of refrigeration cycle [47]

When the refrigerant (gas) is in its liquid form, it takes the heat from the content (inside compartment) and evaporates to form gas thereby, cooling the contents in the refrigerator. Afterwards, this gas is compressed by the compressor to convert it back into liquid again releasing the heat absorbed in the previous step into the atmosphere.

Once the pre-set temperature is reached, the device known as a thermostat (thermal switch), which controls the compressor function, switches off the compressor. When the cabin temperature goes above the set value the thermostat switches on the compressor again and the system will continue cycling keeping the contents cool.

The overall heat transfer takes place by circulation of gas and this function is done by the compressor. Therefore, the compressor is considered the heart of the refrigeration process.

There are various compressor designs that are employed in the refrigeration industry based on their cooling capacity. But the primary drive mechanism of the compressor is accomplished by either AC or DC motors. This means the compressor system is the most energy demanding component in the refrigeration system. As a result more energy-efficient compressors and motor technologies are in continuous development.

5.2 COMPRESSOR TECHNOLOGIES FOR DOMESTIC REFRIGERATORS

In modern refrigerators, there are three types of compressor systems used. They are namely, open refrigerator compressors, semi-hermetic compressors, and hermetic compressors.

The open-type compressors utilize the involvement of pulleys and belts to drive the compressor section by the motor. This type is generally found in large commercial refrigeration. Domestic refrigerators are commonly seen as hermetically sealed type compressors system. The main advantages this type offers are having no moving parts exposed out of the seal casing, minimizing refrigerant gas leakage, minimizes noise, and does not require any maintenance. The semi-hermetic system is similar to the hermetic type, but not completely sealed and accessible for maintenance [48].

Whatever compressor system used, it consists of two main parts. That is the compressor pump and compressor drive motor. The pump moves refrigerant through the system and the motor drives the pump mechanism.

Most domestic refrigerators employ a piston-type (reciprocating) compressor pumps. The principal operation consists of a piston motion to compress refrigerant gas. In this type, the piston is connected to the drive motor via a crankshaft. The motion of the crankshaft creates the suction, compression, and discharge. Figure 5-2 shows such an assembly.

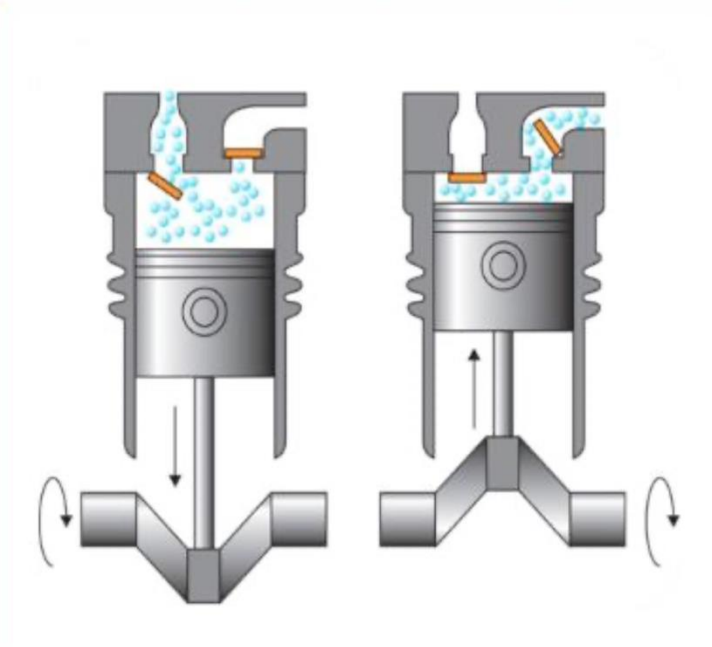

Figure 5-2: A typical reciprocating compressor operation [49]

5.3 Functional differences between a regular refrigerator and an inverter refrigerator

The fundamental difference between these two types of refrigerators is the compressor drive motor. Both use electric motors but of different types. Until recently, the domestic refrigerator compressor was designed to work only with single-phase induction motors. It is either on or off, based on the temperature setting of the thermostat signal. In designing this type of refrigerator, the primary objective is that the equipment must be able to handle peak load conditions. Therefore, at any time it runs at a peak load condition even if the cooling requirement is less. Hence, every time the set temperature goes above the pre-set value, the compressor operates at maximum power, thereby using a lot of energy at each cycle it is on. Furthermore, it increases the wear and tear of the compressor system and creates unwanted noise during operation.

The drive motors used in regular-type refrigerator compressors are either single-phase or three-phase induction motors. Figure 5-3 shows the electrical diagram of a regular refrigerator with a single-phase induction motor.

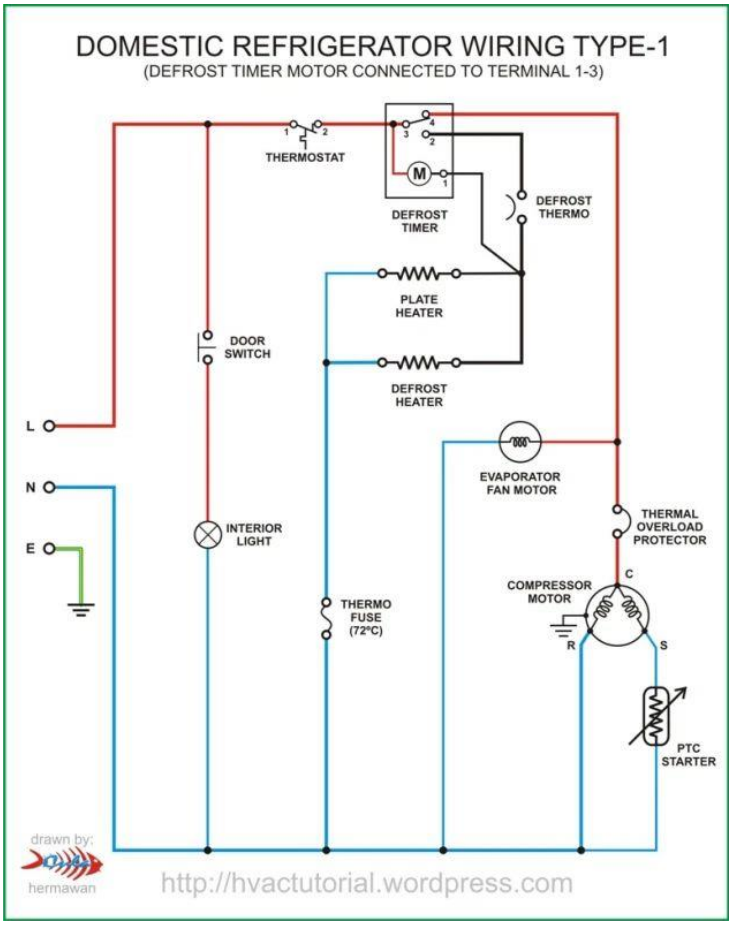

Figure 5-3: Single-phase induction motor refrigerator circuit diagram [50]

Inverter technology has modernized most home appliances. With the significant reduction in energy consumption, they have become more attractive to the consumer. Although they come with different names of inverter technologies commercially, from an engineering point of view, in any inverter technology, the compressor is driven by using a brushless direct current (DC) motor via an intelligently controlled inverter circuit. Figure 5-4 (a) shows a typical block diagram of the inverter module for motor control. The operational significance of this type of system is that the motor allows the compressor to run at different levels of speed depending on the temperature demand and other environmental conditions. In other words, the inverter compressor is a variable-speed compressor that uses a brushless DC motor to operate at variable speed. The most important gain achieved by variable speed drive compressors is the reduction of energy consumption by eliminating unnecessary losses incurred by the sudden power draw from regular refrigerator compressors, as shown in Figure 5-4(b). The most efficient inverter technology available in the market is advertised as allowing, energy saving of up to 40% in comparison to similar capacity regular refrigerator models [50]. [It is a good idea to mention that BLDC motor means a 3 phase variable frequency capable induction motor fed by a 3 phase inverter inside the BLDC motor drive circuit.]

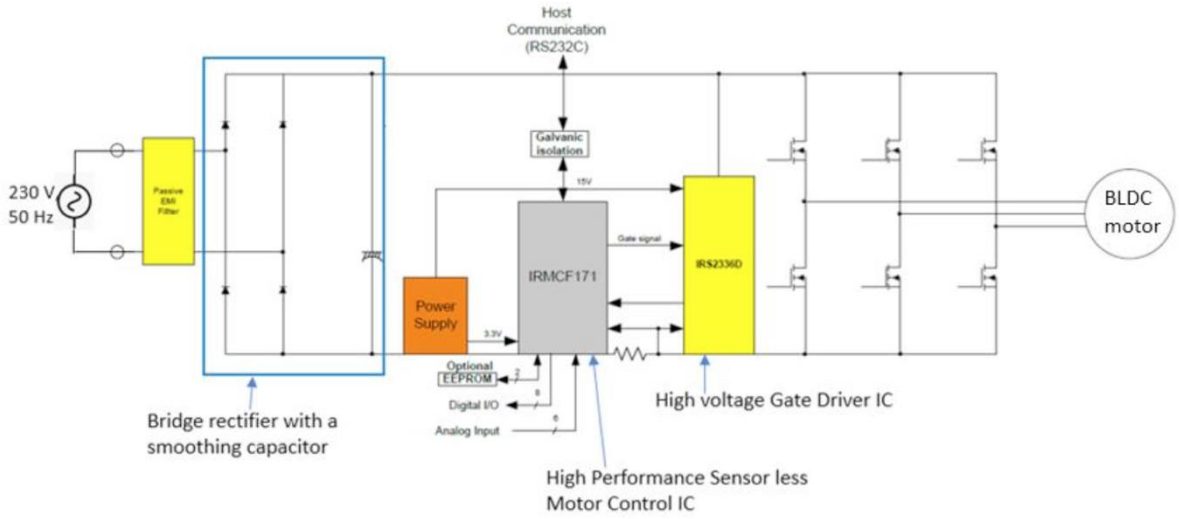

(a)

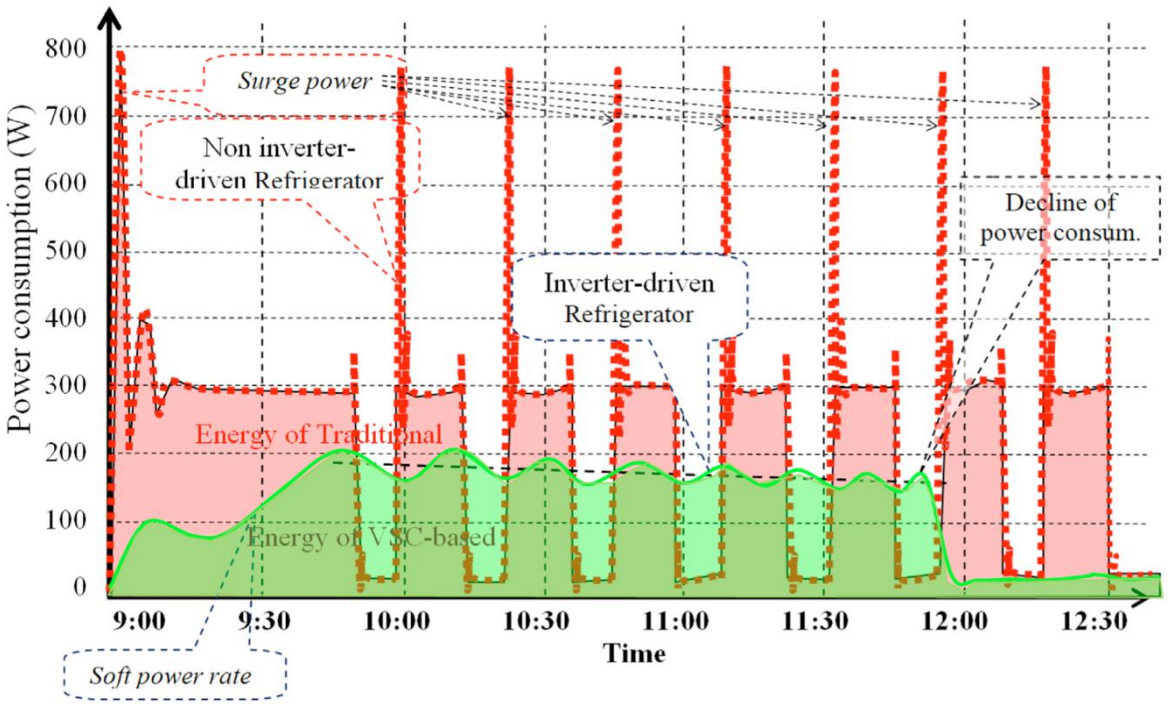

(b)

Figure 5-4: Inverter refrigerator: (a)Block diagram of typical inverter module for motor control, (b) Operational behaviour and power consumption comparison of inverter and non-inverter refrigerator [3, 52] [Your Figure 5-5 (a) is not of good quality. Do you have a possibility to redraw it. Exteranl examiners usually comment (negatively) when complex figures are not easily readable]

Among other benefits, a few important technical benefits are, [53]

(1) Regular motor compressors need 3-4 times more current to start up. But the inverter compressor consists of a variable speed motor that stat up gradually and as a result requires less current during compressor start-up.

(2) Regular Refrigerator motors have a much lower power factor. BDLC motor used in inverter refrigerator have a power factor closer to unity.

(3) Inverter technology can easily work with solar PV systems. Because it consumes less current and hence, not require a high current capable PV system.

5.4 COMPARISON OF THE TWO COMPRESSOR MOTOR TYPES (BLDC VS INDUCTION MOTOR)

Table 5-1: BLDC motor vs Induction motor [54]

Features	BLDC Motors	AC Induction Motors
Speed/Torque Characteristics	Flat – Enables operation at all speeds with rated load.	Nonlinear – Lower torque at lower speeds.
Output Power/ Frame Size	High – Since it has permanent magnets on the rotor, a smaller size can be achieved for a given output power.	Moderate – Since both the stator and rotor have windings, the output power to size is lower than BLDC.
Rotor Inertia	Low – Better dynamic characteristics.	High – Poor dynamic characteristics.
Starting Current	Rated – No special starter circuit is required.	Approximately up to seven times of rated – Starter circuit rating should be carefully selected. Normally uses a Star-Delta starter.
Control Requirements	A controller is always required to keep the motor running. The same controller can be used for variable speed control.	No controller is required for fixed speed; a controller is required only if variable speed is desired.
Slip	No slip is experienced between stator and rotor frequencies.	The rotor runs at a lower frequency than the stator by slip frequency and slip increases with load on the motor.

Chapter 6: Supercapacitor-Assisted Refrigerator (SCA-Ref)

6.1 Refrigerator Specifications

The commercially available camping refrigerator is rated for 12/24V with a max power of 50 W. Table 1 shows the specifications of this camping refrigerator. Exposing the back panel, as shown in Figure 6-1, displays the compressor and the controller with an inverter embedded inside. Sealed inside the compressor unit is a BLDC motor where a three-phase connection is present from the compressor to the control board.

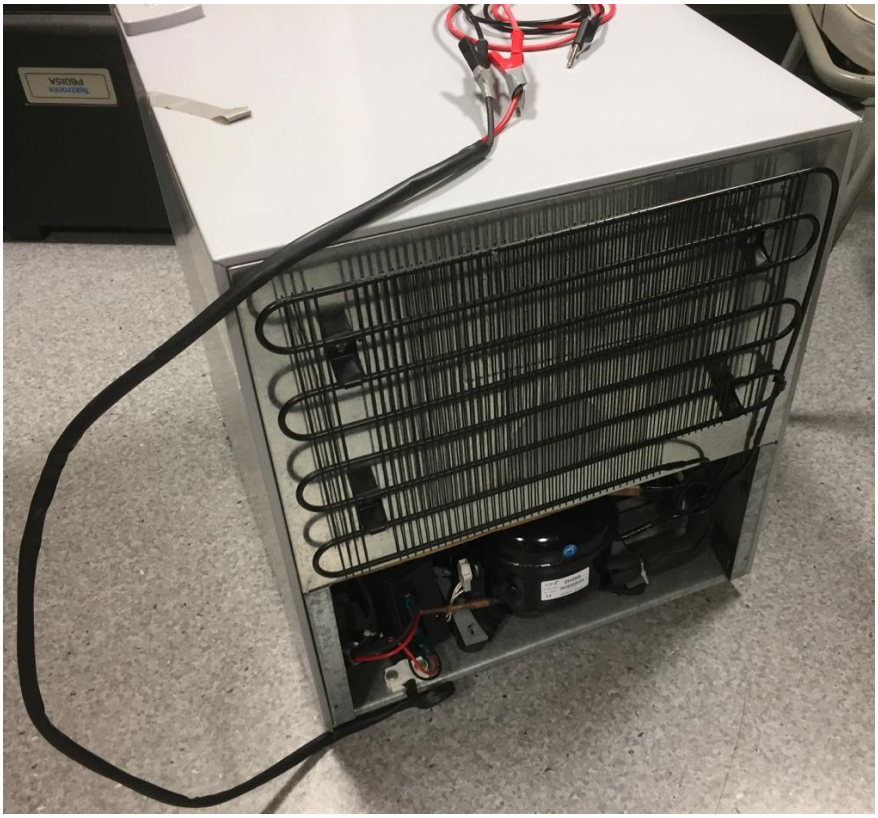

(a)

(b)

(c)

Figure 6-1: 12V/24V DC refrigerator (a) Reverse panel (b) Compressor and controller (c)Controller module

The performance of the refrigerator was measured for thermostat setting 2 and 6, as shown in Figure 6-2 and Figure 6-3.

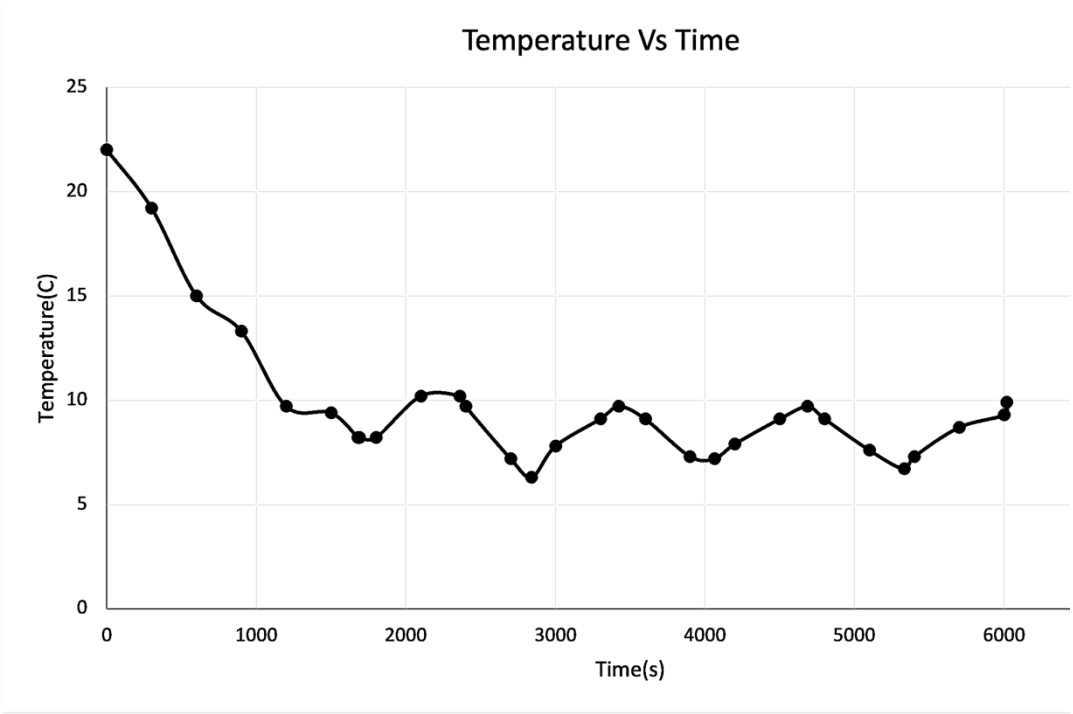

(a)

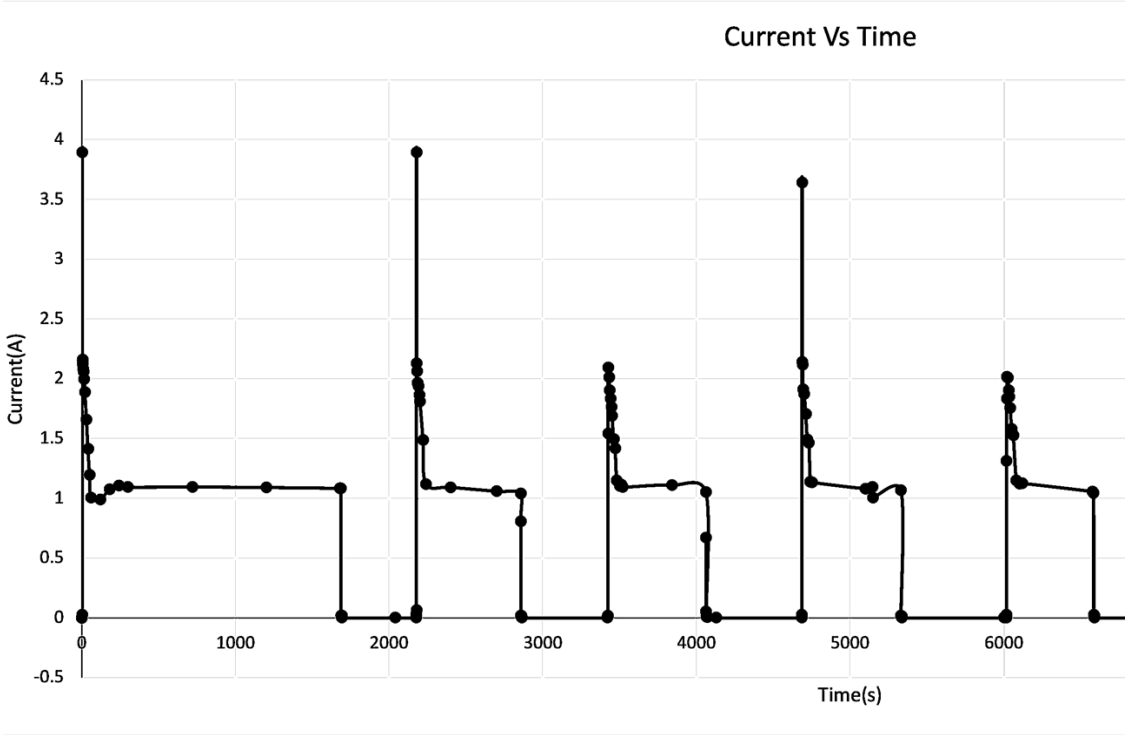

(b)

Figure 6-2: Refrigerator performance : (a) Temperature variation for thermistor setting 2, (b) Current drawn at thermistor setting 2

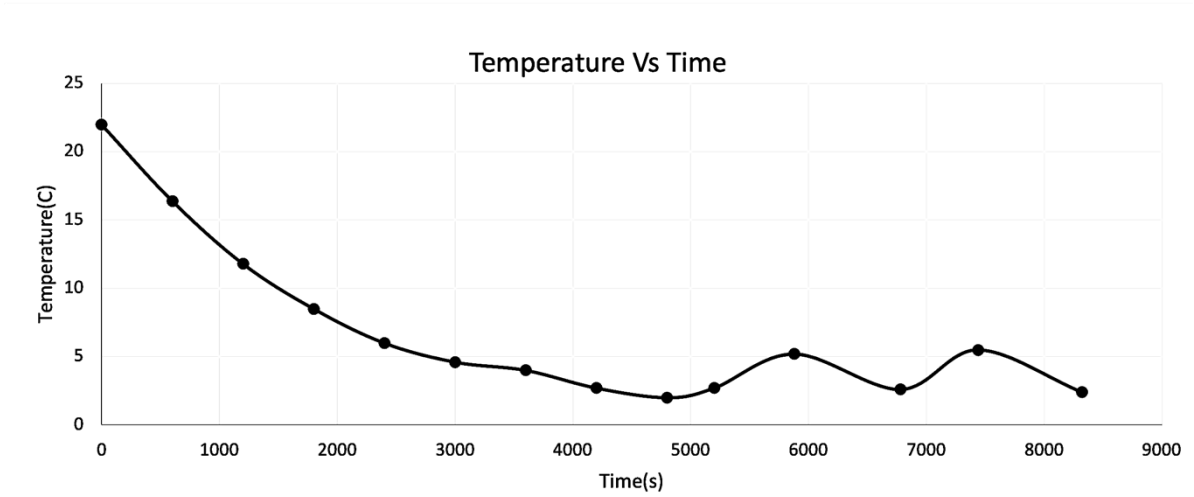

(a)

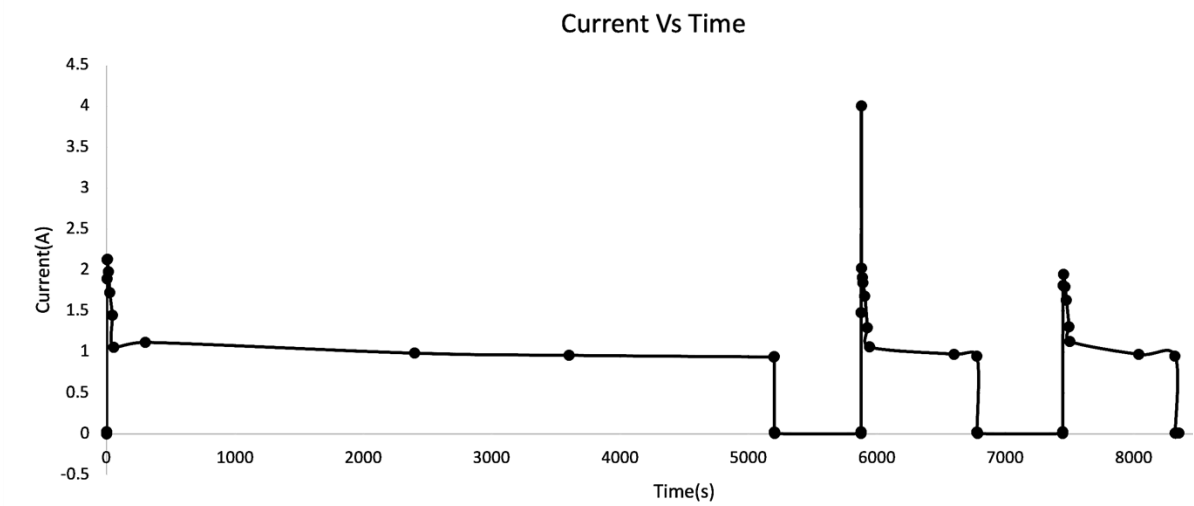

(b)

Figure 6-3: Refrigerator performance : (a) Temperature variation for thermistor setting 6, (b) Current drawn at thermistor setting 6

Table 6-1: Refrigerator specifications

Model	BD-50, single door DC compressor. 12/24V Auto
Input power	50W
Daily rating	30Ah / 12V
	15Ah / 24V
Gross capacity	50 liters

Temperature control	Mechanical setting 1-8
Refrigerant	R134a

6.2 DC-AC conversion

A brushless DC (BLDC) motor is a three phase AC motor, fed by an electronic converter unit which creates a 3 phase AC output from a DC source. Electronic converter unit (commonly called the inverter) has the capability to change the frequency fed to the three phase windings of the motor, so that the synchronous speed of the motor can be variable.

While the refrigerator is powered with DC power, the inverter embedded in the control unit converts the DC power to AC power with varying frequencies to accommodate for the different speeds of the BLDC motor. Figure 6-4 depicts the simplified concept of a BLDC motor system and its inverter which has the ability to change the output frequency of the three-phase motor allowing variable speed drive capability which smoothens out the motor's operation while increasing the efficiency. This kind of a BLDC system allows the overall system to operate over a wide range of DC voltage supplied to the BLDC motor controller.

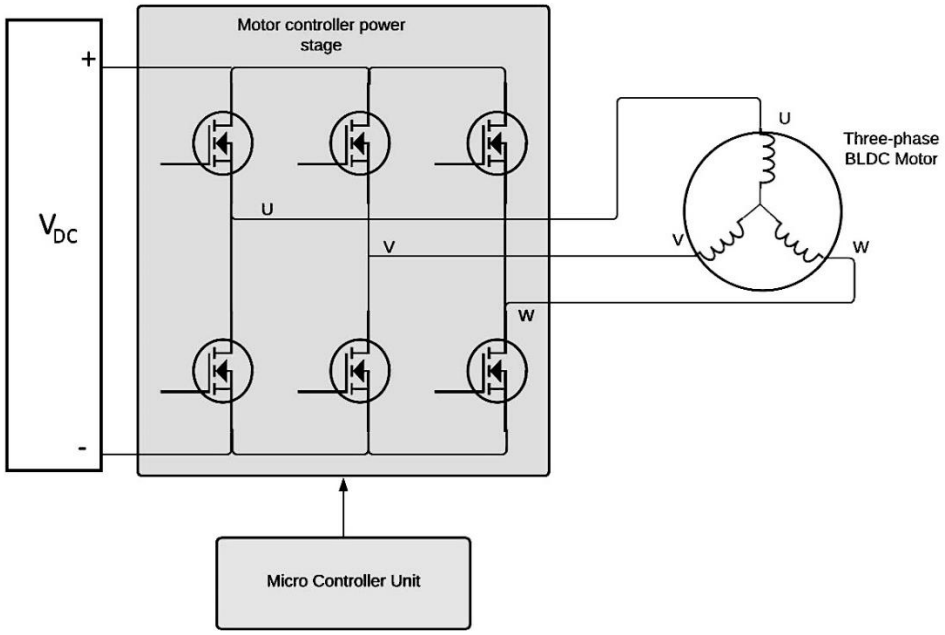

Figure 6-4: AC-DC conversion

6.3 The Supercapacitor-Assisted DC refrigerator (SCA-ref) concept

The refrigerator controller specifications mention the operation voltage of the refrigerator for the 24V setting is between 22.8 VDC and 35VDC. This allows the refrigerator to be powered for a varying range of voltages. This feature combined with charge and discharge profile of a supercapacitor led to the development of a new type of power converter.

The Supercapacitor-Assisted DC refrigerator uses the SCALoM concept discussed in detail in Chapter 5. In the typical RC-circuit, the DC refrigerator is added as a useful load to recover the energy lost in the supercapacitor charging loop. During the first phase the supercapacitor is charged by the DC power supply with the refrigerator in series. The second phase consists of disconnecting the power supply and discharging the supercapacitor across the refrigerator. In this operation, the technique makes use of the wide-DC voltage input range advantage of the BLDC motor system.

In the first phase the DC equivalent resistance of the refrigerator (R_{ref}) is much higher than the parasitic resistance in the loop (r_p). As per the proof of the SCALoM concept, the refrigerator consumes most of the wasted energy in the typical RC circuit while charging. Figure 6-5(a) shows the basic configuration of the first phase. When the supercapacitor has reached the pre-determined voltage value, the converter changes over to the second phase as shown in Figure 6-5(b). V_{DC} in Figure 6-4 is the DC source voltage of the solar input, which acts as the energy supply for powering this DC operable refrigerator.

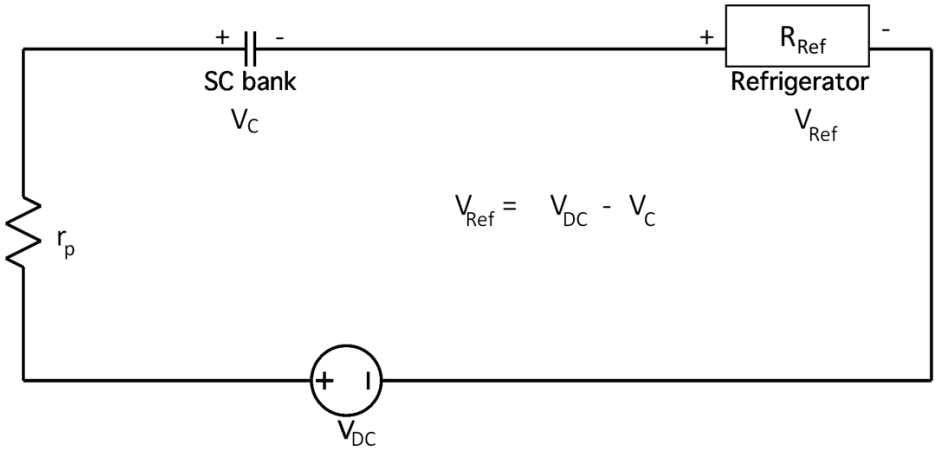

(a)

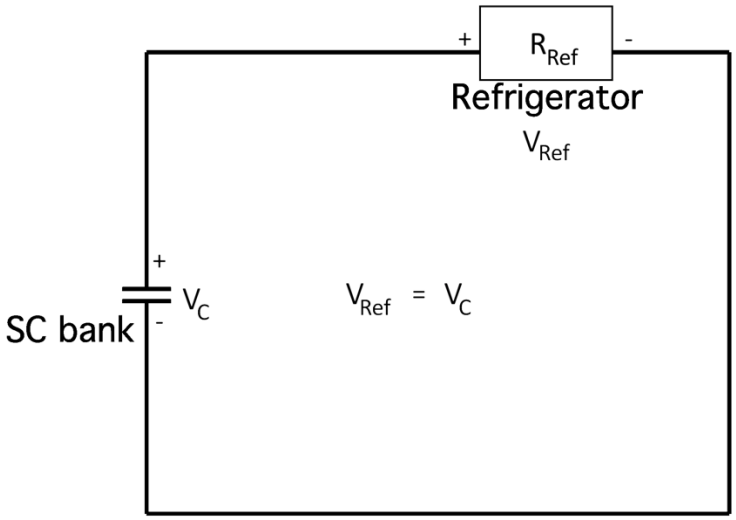

(b)

Figure 6-5: Modes of operation: (a) Charging phase (b) Discharging phase

The following operating parameters need to be established when deciding the operating DC source voltage.

$V_{c(min)}$ - Minimum supercapacitor capacitor pre-charge voltage

$V_{c(max)}$ - Maximum supercapacitor charging voltage

$V_{Ref(min)}$- Minimum voltage of refrigerator (at the end of charge/ beginning of discharge)

$V_{Ref(max)}$- Maximum voltage of refrigerator (at the end of discharge/ beginning of charge)

The DC supply voltage V_{DC} then becomes,

$$V_{DC} = V_{c(\min)} + V_{Ref(\max)} \tag{6.66}$$

$V_{Ref(\min)}$ and $V_{Ref(\max)}$ are important parameters in the system configuration as the refrigerator compressor does not operate below $V_{Ref(\max)}$ and likewise $V_{Ref(\max)}$ is beyond its operation limits. Along with that the supercapacitor should never be charged beyond its rated value.

With reference to the SCALoM concept derived in Chapter 5, the overall efficiency of the RC loop depend on the over voltage factor (over-rated factor) m and pre-charge factor k. Theoretically (m,k) → (1,1). Therefore, supercapacitor pre-charge voltage and over-rated voltage must be selected appropriately. When the values get closer, the operating frequency of the system (charging and discharging cycle) increases but the overall efficiency increases.

6.4 SCA-Ref circuit topology and operation

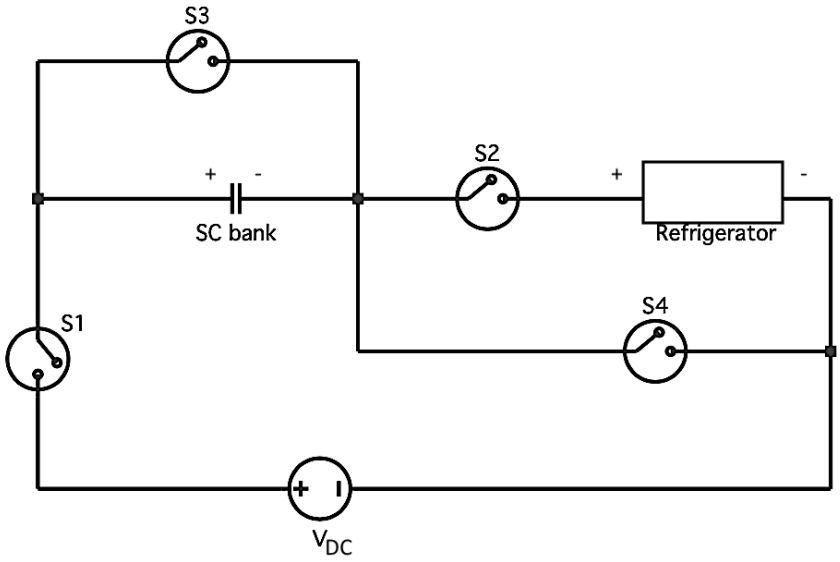

Figure 6-6: SCA-ref topology

Table 6-2: Switch states for the different modes

	S1	S2	S3	S4
Charging phase	ON	ON	OFF	OFF
Discharging phase	OFF	OFF	ON	ON

6.4.1 Charging phase

When set to the charging phase, switches S1 and S2 are turned on while switches S3 and S4 are turned off. The supercapacitor ends up in series with the refrigerator and charging continues until the preset value.

The energy stored in the supercapacitor E_c during charging phase is,

$$E_c = \frac{1}{2} C\left(V_{max}^2 - V_{min}^2\right) \tag{6.67}$$

The average power consumed by the refrigerator during the charging phase is,

$$P_{Ref(average)} = V_{(average)}\, I_{(average)} \tag{6.68}$$

The average energy consumed by the refrigerator $E_{Ref(av)charging}$ then becomes,

$$E_{Ref(av)charging} = V_{(average)}\, I_{(average)}\, t_{charging} \tag{6.69}$$

6.4.2 Discharging phase

When set to the discharging phase, switches S3 and S4 are turned on while switches S1 and S2 are turned off. The supercapacitor is now connected in parallel with refrigerator and discharges across it until the supercapacitor reaches the preset voltage.

The average power consumed by the refrigerator is,

$$P_{Ref(average)} = V'_{(average)}\, I'_{(average)} \tag{6.70}$$

The average energy consumed by the refrigerator during the discharge phase becomes,

$$E'_{Ref(average)} = V'_{(average)} I'_{(average)} t_{discharge} \quad (6.71)$$

Combined total energy E_{DC} provided by the DC power source during charging is,

$$E_{DC} = V_{DC} I_{DC} t_{charging} \quad (6.72)$$

The overall energy efficiency of the SCA-ref converter becomes,

$$\eta = \frac{E_{Ref(av)charging} + E'_{Ref(average)}}{E_{DC}} \quad (6.73)$$

6.5 Switch selection for main circuit

For the charging and discharging cycles, the DC refrigerator require power in correct polarity and the switches S2 and S4 need to be uni directional. Power MOSFETs were considered to fulfill this requirement due to their smaller size and low power needed for control. Switches S1 and S3, as shown in Figure 6-6, are high-side switches. Considering the possible power losses due to conduction losses in the switch, N-Channel MOSFETs with very low $R_{DS(on)}$ are favorable. However, using N-channel MOSFETs for high side switching require complex circuitry involving high frequency operation or additional power sources. While P-channel MOSFETs have higher R_{DS}(0n) compared to N-channel MOSFETs, they are easier to control as high side switches. Therefore, P-channel MOSFETs were utilized for switches S1 and S3.

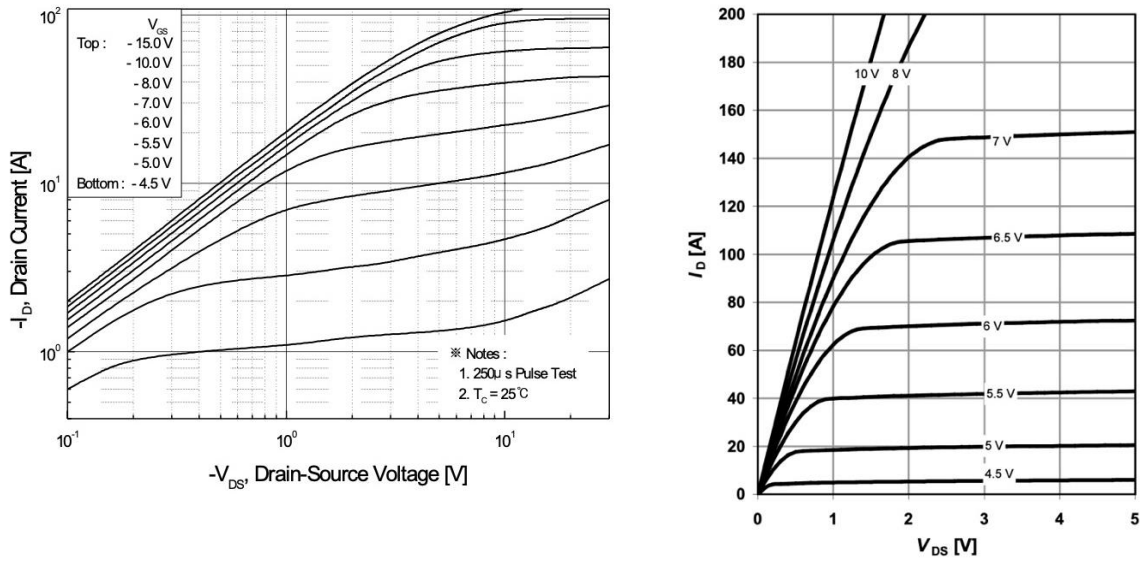

(a) *(b)*

Figure 6-7: Typical output characteristics: (a)P-Channel MOSFET (b) N-Channel MOSFET

MOSFETs only block current in one direction. This is due to the presence of a body diode in parallel to the switch inside the MOSEFT. When a MOSFET is used for switch S4, during off condition the body diode will create a short circuit path for the supercapacitor to discharge through. To mitigate this effect, two MOSFETs can be placed in series with opposing polarity. This does add complexity to the circuit to ensure both MOSFETs receive the proper gate-source voltage (V_{GS}) to turn on completely. To make the design process of control circuit simpler and reduce the component count, a Schottky diode was chosen. Likewise during the discharging phase when switch S3 is turned on, a MOSFET for switch S2 also has the issues of its body diode providing a short circuit path for the supercapacitor. As such this was also replaced with a Schottky diode. The final power stage consists of only two P-channel MOSFETs and two Schottky diodes as shown in Figure 6-8.

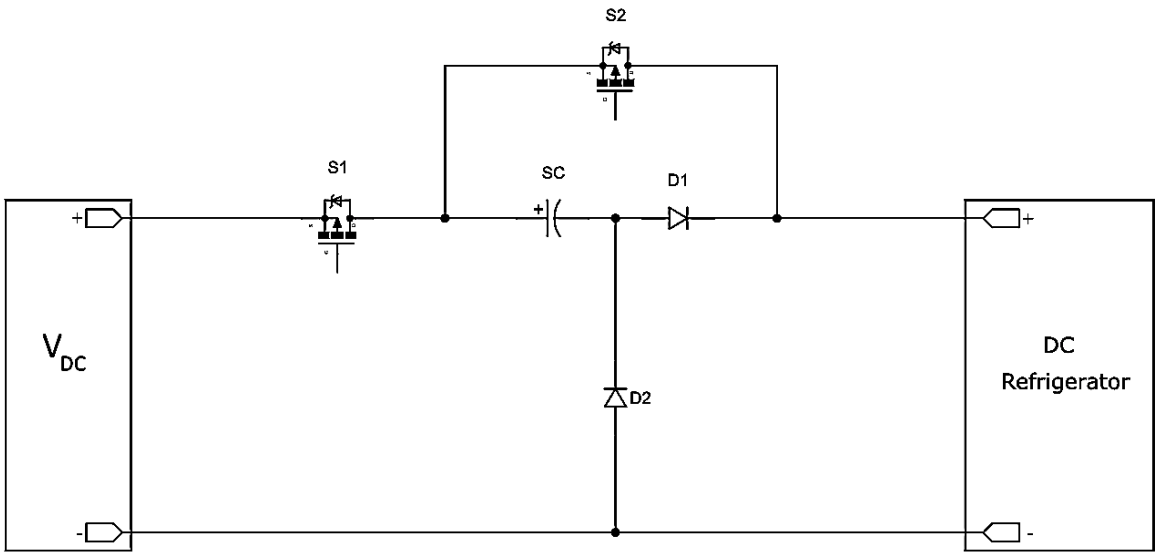

Figure 6-8:Power stage

6.6 Control circuit design

The control circuit was designed to accurately sequence the switching of the two MOSFET switches S1 and S3. During the charging phase S1 will conduct while S3 is left off. Once the charging phase is completed after charging the supercapacitor to the predetermined value, switch S3 will start conducting with S1 now turned off until the completion of the discharge phase. In order to achieve control of the switches at the correct sequency, the fundamentals of the Schmitt trigger circuit was implemented.

Schmitt trigger is a bi-stable multivibrator. The Schmitt trigger is able to convert triangular periodic signals into square pulses, as shown in Figure 6-9 .

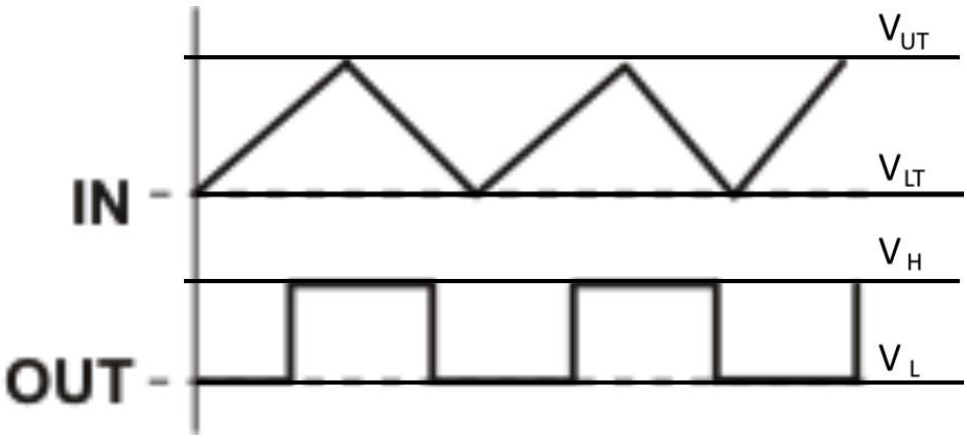

Figure 6-9: Schmitt trigger waveform

V_{UT} – Upper threshold voltage

V_{LT} – Lower threshold voltage

V_H – High voltage out

V_L – Low voltage out

6.6.1 Non-Inverting Schmitt trigger (Non-symmetrical Schmitt trigger)

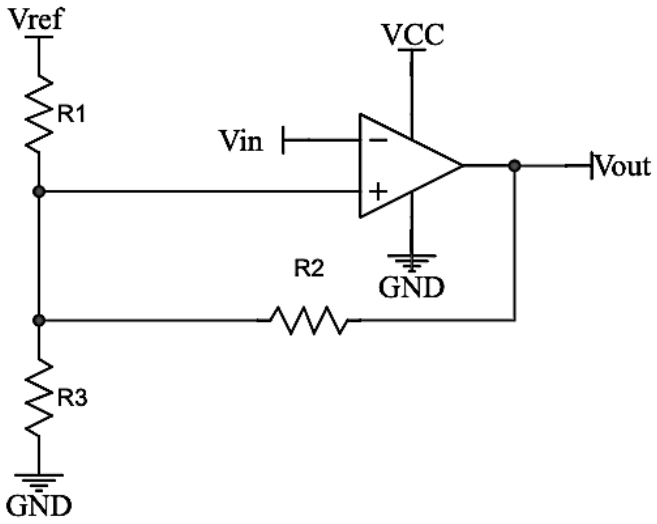

Figure 6-10: Schmitt trigger circuit

Charging and discharging voltage of the supercapacitor bank, shown in Figure 6-8, is monitored and sampled by a resistor divider. For the circuit to switch between the two modes of operation, the Schmitt trigger action is used. The upper and lower thresholds are calculated as follows.

$$V_{LT} = \left(\frac{R_2 // R_3}{R_1 + R_2 // R_3}\right) V_{ref} \tag{6.74}$$

$$V_{UT} = \left(\frac{R_2}{R_2 + R_1//R_3}\right) V_{ref} \tag{6.75}$$

The output of the Schmitt trigger is then fed to an op-amp circuit to generate the drive signals for the two switches via two opto-couplers in order to supply the required gate-to-source voltage (V_{GS}) for the P-channel MOSFETs. The schematic of circuit for driving switch S1 and S2 are shown in Figure 6-11.

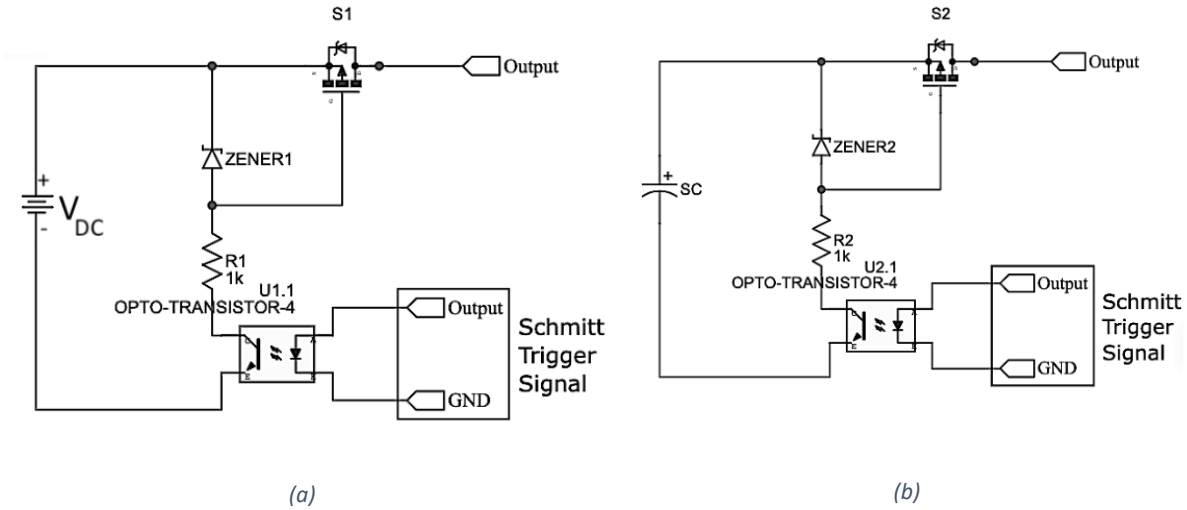

(a) *(b)*

Figure 6-11: Driving P-channel MOSFETs (a) Charging phase (b) Discharging phase

6.6.2 Regulator for the control circuit

The power required for the control circuit was provided through the supercapacitor with a linear regulator. A linear regulator was chosen due to simplicity of design and due to the low power requirement of the control circuit. For linear regulators, the efficiency is found to be,

$$\eta = \frac{V_{out}}{V_{in}} \times 100\ \% \tag{6.76}$$

As a result, using the main DC power source with a double the supercapacitor voltage would result in lower efficiencies. Hence the use of the pre-charged supercapacitor to power the control unit was decided.

6.7 Efficiency of SCA-Ref

The lab set-up consisted of a DC power supply with some FLUKE digital multimeters (DMMs) and a Tektronix PA3000 power analyzer for measurements, as shown in Figure 6-12.

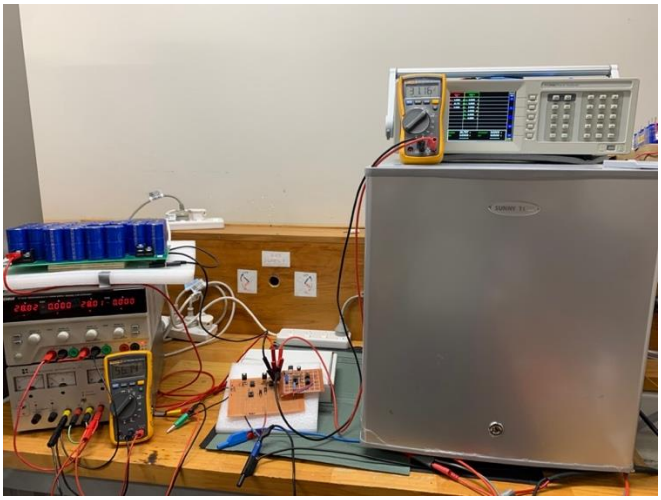

(a)

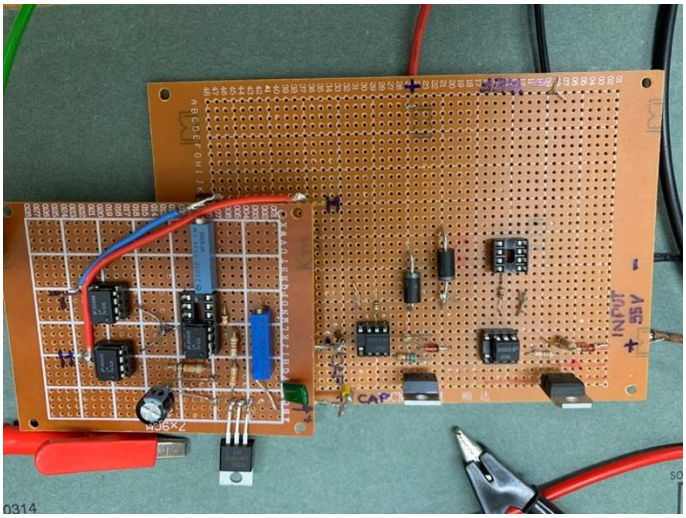

(b)

Figure 6-12: Experimental set-up: (a) Measurement set-up (b) Prototype circuit board.

The power is supplied to SCA-Ref converter for half the time operation. This requires the efficiency to be calculated by the energy that is transferred as per Equation 6.8. The refrigerator has 5 distinct thermistor settings. Average power utilized by the refrigerator was found for each setting and the energy content that was utilized for the whole cycle was calculated. To validate efficiency, thermistor setting 2 and thermistor setting 5 were analysed.

From Figure 6-13, time period starting from 9.24 minutes and ending at 25.37 minutes was observed. The time spent in the charging phase t_{ch} was 7.88 minutes and the time spent in the discharging phase t_{dis} was 8.33 minutes. Average values for the power consumed by the fridge for the two phases and the average current drawn are shown in Table 6-3.

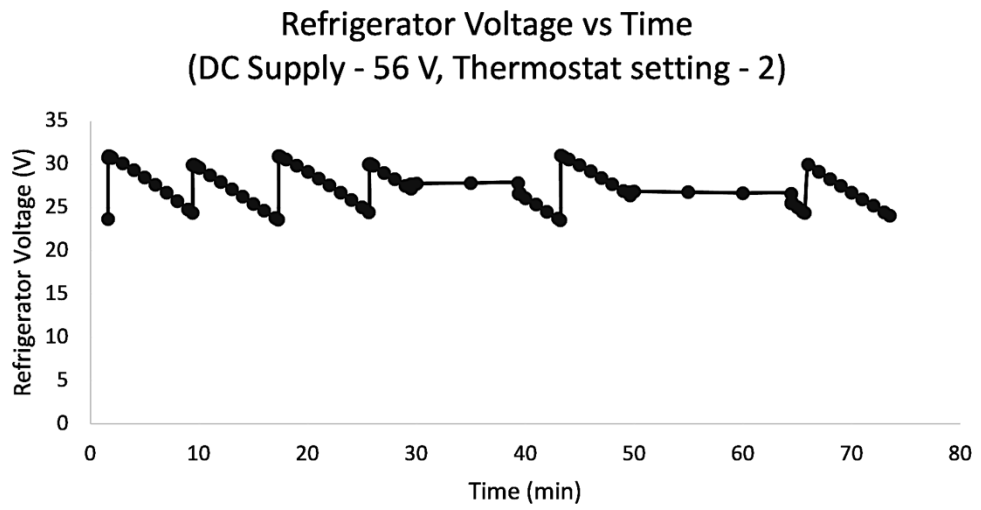

(a)

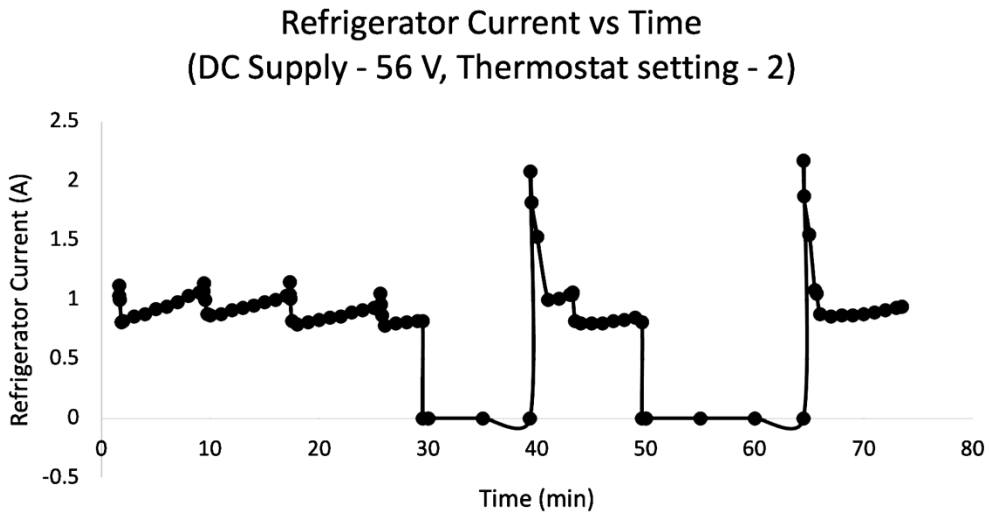

(b)

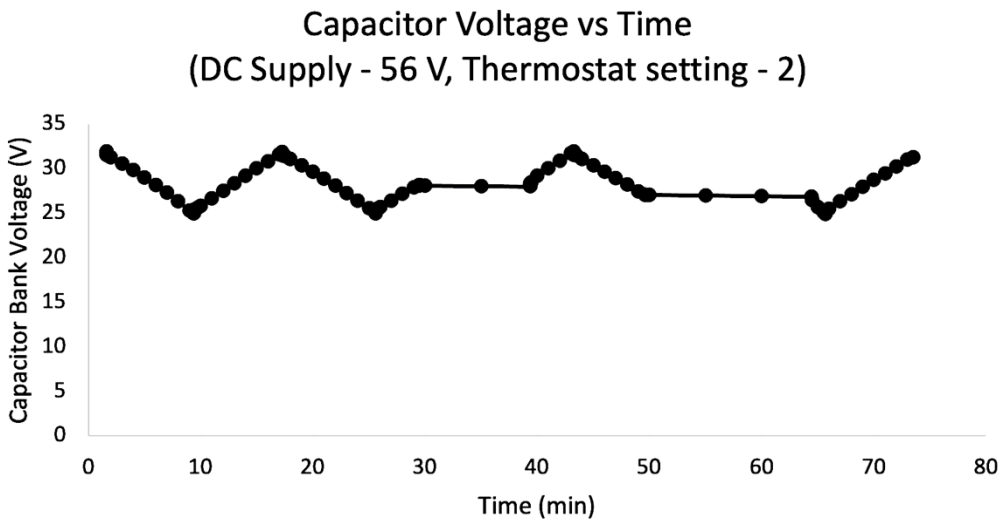

(c)

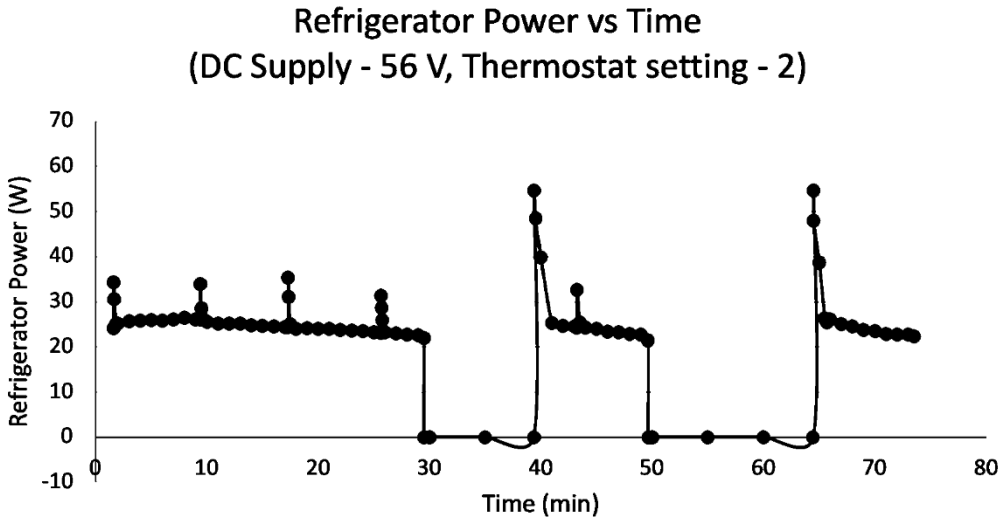

(d)

Figure 6-13: SCA-Ref waveforms for temperature setting 2: (a) Refrigerator voltage vs time, (b) Refrigerator current vs time, (c) Capacitor voltage vs time, (d)Refrigerator power vs time

The energy consumed by the refrigerator for each phase was then calculated using,

$$Energy\ consumed\ [Wh] = Average\ power[W] * \frac{time[\min]}{60} \tag{6.77}$$

Where time is either t_{ch} or t_{dis}.

Table 6-3:Data collected for SCA-Ref at thermistor setting 2

	Charging phase	Discharging phase
Time (min)	7.88	8.33

Average power (W)	24.9	23.9
Average current drawn (A)	0.96	0.96
Average energy (Wh)	3.27	3.32

As the power supply only provides energy during the charging phase, input energy is calculated by Equation 6.7,

$$E_{DC} = V_{DC}\, I_{DC} t_{charging} \tag{6.78}$$

Efficiency is then calculated as per equation 6.8

$$\eta = \frac{E_{Ref(av)charging} + E'_{Ref(average)}}{E_{DC}} \tag{6.79}$$

Table 6-4: Efficiency of SCA-Ref at thermistor setting 2

$E_{DC}\ [Wh]$	7.06
$E_{utilized}[Wh] = E_{Ref(av)charging} + E'_{Ref(average)}$	$3.27 + 3.32 = 6.59$
Efficiency, η	93.3%

Likewise, the efficiency of SCA-Ref was found for thermistor setting 6.

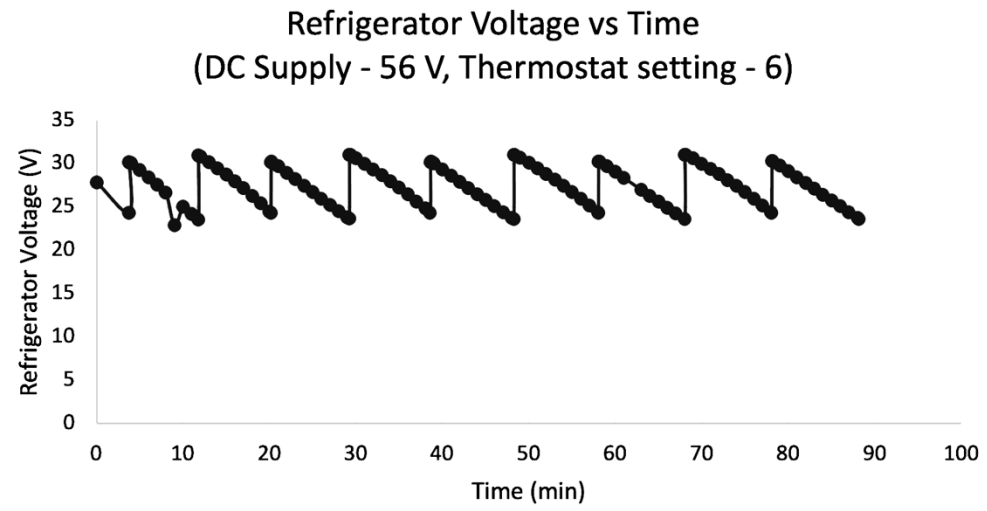
Refrigerator Voltage vs Time
(DC Supply - 56 V, Thermostat setting - 6)
Refrigerator Voltage (V)
35
30
25
20
15
10
5
0
0
10
20
30
40
50
60
70
80
90
100
Time (min)

(a)

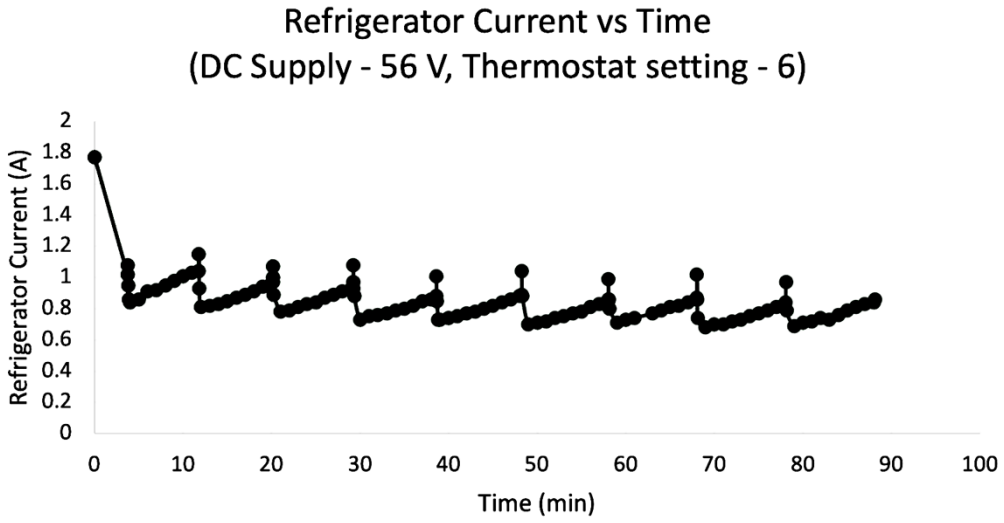
Refrigerator Current vs Time
(DC Supply - 56 V, Thermostat setting - 6)
Refrigerator Current (A)
2
1.8
1.6
1.4
1.2
1
0.8
0.6
0.4
0.2
0
0
10
20
30
40
50
60
70
80
90
100
Time (min)

(b)

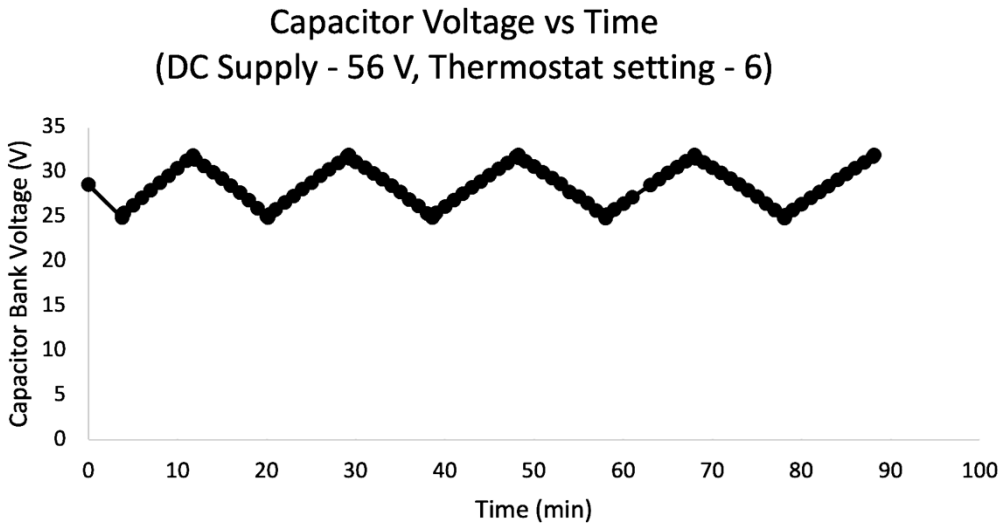

(c)

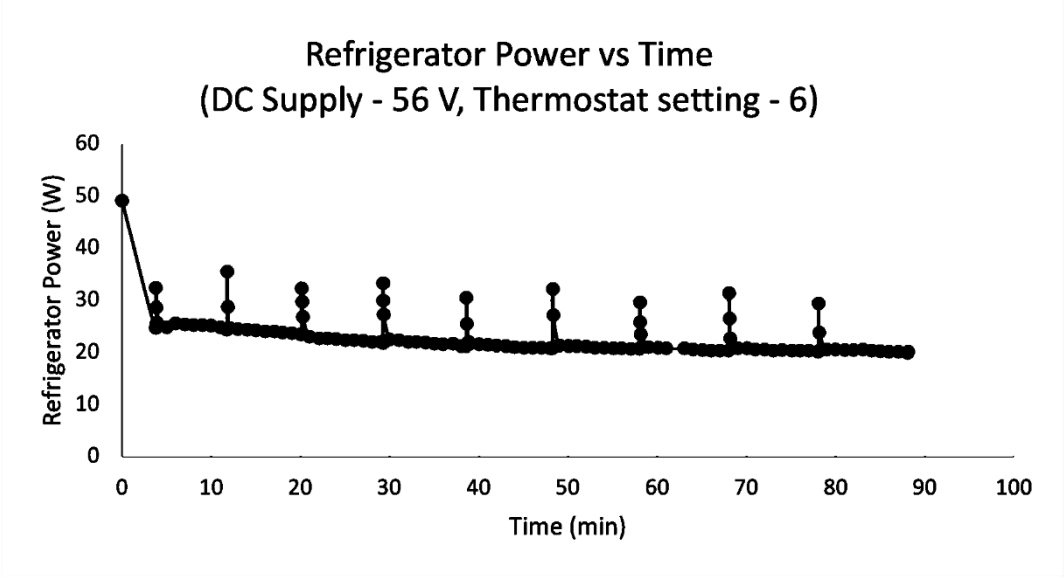

(d)

Figure 6-14: SCA-Ref waveforms for thermistor setting 6: (a) Refrigerator voltage vs time, (b) Refrigerator current vs time, (c) Capacitor voltage vs time, (d)Refrigerator power vs time

From Figure 6-14, time period starting from 49.31 minutes and ending at 68.52 minutes was observed. The time spent in the charging phase t_{ch} was 9.39 minutes and the time spent in the discharging phase t_{dis} was 9.42 minutes. Average values for the power consumed by the fridge for the two phases and the average current drawn are shown in Table 6-5.

Table 6-5: Data collected for SCA-Ref at thermistor setting 6

	Charging phase	Discharging phase
Time (min)	9.39	9.42
Average power (W)	21.8	21.7
Average current drawn (A)	0.83	0.85
Average energy (Wh)	3.5	3.51

Table 6-6: Efficiency of SCA-Ref at thermistor setting 6

$E_{DC}\ [Wh]$	7.49
$E_{utilized}[Wh] = E_{Ref(av)charging} + E'_{Ref(average)}$	$3.5 + 3.51 = 7.01$
Efficiency, η	93.6%

The efficiency values were consistently above 90% proving the viability of SCA-Ref concept.

Chapter 7: Conclusion

7.1 Summary of results

The main objectives of the project were,

- To access the viability of SCALoM concept to a DC powered refrigerator
- To develop an effective SCA-Ref converter, with ultra-low switching frequency, to power the refrigerator using a DC power source simulating a solar photovoltaic panel
- For the supercapacitor bank to provide an energy buffer during any power fluctuations due to solar irradiation
- To complete objectives within the time frame of a Master of Engineering programme

The viability of a supercapacitor assisted refrigerator (SCA-Ref) was proven and prototype was built for demonstration.

A prototype circuit for switching between the charging and discharging phase was successfully developed. The use of an analogue circuit blocks for transitioning automatically between the two phases and the MOSFET switching circuitry depending on the state of charge of supercapacitor bank offers reliable operation.

7.2 Future work

The project proved that the SCALoM concept of coupling a supercapacitor bank with a DC load like a refrigerator is viable for (i) operating the refrigerator from a solar panel based fluctuating DC supply (ii) a supercapacitor bank can be used to buffer the energy source voltage fluctuations (iii) maintaining a high system efficiency. The performance of the protype was consistent at each thermostat setting while having efficiencies above 92%. The refrigeration device under test was a 24VDC camper fridge. For household use, 240Vac refrigerators are used. For future DC homes to be viable it is important to help with transition from AC powered devices to DC devices. Since most devices internally run on DC power, the SCA-ref converter should be able to be directly implemented on commercial devices. A 240Vac refrigerator was brought in for further development for SCA-Ref

for higher power. The validity of the protype has spawned a PhD project for the completion of the SCA-Ref prototype over the next four years.

References

[1] R.Singh, G.F.Alapatt, G.Bedi, “Why and How Photovoltaics will provide cheapest electricity in the 21st century ”, FACTA universitatis, Electronics and Energetics, Vol 27, no.2, pp 275-298, June 2014.

[2] V.Vossos, K.Garbesi, H.Shen, “Energy savings from direct-DC in US. Residential Buildings”, Energy and Building, Vol 68, pp 223-23, 2014.

[3] A.Sabry, P.Ker, “Improvement on energy consumption of a refrigerator within PV system including battery storage”, Energy reports, Vol 7, pp 430-438, January 2021.

[4] Z.Zhang, T.Ding, Q.Zhou, Y.Sun, M.Qu, Z.Zeng, Y.Ju, L.Li, K.Wang, F.Chi, “A Review of Technologies and Applications on versatile energy storage systems”, Renewable and Sustainable Energy Reviews, no.148, pp 1-31, 2021.

[5] N.Kularatna, K.Gunawardane, “Energy Storage Devices for Renewable Energy-Based Systems; Rechargeable Batteries and Supercapacitors”, 2nd Edition, ACADEMIC PRESS, 2021.

[6] Ariyarathna, Thilanga et al. “Development of Supercapacitor Technology and Its Potential Impact on New Power Converter Techniques for Renewable Energy.” *IEEE journal of emerging and selected topics in industrial electronics (Print)* 2.3 (2021): 267–276. Web.

[7] D.Kumar, F.Zare, A.Ghosh, “Dc Microgrid Technology; System Architecture: AC Grid interfaces, Grounding Schemes, Power Quality, Communication Networks, Applications and standardizations Aspect”, IEEE Access, Special section on Power quality and harmonics issues of future and smart grid, Vol 5, pp 12230-12241, 2017.

[8] T.Christen, M.W.Carlen, “Theory of Ragone Plot”, Journal of Power Source 91, pp 210-216, 2000.

[9] N.Guerra, M.Guevara, C.Palacios, F.Crupi, “Operation and Physics of Photovoltaic Solar Cells; An Overview” Revista de 1+D Technologico, Vol 4, no 14, pp 84-95, 2018.

[10] Solar Energy Overview. Available online. hppts://www.irena.org>Energy-Transition>Technology Solar energy-IRENA-International Renewable Energy Agency. (Accessed on 20.05.2023)

[11] K.Jager, O.Isabella, A.H.M.Smels, R.Van Swaaij, M.Zeman, “Solar Energy; Fundamentals, Technology, and Systems”, 1st Edition, Delft university of Technology, 2014.

[12] Solar Cells: A Guide to theory and Measurements. Available online. https://www.ossila.com/pages/solar-cells-theory (Accessed on 14.05.2023)

[13] How a Solar cell works- American chemical society. Available online. https://www.acs.org>archive-2013-2014>how-a-solar-cell-work. (Accessed on 30.05.2023)

[14] M.Diantoro, T.Suprayogi, A.Hidayat, A.Taufiq, A.Faud, R.Suryana, “Shockley’s equation fit Analysis for solar cell parameters from I-V curves”, International Journal of Photoenergy, Vol 2018, Article ID 9214820, 2018.

[15] PV Cells 101: A primer on the Solar Photovoltaic cell. Available online. https://www.ernergy.gov/eere/solar/articles/pv-cells-101-primer-solar-photovoltaic-cell (Accessed on 20.05.2023)

[16] C.Hu, R.M.White, “Solar Cells; From basics to Advance Systems”, McGraw-Hill Book, NewYork, USA, 1983

[17] A.K.Podder, N.K.Roy, H.R.Pota, “MPPT Methods for Solar PV Systems; A Critical Review based on tracking nature”, IET Renewable Power Generations, Vol 13, no.10, pp 1615-1632, 2019.
[18] M.Rosu-Hamzescu, S.Opera, “Practical Guide to Implementing Solar Panel MPPT Algorithms”, Microchip Technology Inc, AN 1521, D500001521A, 2013.
[19] R.F.Coelho, F.M.Concer, D.C.Martin, “A MPPT approach based on Temperature Measurement Applied in PV System”, IEEE International Conference on Sustainable Energy Technologies (ICSET), pp 1-6, 2010.
[20] D.Jayananda, N.Kularatne, D.A.Steyn-Ross, “A Validity of MPPT Technique using Supercapacitors as Energy Storage Devices”, IEEE, 2019, pp 2301-2306.
[21] G.W.A Dummer, Electronic Inventions and Discoveries, 4th edition,Bristol, U.K.; Institute Of Physics publishing, p.74, 1997.
[22] J.Ho, R.Jow, S.Boggs, “Historical Introduction to Capacitor Technologies”, IEEE Electr. Insul. Mag. Vol 26, pp 20-25, 2010.
[23] M.E.Sahin, F.Blaabjerg, A.Sangwongwanich, “A Comprehensive Review on Supercapacitor Applications and Developments”, Energies, Vol 15, 674, 2022.
[24] K.Remi, “Supercapacitor: A Short Literature Review”. https://www.researchgate.net/publication/331471216.
[25] F.Naseri, S.Karimi, E.Farjah, E.Schaltz, “A comprehensive review of modeling, estimation, balancing and protection techniques”, Renewable and Sustainable Energy Reviews, Vol 155, pp 1-19,2022.
[26] A.Schneuwly, R.Gallay, “Properties and application of supercapacitors From the state-of-the-art to future trends”, Proceeding PCIM 2000.
[27] A.Burke, “R&D consideration for the performance and application of electrochemical capacitors”, Electrochim, Vol 52, pp 1089-1091, 2007.
[28] M.Selanne, “Ionic Liquids for Supercapacitor Applications”, Top Curr Chem 375; 63, 2017.
[29] A.Schneuwly, R.Gallay, “Properties and applications of supercapacitors From the state-of-the-art to future trends”, Proceeding PCIM, 2000.
[30] B.Schweber, “Energy storage by the Farad-part 3; Hybridcapacitor”, Power electronics tips, June, 2021.
[31] M.E.Sahin, F.Blaabjerg, A.Sangwongwanioh, “Modelling of Supercapacitor based on simplified Equivalent Circuit”, CPSS Transactions on power electronics and applications, Vol 6, no.1, March 2021,
[32] The major difference between supercapacitors and batteries. Available online; https://www.eaton.com>topics>supercapacitors-vs-batteries (Accessed on 26.04.2023)
[33] I.P.D.Faria, A.C.G.M.Ferandes, I.A.N>Pombo, M.R.A.Calado, S.I.P.S Mariano, “SC Voltage Balancing method: A comprehensive review”, IEEE, 2022.
[34] Y.Qu, T.ZHu, J.Hu, B.Holliday, “Overview of SC cell voltage balancing Method for an electric vehicles”, IEEE ECCE Asia Downunder, 2013, pp 810-814.
[35] R.Kalbitz, “Keep the Balance- Balancing of Supercapacitors”, Wurth Elektronik, Application note and Design Guide, AnPO90, 2021.
[36] C.Ionescu, A.Drumea, P.Svasta, A.Vasile, N.Codreanu, “Evaluation of Active Balancing circuits for Supercapacitors”, 2nd PCNS, 2019.
[37] Voltage balancing techniques for series supercapacitors connection. Available online. https://www.analog.com>en>design-notes (Accessed on 28.04.2023).

[38] U.G.D.U.K.Jayananda, “Supercapacitor Assisted LED (SCALED) Converter Technique for Solar Powered DC-Microgrids, (Thesis, Doctor of Philosophy)”, the University of Waikato, 2020.

[39] N.Kularatna, “Supercapacitor Assisted low Dropout Regulator (SCALDO) for high efficiency DC-DC converters for DC microgrid applications”, 2015 IEEE first International Conference on DC microgrid (ICDCM). Atlanta.GA, USA. pp 333-338, 2015.

[40] N.Kularatna, D.Jayananda, “Supercapacitor-based long time-constant circuits: A unique design opportunity for new power electronic circuit topologies”, IEEE Industrial Electronics Magazine, Vol 14, no.2, pp 40-56, June 2020.

[41] J.Fernando, N.Kularatne, H. Round and S.Taele, “Implementation of the supercapacitor-assisted surge absorber (SCASA) technique in a practical surge protector”. IECON 2014- 40th Annual conference of the IEEE Industrial Society. Dallas. TX, USA. pp 5191-5195, 2014.

[42] N.Gurusinghe, N.Kularatne, S.A.Charleston and J.Fernando, “System implementation aspects of supercapacitor based fast in-line water heating system”, IEEE-ISIE, Brasil, pp 1313-1317, 2015.

[43] D.Jayananda, N.Kularatna and D.A.Steyn-Ross, “Design approach for Supercapacitor Assisted LED lighting (SCALED) technique for DC-microgrid”, 2018 IEEE International Conference on Industrial Electronics for Sustainable Energy Systems (IESES), Hamilton, New Zealand, pp 27-31,2018.

[44] The 4 main Refrigeration Cycle components. Available online: https://www.superradiatorcoils.com/blog/4-main-refrigeration-cycle-components. (Accessed on 13.06.2023)

[45] The Different Types of Refrigeration Compressors. Available online: https://www.compressorsunlimited.com/blog/the-different-types-of-refrigeration-compressor. (Accessed on 13.06.2023)

[46] A.Ahmed, A.Al-Farhan, A.Mahmoud, A.Hammouda, “Control of inverter compressors”, International Journal of Scientific and Technology research, Vol10, no.11, 2021, pp 27-33.

[47] Wiring Diagram of Refrigerator, Available online: https://www.hvactutorial.wordpess.com/refrigeration-system-refrigertorfreezer-system/domestic-refrigerator-wiring/ (Accessed on 14.06.2023)

[48] What are the advantages of having a digital inverter compressor in refrigerator? Available online: https://www.samsung.com/nz/support/home-appliances/what-are-the-advantages-of-having-a-digital-inverter-compressor-in-refrigerator/. (Accessed on 13.06.2023)

[49] International Rectifier, “High-Performance sensor less Moter control IC”, IRMCF 171, datasheet, April 2013.

[50] Refrigerators with Inverter technology can help save electricity. Available online: https://www.bijibachao.com/refrigerators/refrigerators-with-inverter-technology-can-help-save-electricity.html. (Accessed on 28.03.2023)

[51] P.Yedamale, “Brushes DC (BDLC) Motor Fundamentals”, Microchip Technology Inc, DS 00885A, 2003.

A. Appendix

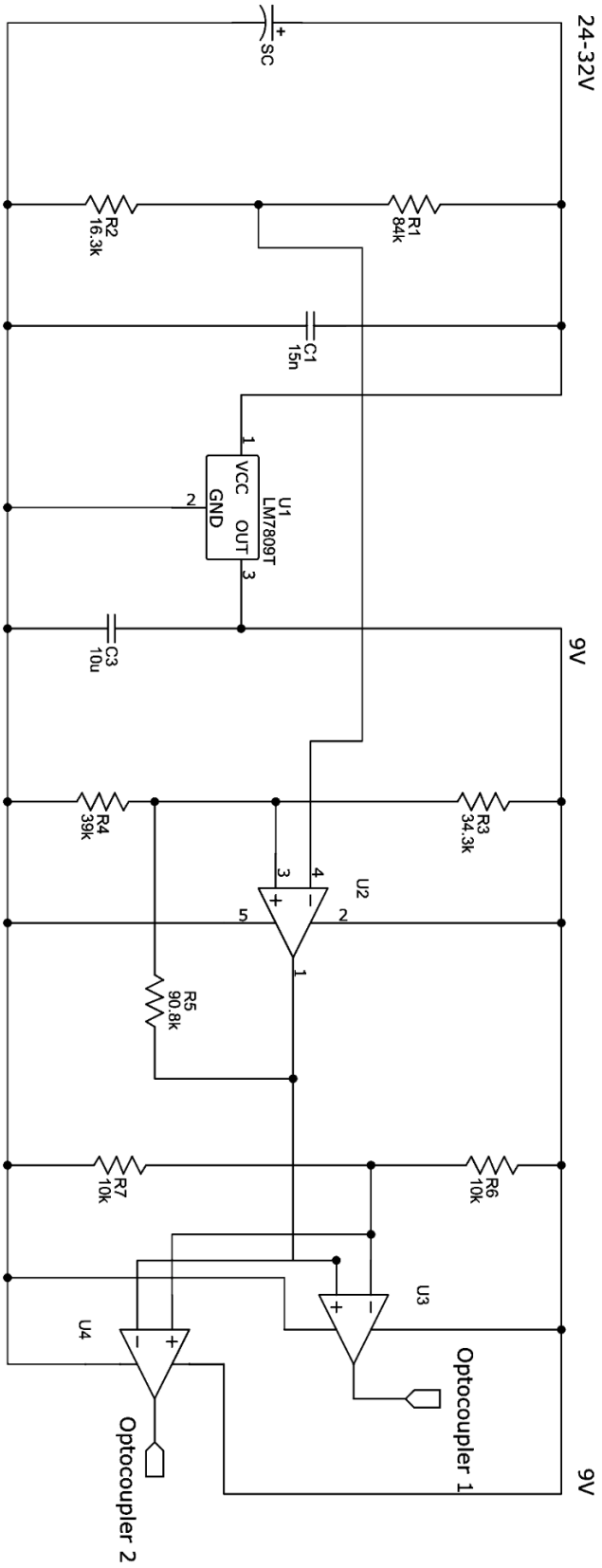

Figure A-1: Control circuit

onsemi

DATA SHEET
www.onsemi.com

Voltage Regulators – Positive

1.0 A

MC7800, MC7800A, MC7800AE, NCV7800

These voltage regulators are monolithic integrated circuits designed as fixed−voltage regulators for a wide variety of applications including local, on−card regulation. These regulators employ internal current limiting, thermal shutdown, and safe−area compensation. With adequate heatsinking they can deliver output currents in excess of 1.0 A. Although designed primarily as a fixed voltage regulator, these devices can be used with external components to obtain adjustable voltages and currents.

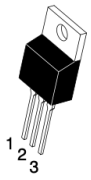

TO−220
T SUFFIX
CASE 221AB

Heatsink surface connected to Pin 2.

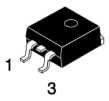

Pin 1. Input
2. Ground
3. Output

D²PAK−3
D2T SUFFIX
CASE 936

Heatsink surface (shown as terminal 4 in case outline drawing) is connected to Pin 2.

DPAK−3
DT SUFFIX
CASE 369C

Features

- Output Current in Excess of 1.0 A
- No External Components Required
- Internal Thermal Overload Protection
- Internal Short Circuit Current Limiting
- Output Transistor Safe−Area Compensation
- Output Voltage Offered in 1.5%, 2% and 4% Tolerance
- Available in Surface Mount D²PAK−3, DPAK−3 and Standard 3−Lead Transistor Packages
- NCV Prefix for Automotive and Other Applications Requiring Unique Site and Control Change Requirements; AEC−Q100 Qualified and PPAP Capable
- These are Pb−Free Devices

MAXIMUM RATINGS (T_A = 25°C, unless otherwise noted)

Rating	Symbol	Value			Unit
		369C	221A	936	
Input Voltage (5.0 − 18 V) (24 V)	V_I	35 40			Vdc
Power Dissipation	P_D	Internally Limited			W
Thermal Resistance, Junction−to−Ambient	$R_{\theta JA}$	92	65	Figure 15	°C/W
Thermal Resistance, Junction−to−Case	$R_{\theta JC}$	5.0	5.0	5.0	°C/W
Storage Junction Temperature Range	T_{stg}	−65 to +150			°C
Operating Junction Temperature	T_J	+150			°C

Stresses exceeding those listed in the Maximum Ratings table may damage the device. If any of these limits are exceeded, device functionality should not be assumed, damage may occur and reliability may be affected.

*This device series contains ESD protection and exceeds the following tests:
Human Body Model 2000 V per MIL_STD_883, Method 3015.
Machine Model Method 200 V.

STANDARD APPLICATION

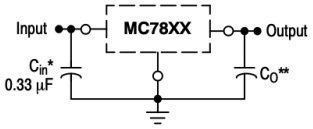

A common ground is required between the input and the output voltages. The input voltage must remain typically 2.0 V above the output voltage even during the low point on the input ripple voltage.

XX, These two digits of the type number indicate nominal voltage.

* C_{in} is required if regulator is located an appreciable distance from power supply filter.

** C_O is not needed for stability; however, it does improve transient response. Values of less than 0.1 μF could cause instability.

ORDERING INFORMATION

See detailed ordering and shipping information in the package dimensions section on page 21 of this data sheet.

DEVICE MARKING INFORMATION

See general marking information in the device marking section on page 24 of this data sheet.

Figure A-2: 9V linear regulator datasheet

ELECTRICAL CHARACTERISTICS (V_{in} = 15 V, I_O = 500 mA, T_J = T_{low} to 125°C (Note 9), unless otherwise noted)

Characteristic	Symbol	MC7809B/NCV7809B			MC7809C			Unit
		Min	Typ	Max	Min	Typ	Max	
Output Voltage (T_J = 25°C)	V_O	8.65	9.0	9.35	8.65	9.0	9.35	Vdc
Output Voltage (5.0 mA ≤ I_O ≤ 1.0 A, P_D ≤ 15 W) 11.5 Vdc ≤ V_{in} ≤ 24 Vdc	V_O	8.55	9.0	9.45	8.55	9.0	9.45	Vdc
Line Regulation, T_J = 25°C (Note 10) 11 Vdc ≤ V_{in} ≤ 26 Vdc 11.5 Vdc ≤ V_{in} ≤ 17 Vdc	Reg_{line}	– –	6.2 1.8	32 16	– –	6.2 1.8	32 16	mV
Load Regulation, T_J = 25°C (Note 10) 5.0 mA ≤ I_O ≤ 1.5 A	Reg_{load}	–	1.5	35	–	1.5	35	mV
Quiescent Current	I_B	–	3.4	8.0	–	3.4	8.0	mA
Quiescent Current Change 11.5 Vdc ≤ V_{in} ≤ 26 Vdc 5.0 mA ≤ I_O ≤ 1.0 A	ΔI_B	– –	– –	1.0 0.5	– –	– –	1.0 0.5	mA
Ripple Rejection 11.5 Vdc ≤ V_{in} ≤ 21.5 Vdc, f = 120 Hz	RR	56	61	–	56	61	–	dB
Dropout Voltage (I_O = 1.0 A, T_J = 25°C)	$V_I - V_O$	–	2.0	–	–	2.0	–	Vdc
Output Noise Voltage (T_A = 25°C) 10 Hz ≤ f ≤ 100 kHz	V_n	–	10	–	–	10	–	$\mu V/V_O$
Output Resistance f = 1.0 kHz	r_O	–	1.0	–	–	1.0	–	mΩ
Short Circuit Current Limit (T_A = 25°C) V_{in} = 35 Vdc	I_{SC}	–	0.2	–	–	0.2	–	A
Peak Output Current (T_J = 25°C)	I_{max}	–	2.2	–	–	2.2	–	A
Average Temperature Coefficient of Output Voltage	TCV_O	–	−0.5	–	–	−0.5	–	mV/°C

9. T_{low} = 0°C for MC78XXC, MC78XXAC,
   = −40°C for NCV78XX, MC78XXB, MC78XXAB, and MC78XXAEB
10. Load and line regulation are specified at constant junction temperature. Changes in V_O due to heating effects must be taken into account separately. Pulse testing with low duty cycle is used.

Figure A-3:9V linear regulator datasheet continued

STP12PF06
STF12PF06

P-CHANNEL 60V - 0.18 Ω - 12A TO-220/TO-220FP
STripFET™ II POWER MOSFET

Table 1: General Features

TYPE	V_{DSS}	$R_{DS(on)}$	I_D
STP12PF06	60 V	< 0.20 Ω	12 A
STF12PF06	60 V	< 0.20 Ω	12 A

- TYPICAL R_{DS}(on) = 0.18 Ω
- EXCEPTIONAL dv/dt CAPABILITY
- 100% AVALANCHE TESTED
- LOW GATE CHARGE
- APPLICATION ORIENTED CHARACTERIZATION

DESCRIPTION

This Power MOSFET is the latest development of STMicroelectronis unique "Single Feature Size™" strip-based process. The resulting transistor shows extremely high packing density for low on-resistance, rugged avalanche characteristics and less critical alignment steps therefore a remarkable manufacturing reproducibility

APPLICATIONS

- MOTOR CONTROL
- DC-DC & DC-AC CONVERTERS

Figure 1:Package

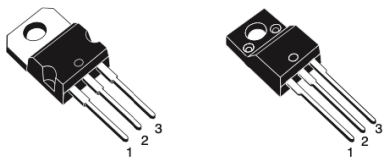

TO-220 TO-220FP

Figure 2: Internal Schematic Diagram

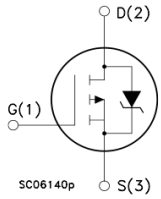

Table 2: Order Codes

PART NUMBER	MARKING	PACKAGE	PACKAGING
STP12PF06	P12PF06	TO-220	TUBE
STF12PF06	F12PF06	TO-220FP	TUBE

Table 3: ABSOLUTE MAXIMUM RATINGS

Symbol	Parameter	Value		Unit
		STP20PF06	STF20PF06	
V_{DS}	Drain-source Voltage (V_{GS} = 0)	60		V
V_{DGR}	Drain-gate Voltage (R_{GS} = 20 kΩ)	60		V
V_{GS}	Gate- source Voltage	± 20		V
I_D	Drain Current (continuous) at T_C = 25°C	12	8	A
I_D	Drain Current (continuous) at T_C = 100°C	8.4	5.6	A
I_{DM}(•)	Drain Current (pulsed)	48	32	A
P_{tot}	Total Dissipation at T_C = 25°C	60	225	W
	Derating Factor	0.4	0.17	W/°C
dv/dt (1)	Peak Diode Recovery voltage slope	6		V/ns
E_{AS} (2)	Single Pulse Avalanche Energy	200		mJ
T_{stg}	Storage Temperature	-55 to 175		°C
T_j	Operating Junction Temperature			

(•) Pulse width limited by safe operating area.
NOTE:For the P-CHANNEL MOSFET actual polarity of voltages and current has to be reversed.

(1) I_{SD} ≤12A, di/dt ≤200A/μs, V_{DD} ≤ $V_{(BR)DSS}$, T_j ≤ T_{JMAX}
(2) Starting T_j = 25 °C, I_D = 12A, V_{DD}= 25V

Figure A-4: P-Channel MOSFET datasheet

Table 4: THERMAL DATA

			TO-220	TO-220FP	
Rthj-case	Thermal Resistance Junction-case	Max	2.5	5.35	°C/W
Rthj-amb T_l	Thermal Resistance Junction-ambient Maximum Lead Temperature For Soldering Purpose	Max	62.5 300		°C/W °C

ELECTRICAL CHARACTERISTICS (T_{CASE} = 25 °C UNLESS OTHERWISE SPECIFIED)

Table 5: OFF

Symbol	Parameter	Test Conditions	Min.	Typ.	Max.	Unit
$V_{(BR)DSS}$	Drain-source Breakdown Voltage	I_D = 250 μA, V_{GS} = 0	60			V
I_{DSS}	Zero Gate Voltage Drain Current (V_{GS} = 0)	V_{DS} = Max Rating V_{DS} = Max Rating T_C = 125°C			1 10	μA μA
I_{GSS}	Gate-body Leakage Current (V_{DS} = 0)	V_{GS} = ± 20V			±100	nA

Table 6: ON (*)

Symbol	Parameter	Test Conditions	Min.	Typ.	Max.	Unit
$V_{GS(th)}$	Gate Threshold Voltage	V_{DS} = V_{GS} I_D = 250 μA	2	3.4	4	V
$R_{DS(on)}$	Static Drain-source On Resistance	V_{GS} = 10 V I_D = 10 A		0.18	0.20	Ω

Table 7: DYNAMIC

Symbol	Parameter	Test Conditions	Min.	Typ.	Max.	Unit
g_{fs} (2)	Forward Transconductance	V_{DS} = 15 V I_D = 6 A	2.5	6		S
C_{iss} C_{oss} C_{rss}	Input Capacitance Output Capacitance Reverse Transfer Capacitance	V_{DS} = 25V f = 1 MHz V_{GS} = 0		850 230 75		pF pF pF

Figure A-5:P-Channel MOSFET datasheet continued

ELECTRICAL CHARACTERISTICS (continued)

Table 8: SWITCHING ON

Symbol	Parameter	Test Conditions	Min.	Typ.	Max.	Unit
$t_{d(on)}$ t_r	Turn-on Delay Time Rise Time	V_{DD} = 30 V I_D = 6 A R_G = 4.7 Ω V_{GS} = 10 V (Resistive Load, Figure 19)		20 40		ns ns
Q_g Q_{gs} Q_{gd}	Total Gate Charge Gate-Source Charge Gate-Drain Charge	V_{DD}= 48 V I_D= 12 A V_{GS}= 10 V		16 4 6	21	nC nC nC

Table 9: SWITCHING OFF

Symbol	Parameter	Test Conditions	Min.	Typ.	Max.	Unit
$t_{d(off)}$ t_f	Turn-off Delay Time Fall Time	V_{DD} = 30 V I_D = 6 A R_G = 4.7Ω, V_{GS} = 10 V (Resistive Load, Figure 19)		40 10		ns ns

Table 10: SOURCE DRAIN DIODE

Symbol	Parameter	Test Conditions	Min.	Typ.	Max.	Unit
I_{SD} I_{SDM} (1)	Source-drain Current Source-drain Current (pulsed)				10 40	A A
V_{SD} (2)	Forward On Voltage	I_{SD} = 12 A V_{GS} = 0			2.5	V
t_{rr} Q_{rr} I_{RRM}	Reverse Recovery Time Reverse Recovery Charge Reverse Recovery Current	I_{SD} = 12 A di/dt = 100A/μs V_{DD} = 30 V T_j = 150°C (see test circuit, Figure 21)		100 260 5.2		ns nC A

(1) Pulse width limited by safe operating area.
(2) Pulsed: Pulse duration = 300 μs, duty cycle 1.5 %.

Figure 3: Safe Operating Area for TO-220

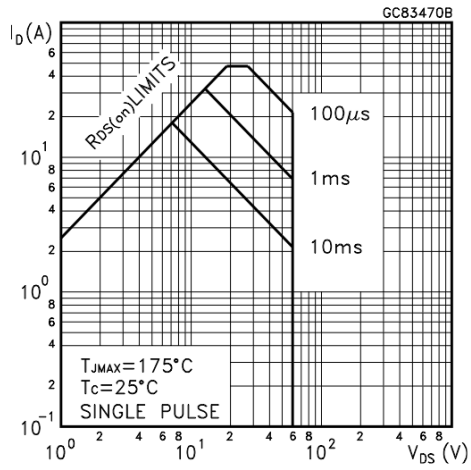

Figure 4: Safe Operating Area for TO-220FP

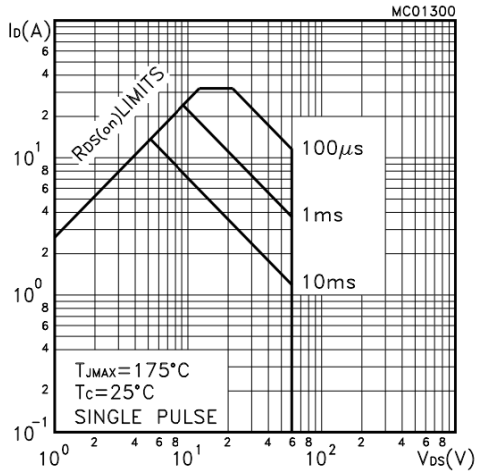

Figure A-6:P-Channel MOSFET datasheet continued

Figure 5: Thermal Impedance

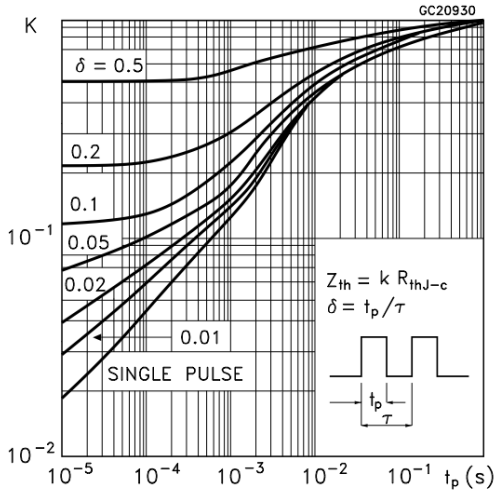

Figure 6: Thermal Impedance for TO-220FP

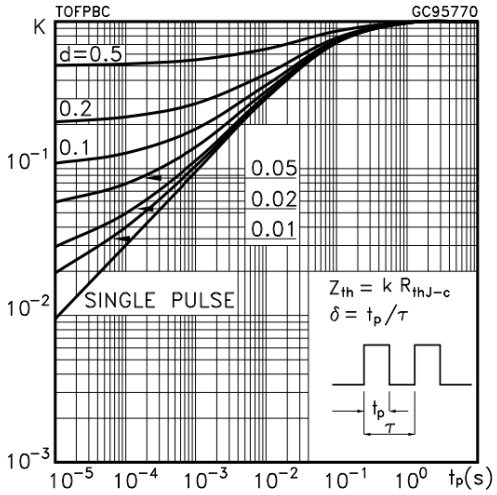

Figure 7: Output Characteristics

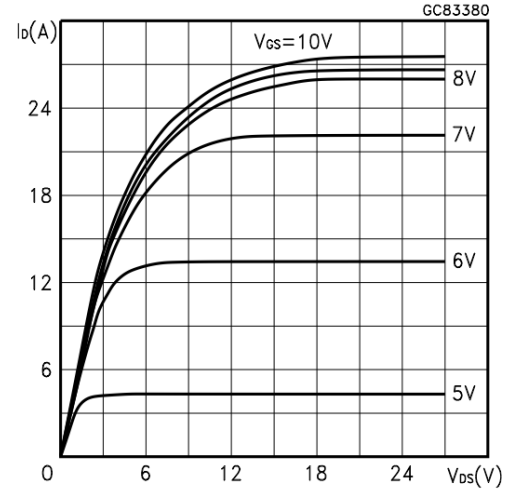

Figure 8: Transfer Characteristics

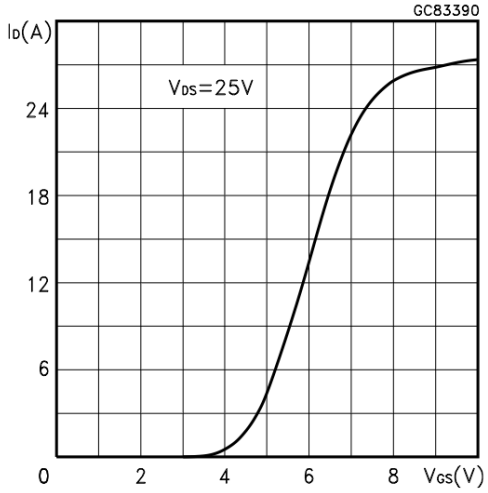

Figure 9: Transconductance

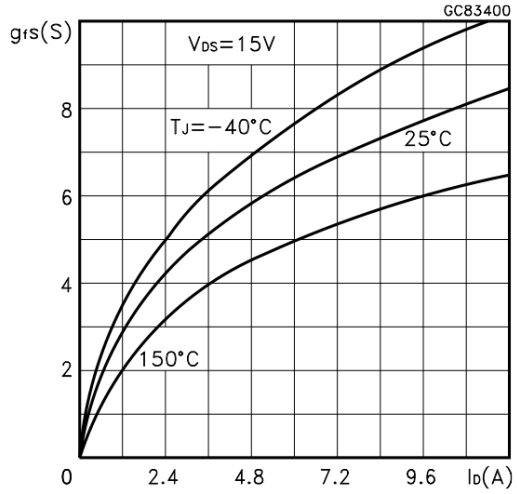

Figure 10: Static Drain-source On Resistance

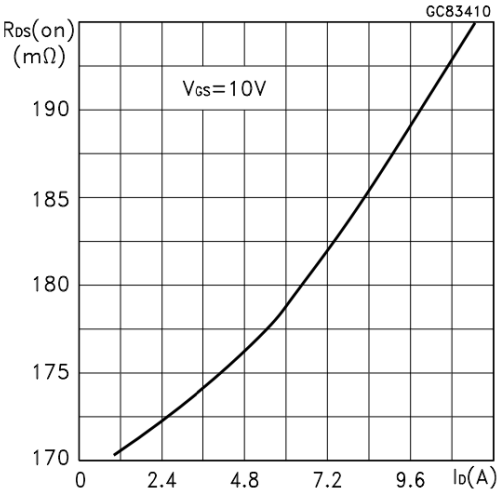

Figure A-7:P-Channel MOSFET datasheet continued

RECTRON SEMICONDUCTOR
TECHNICAL SPECIFICATION

SR520 THRU SR5200

SCHOTTKY BARRIER RECTIFIER

VOLTAGE RANGE 20 to 200 Volts CURRENT 5.0 Amperes

FEATURES

* High reliability
* Low switching loss
* Low forward voltage drop
* High current capability
* High switching capability

MECHANICAL DATA

* Epoxy: Device has UL flammability classification 94V-O
* Case: Molded plastic
* Lead: MIL-STD-202E method 208C guaranteed
* Mounting: position: Any
* Weight: 1.18 grams

DO-201AD

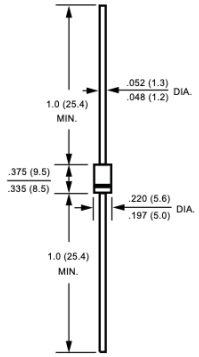

Dimensions in inches and (millimeters)

MAXIMUM RATINGS AND ELECTRICAL CHARACTERISTICS

Ratings at 25 °C ambient temperature unless otherwise specified.
resistive or inductive load.

MAXIMUM RATINGS (@ TA=25 °C unless otherwise noted)

RATINGS	SYMBOL	SR520	SR530	SR540	SR550	SR560	SR580	SR5100	SR5150	SR5200	UNITS
Maximum Recurrent Peak Reverse Voltage	V_{RRM}	20	30	40	50	60	80	100	150	200	Volts
Maximum RMS Voltage	V_{RMS}	14	21	28	35	42	56	70	105	140	Volts
Maximum DC Blocking Voltage	V_{DC}	20	30	40	50	60	80	100	150	200	Volts
Maximum Average Forward Rectified Current at Derating Lead Temperature	I_O	5.0									Amps
Peak Forward Surge Current 8.3 ms single half sine-wave superimposed on rated load (JEDEC method)	I_{FSM}	150									Amps
Typical Current Squared Time	I^2T	93.3									A^2S
Typical Thermal Resistance (Note 1)	$R_{\theta JA}$	25									°C/W
	$R_{\theta JL}$	8									
Typical Junction Capacitance (Note 3)	C_J	200									pF
Operating Temperature Range	T_J	150									°C
Storage Temperature Range	T_{STG}	-55 to + 150									°C

ELECTRICAL CHARACTERISTICS(@TA=25 °C unless otherwise noted)

CHARACTERISTICS		SYMBOL	SR520	SR530	SR540	SR550	SR560	SR580	SR5100	SR5150	SR5200	UNITS
Maximum Instantaneous Forward Voltage at 5.0A DC		V_F	.55			.75		.85				Volts
Maximum Average Reverse Current	@T_A = 25°C	I_R	0.2									mA
at Rated DC Blocking Voltage	@T_A = 100°C		2									mA

NOTES : 1. Thermal Resistance : At 9.5mm lead lengths, PCB mounted.
2. Measured at 1 MHz and applied reverse voltage of 4.0 volts.□
3. "Fully ROHS compliant", "100% Sn plating (Pb-free)".

2009-10
REV:A

Figure A-8: Diode datasheet

RATING AND CHARACTERISTICS CURVES (SR520 THRU SR5200)

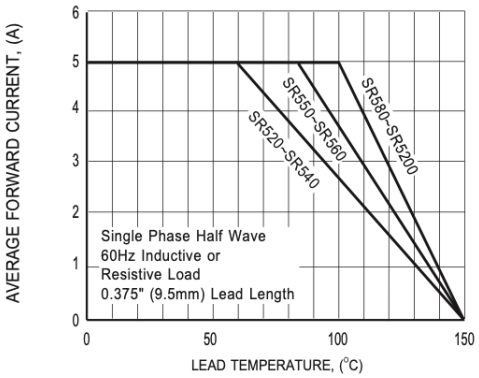

FIG.1 TYPICAL FORWARD CURRENT DERATING CURVE

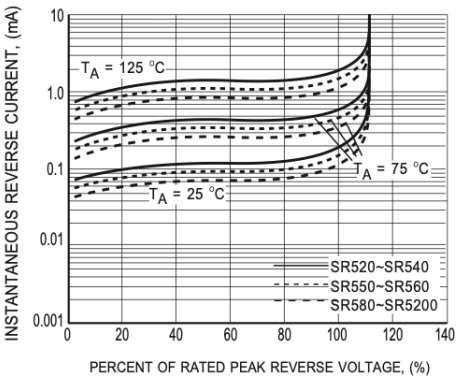

FIG.2 TYPICAL REVERSE CHARACTERISTICS

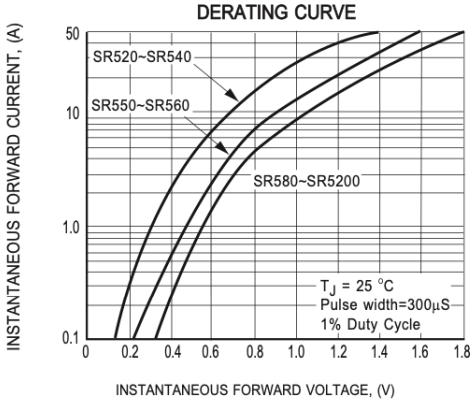

FIG.3 TYPICAL INSTANTANEOUS FORWARD CHARACTERISTICS

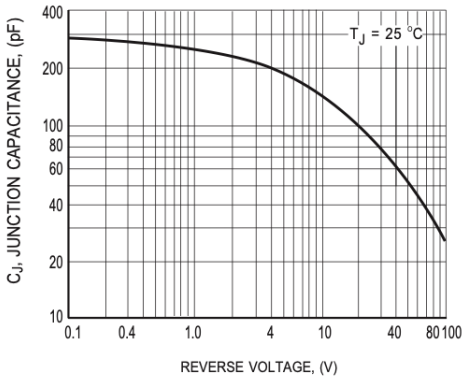

FIG.4 TYPICAL JUNCTION CAPACITANCE

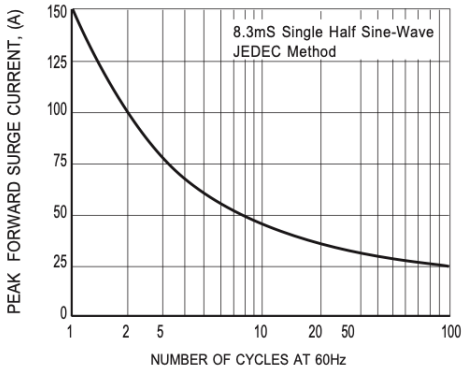

FIG.5 MAXIMUM NON-REPETITIVE FORWARD SURGE CURRENT

RECTRON

Figure A-9:Diode datasheet continued